THESIS / THÈSE

MASTER IN BIOCHEMISTRY AND MOLECULAR AND CELL BIOLOGY RESEARCH FOCUS

Deciphering the role of non-homologous-end joining and homologous recombination during the DNA repair mechanism of the bdelloid rotifer Adineta vaga

Boutsen, Anaïs

Award date:
2020

Awarding institution:
University of Namur

Link to publication

Faculté des Sciences

DECIPHERING THE ROLE OF NON-HOMOLOGOUS END-JOINING AND HOMOLOGOUS RECOMBINATION DURING THE DNA REPAIR MECHANISM OF THE BDELLOID ROTIFER *ADINETA VAGA*

Mémoire présenté pour l'obtention

du grade académique de master 120 en biochimie et biologie moléculaire et cellulaire

Anaïs BOUTSEN

Janvier 2020

Acknowledgment

For ten past months, in the LEGE labs I have been doing my Master thesis and what an adventure rich in emotions. It was a chance to have a master during which I could learn a lot and have fun.

First of all, I would like to thank my promotor, Karine Van Doninck, for allowing me to do my master thesis in her lab during the last 10 months. It was very formative and I learned a lot.

Obviously, I want to say a huge THANK YOU to my advisor Emilien Nicolas. He taught me many things from experiments to perseverance. I would not have been able to finish this thesis if it wasn't for his help and good advices. I wish him good luck for his future fishing.

I also want to particularly thank Mathilde Colinet, cloning master, for helping me through the thesis even though bdelloid rotifers are resistant to molecular analyses. It was thank to her and the other two Daltons, Lucie Bruneau and Laura Petit, my co-memorant, that coming to the lab was a pleasure, especially when going to look for cupcakes between experiments.

I want to thank Paul Simion, Rohan Arora, Matthieu Terwagne and Boris Hespeels for answering my questions and helping me understands some of the rotifers particularities. Also thanks to Rohan for making me discover some Indian sweets.

Finally, I would like to thank Antoine Houtain for his advices, his good mood and the nice green touch he added to the office.

I would like to thank everyone for their cheerfulness and support.

TABLE OF CONTENTS

ABBREVIATIONS

Ac	Acetone
BIR	Break-Induced Replication
BSA	Bovine Serum Albumine
CHAPS	3-[(3-cholamidopropyl)diméthylammonio]-1-propanesulfonate
CRISPR	Clustered Regularly Interspaced Short Palindromic Repeats
Ct	Cycle Treshold
DAPI	4',6-diamidino-2-phénylindole
DDR	DNA damages repair
DNA	Deoxyribonucleic acid
cDNA	complementary DNA
mtDNA	mitochondrial DNA
nDNA	nuclear DNA
ssDNA	single-stranded DNA
DSB	Double Strand Break
DSBR	Double Strand Break Repair
EDTA	Ethylenediaminetetraacetic acid
FA	Formaldehyde
FC	Freeze Crack
GAPDH	Glyceraldehyde-3-Phosphate Dehydrogenase
GC	Gene Conversion
GFP	Green Fluorescent Protein
HR	Homologous recombination
HSB	High Salt Buffer
HSP70	Heat Shock Protein 70
Indel	Insertion - Deletion
IF	Immunofluorescence
IR	Ionizing Radiation
LB	Lysogeny Broth
LDS	Lithium Dodecyl Sulfate
LEA	Late Embryogenesis Abundant
MeOH	Methanol
MMEJ	Microhomology-Mediated End-Joining
NFDM	Non Fat Dry Milk

NHEJ	Non Homologous End Joining
NI	Non Irradiated
OD	Optical Density
PAM	Protospacer Adjacent Motif
PBS	Phosphate-Buffered Saline
PCR	Polymerase Chain reaction
qPCR	quantitative PCR
PFGE	Pulse Field Gel Electrophoresis
PTM	Post Translational Modification
PVDF	Polyvinylidene Fluoride
RISC	RNA-Induced silencing complex
RIPA	Radio-Immuno-Precipitation Assay
RNA	Ribonucleic acid
dsRNA	double stranded RNA
gRna	guide RNA
mRna	messenger RNA
RNAi	RNA interference
shRNA	short hairpin RNA
siRNA	short interferent RNA
ssRNA	single stranded RNA
Rad51_L1	Rad51 Like protein 1
Rad51_L2	Rad51 Like protein 2
RNS	Reactive Nitrogen Species
ROS	Reactive Oxygen Species
RT	Reverse Transcription
Sc	*Saccharomyces cerevisiae*
SDS	Sodium Dodecyl Sulfate
SDSA	Synthesis-Dependent Strand Annealing
SSA	Single Strand Annealing
SSD	Solid State Drive
TAE	Tris base, Acetic acid, EDTA
TBST	Tris-Buffered Saline, 0.5% Tween 20
WB	Western Blot

Décryptage du rôle de la Jonction d'extrémités non-homologues et de la recombinaison homologue au cours du mécanisme de réparation de l'ADN du rotifère bdelloïde *Adineta vaga*

BOUTSEN Anaïs

Résumé

   Adineta vaga, rotifère bdelloïde, est un micro-organisme capable de survivre dans des conditions extrêmes et de se reproduire de manière asexuée depuis des millions d'années. Leur grande capacité de tolérance au stress s'illustre notamment grâce à une résistance à de fortes doses de radiation ionisante pouvant atteindre 2,000 Gy. La grande majorité des organismes eucaryotes sont sensibles à ces radiations, la résistance moyenne des cellules humaines ne dépasse pas 4 Gy. De telles doses de rayonnements ionisants entraînent un taux élevé de cassure double brin (DSB) de l'ADN activement réparées chez les rotifères bdelloïdes.

   Durant ce mémoire, nous avons tenté de décrypter quel(s) mécanisme(s) de réparation de l'ADN se cache(nt) derrière cette grande résistance. Les mécanismes de réparation de DSB habituels chez les métazoaires impliquent soit une jonction d'extrémité non homologue (NHEJ), soit une recombinaison homologue (RH). Suite à des irradiations de 800Gy*,* la variation d'expression de gènes impliqués dans NHEJ ou RH, *Xrcc4* ou *Rad51*, respectivement, soutien l'hypothèse de la présence de ces mécanismes. Une fois parfaitement mises au point, les méthodes d'analyse d'expression et de localisation de protéines fourniront des informations supplémentaires sur le mécanisme extraordinaire de l'ADN chez les rotifères bdelloïdes.

   La compréhension de ce mécanisme pourrait également donner des pistes sur la stratégie développée par les organismes asexués pour évoluer et se diversifier en l'absence de reproduction sexuée, choix évolutif par excellence pour créer de la diversité dans une population.

Deciphering the role of non-homologous-end joining and homologous recombination during the DNA repair mechanism of the bdelloid rotifer *Adineta vaga*

BOUTSEN Anaïs

Summary

Adineta vaga, bdelloid rotifer, is a peculiar micro-organism able to survive in extreme conditions and to reproduce asexually since millions of years. As an illustration of their high capacity of stress tolerance, bdelloid rotifers exhibit a resistance to high doses of ionizing radiation up to 2,000Gy. Such doses of ionizing radiation lead to a high level of DNA double strand break (DSB) that are actively repaired by bdelloid rotifers.

During this master thesis, we tried to decipher the DNA repair mechanisms behind the bdelloid extreme resistance to ionizing radiation and their DNA DSB. Usual repair mechanisms of DSB in metazoans involve either non-homologous end joining (NHEJ) or homologous recombination (HR). Following 800Gy irradiations, variation of gene expression implicated in NHEJ or HR support the, for now hypothetical, presence of those mechanisms. Once the methods perfectly optimized, protein expression and localization analyses will provide further insights on the extraordinary DNA mechanism undergoing in bdelloid rotifers.

The understanding of this mechanism might also give us lead on what strategy asexual organisms developed to evolve and diversify in the absence of a sexual reproduction, which is the gold standard evolutionary choice to create diversity in a population.

INTRODUCTION

Adineta vaga is a bdelloid rotifer, an eutelic animal composed of approximately 1,000 somatic cells and a few germinal cells. This microscopic aquatic organism is characterized by an obligate parthenogenesis (i.e., asexual mode of reproduction) and a high resistance level to environmental stresses such as complete desiccation, low temperature or ionizing radiation (Ricci & Fontaneto, 2009). Ionizing radiation, such as X-rays, are high energy electromagnetic waves that causes lots of impacts on cells resulting in numerous damages often ending with a deadly outcome (Azzam *et al.*, 2012). Therefore, organisms from unicellular bacteria to pluricellular eukaryotes are sensitive to these rays. When the majority of organisms are killed by doses that are inferior to 500Gy, *A. vaga* has the ability to survive to doses that can go higher than 2,000Gy (Daly, 2012).

Ionizing irradiation can cause damages to the DNA such as double strand breaks (DSB) (Azzam *et al.*, 2012). These cytotoxic lesions occur when two complementary strands of DNA helix are broken simultaneously (Jackson, 2002). When these DNA damages arise, two main repair mechanisms can restore the duplex structure: Non-Homologous End Joining (NHEJ) and Homologous Recombination (HR) (Jackson, 2002; Khanna & Jackson, 2001; Shrivastav *et al.*, 2007). Even though *A. vaga* possesses an extreme resistance to ionizing radiation their DNA is still impacted and undergo DSB. However, these DSBs are efficiently repaired within 48h following radiation and this rapid DNA repair mechanism probably explains their high resistance to radiation (Hespeels, Knapen, *et al.*, 2014). Moreover, their proteins appear protected since the DNA repair machinery is active following ionizing radiation exposure. DNA repair mechanisms are highly conserved among all eukaryotes and bacteria poseess similar DNA repair mechanisms. It has been showed that *A. vaga* possesses proteins involved in NHEJ and HR mechanisms (Daly, 2012; Hecox-Lea & Mark Welch, 2018). Therefore we chose to work with two highly conserved proteins implicated in these DSBs repair mechanisms: RAD51 and XRCC4. RAD51 is implicated in HR DNA mechanism and XRCC4 is a small nuclear protein that plays a role in NHEJ (see below) (Burma *et al.*, 2006; Hecox-Lea & Mark Welch, 2018).

Finally, we asked ourselves: How does this animal resist to such high doses of ionizing radiation? Discovering the DNA repair mechanism(s) active in such resistant organisms could give us some lead about some evolutionary process such as repair mechanism conservation, adaptation to extreme environment or the impact of their life style.

Adineta vaga

Bdelloid rotifers are microscopic freshwater invertebrates present on earth for 35 to 40 million years. *Adineta vaga* is one of the 450 morphologically described bdelloid species (Ricci & Fontaneto, 2009). Those animals can be found all around the world in semi-terrestrial environments such as lichens, mosses, habitats subjected to frequent drought periods or in freshwater environments like lakes, ponds and streams (Flot *et al.*, 2013; Ricci & Fontaneto, 2009). They can also be found in Antarctica and above 4000m (Ricci & Fontaneto, 2009). In those extreme environments such as permafrosts, thaw lakes and semi-terrestrial habitats bdelloid rotifers are abundant and can sometimes represent >50% of the microorganisms (Bégin & Vincent, 2017).
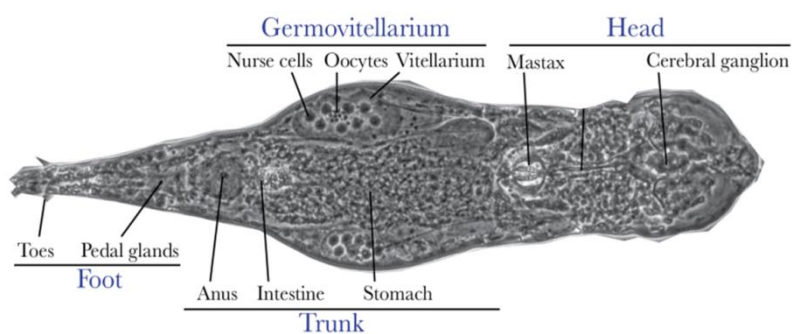
Figure 1 - Picture of *Adineta vaga* individual

Full size adult individual of *Adineta vaga*, microscopic bdelloid rotifers, around 200µm. Its body is divided in three main parts: head, trunk and foot. The head possess a ciliated corona allowing rotifers to nourish themselves by filter feeding. The food goes through the mastax (composed of trophi) to pass by the stomach, intestine and anus; they have a complete digestive system. In the germovitellarium, part of the reproductive system, the nurse cells, the oocytes and the vitellarium can be seen. In the foot the pedal gland and toe allow them to fix themselves to their substrate.
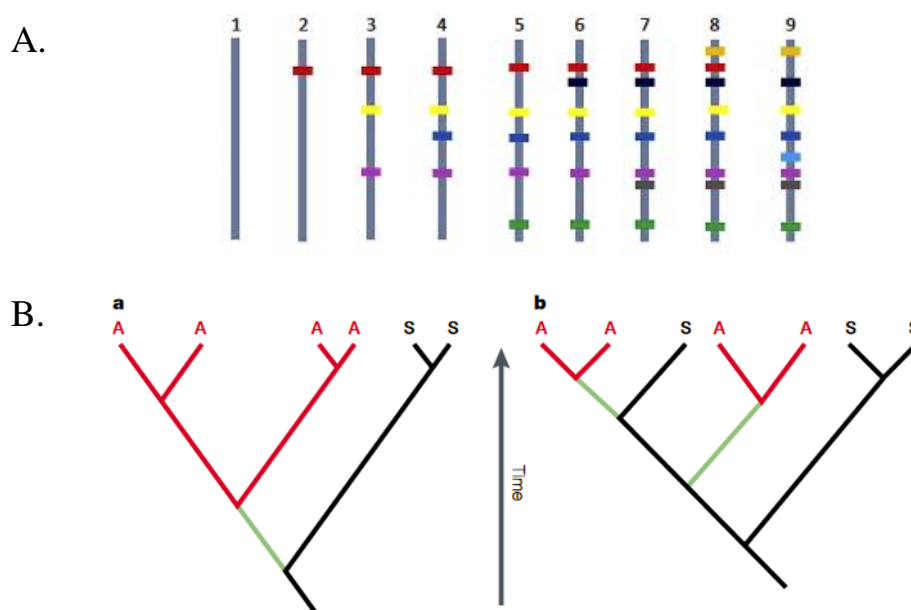
Figure 2 – Impact of time on the apparition of asexual lineages and on the accumulation of mutations (Muller's Ratchet)

(A) A chromosome (grey/blue line) (1) undergoes a mutation (red bar) (2) which is propagated to the next asexual generations (3-8). Some more mutations can appear with time (4–9). Even though some mutations like the red one can be reversed (generation 9), the general trend is translated by an increase in the number of mutations, ultimately leading to an extinction of the species (Maciver, 2016). (B) Two examples of phylogenetic distributions of asexual (A) and sexual (S) lineages in a clade. Origin of asexuality can have one or multiple origins but often asexuality derives from a lineage reproducing sexually (Butlin, 2002).

Bdelloid rotifers, eutelic organisms, possess a fixed number of somatic cells. Those somatic cells are therefore in a quiescent cell cycle phase G0/G1 as they do not divide anymore. On the opposite, their oocytes are in a G2 state. They seem to be dividing by a mitotic division or some modified meiosis since males and syngamy, i.e. fertilization resulting in the fusion of gametes to form a zygote, has never been observed. (Terwagne M., in prep.; Flot *et al*., 2013). Furthermore, the germoviteallarium of *Adinata vaga* includes large cells called nurse cells. In *Drosophila melanogaster* females, nurse cells can undergo multiple endoreplications resulting in highly polyploid cells. Those cells form an "interconnected cyst" with the oocytes by sharing cytoplasm. This phenomenon supports the oogenesis through transfer of mRNA or proteins to the developing oocyte (Lee *et al*., 2009). Finally, an *Adineta vaga* individual has a lifespan around 16,2 days and possesses a reproductive rate of 21,26 eggs per individual lifetime (Latta *et al*., 2019).

Bdelloid individuals possess an elongated body with a "subdivision" in head, trunk and foot (Figure 1). On top of their head can be seen a ciliated corona used for filter feeding on bacteria, algae and unicellular fungi. *Adineta vaga* individuals possess muscles, neurons, a digestive system and a paired germovitellarium. Those gonads are composed of an ovary (germarium) containing oocytes lodged in a syncytial nurse gland (vitellarium) (Ricci & Fontaneto, 2009). *Adineta vaga* populations are composed of female organisms, no males, vestigial male structures nor hermaphrodites have ever been observed. Females bdelloid rotifers reproduce by a clonal mode of reproduction called obligate parthenogenesis but the details of their parthenogenetic reproductive mode remain unknown (Hespeels, Knapen, *et al*., 2014).

Asexual reproduction and obligate parthenogenesis

In the animal tree of life, sexual reproduction is widespread. The evolutionary success of sexual reproduction is believed to be due to the genome plasticity allowed by the mixing and recombination of genes (Danchin *et al*., 2011). However sex seems quite costly as transmission recombination breaks up favourable gene combinations faster than creating new ones in addition to the reproduction process itself during which organisms need to find mates, risk illness transmissions, etc. (Butlin, 2002). On the other hand, sex might give a better adaptability as the production of individual variability, on which natural selection can act, helps overcome environmental modifications and accumulation of deleterious mutations. Strictly asexual species do not seem to survive in the long term leading to an evolutionary dead-end because in the absence of gene mixing and recombination they are less likely to adapt (Butlin, 2002; Danchin *et al*., 2011). Furthermore, according to the Muller's ratchet principle, asexual species are bound to extinction due to the accumulation of deleterious mutations (Figure 2A) (Maciver, 2016). Another cost of asexual reproduction can be observed with the "Hill-Robertson effect". In sexual population recombination enhance the elimination of deleterious alleles and brings together favourable mutations present in different individuals. Therefore, in asexual population, over time, absence of recombination might enhance (i) the frequency of deleterious mutations linked to advantageous ones might increase (genetic hitch-hiking) (ii) elimination beneficial mutations linked to unfavourable ones (background selection) (Desai & Fisher, 2007).

Finally, most known asexual animal species emerged recently and are dispersed among clades of sexually reproducing animals in the tree of life (Figure 2B). Asexual lineages therefore often possess part of the genotypic diversity of sexuals and occupy a more restricted ecological niche than their ancestors (Butlin, 2002; Danchin *et al*., 2011).
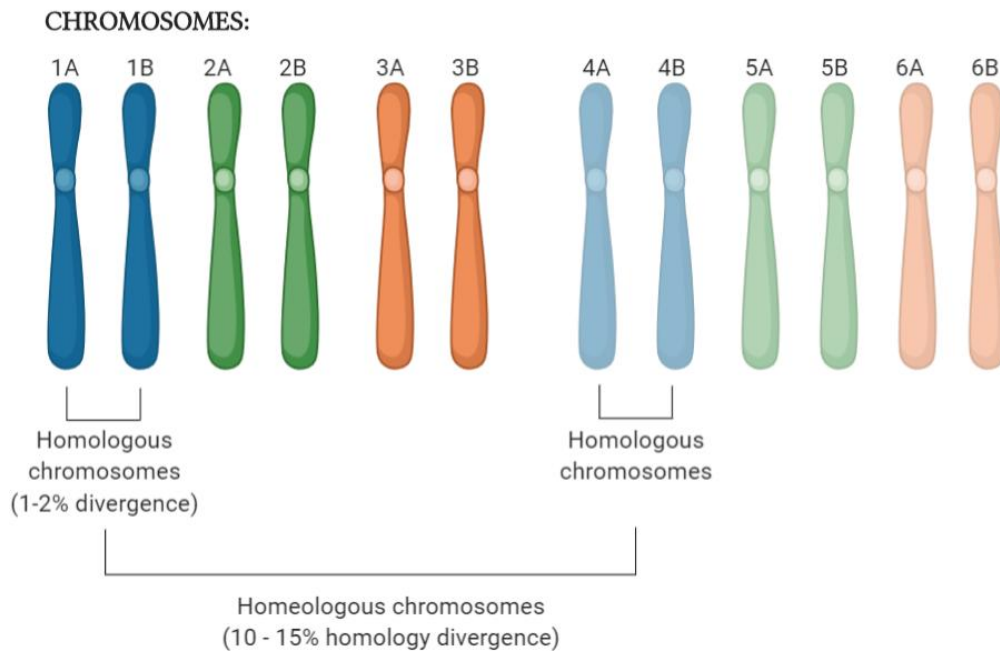
Figure 3 – Illustration of *Adineta vaga* degenerate tetraploidy

Illustration of *A. vaga* chromosomes without sister chromatid as somatic cells are in a G0/G1 cell cycle phase. Homologous chromosomes are represented by the same number but a different letter. Homeologous chromosomes, being the result of a genome duplication or hybridization event in the bdelloid rotifer ancestor, are represented here by matching colours.
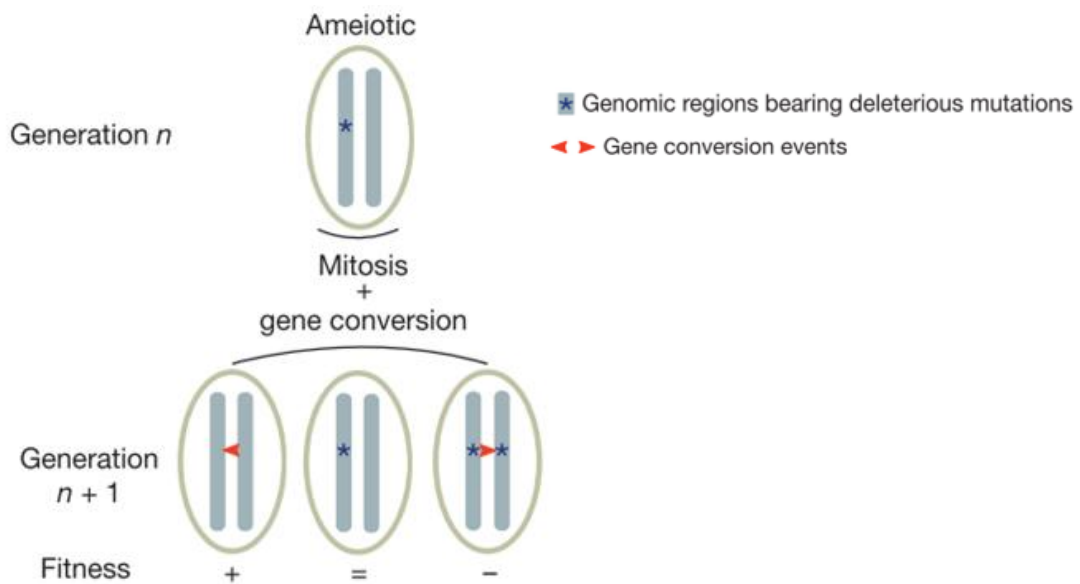
Figure 4 – Gene conversion may allow bdelloid rotifers to homogenise their genome

Illustration of a gene conversion event. Stars represent deleterious mutations and red arrows the gene conversion events. This phenomenon can lead to the loss of the mutation (+) or its acquisition (-) impacting the fitness of the individual (Flot *et al.*, 2013).

Knowing this, asexual lineages appear to be short-lived and ancient, species-rich asexual taxa should not exist (Butlin, 2002). However, bdelloid rotifers are an exemption since they have been reproducing asexually by obligate parthenogenesis for millions of years and diversified into more than 400 morphospecies. Bdelloid rotifers have therefore been named an "ancient asexual scandal" or an "evolutionary scandal" (Hespeels, Knapen, *et al.*, 2014).

Obligate parthenogenesis is an asexual mode of reproduction during which individuals develop from unreduced gametes without fertilization. Obligate parthenogenesis are called "obligate" because organisms can only reproduce asexually (males are never observed) in contrast with facultative parthenogenesis during which animals can switch between sexual and asexual reproduction (Galis & van Alphen, 2019).

Nevertheless, asexual or uniparental reproduction can also provide some advantages. Asexual organisms do not need partners in order to reproduce. This can be seen as a more secure reproductive strategy. There are no risk for low encounter probability and a single animal is enough to start a new population. Furthermore, asexual organisms pass on its entire genome, knowing that the driving force of evolution is to pass on genetic information. This can be seen as an advantage in comparison to sexual reproduction during which only half of the information is transmitted to the descendants (Maciver, 2016; Ricci & Fontaneto, 2009). Under some stressful conditions, it has been shown that the asexual mother can produce daughter of increased fitness and longevity, this is an interesting ability for organisms that can display high resistance to stress.

The genome of *Adineta vaga*

Bdelloid rotifers derived from an ancient genome duplication or hybridization event generating asexual degenerate tetraploid lineages. This event occurred before the actual bdelloid rotifer species divergence (Hur *et al.*, 2008) since several bdelloid species have a degenerate tetraploid genome structure. In *Adineta vaga* the genome is composed of 12 chromosomes made up of three quartets of two homologous pairs (illustrated in figure 3) (Hur *et al.*, 2008). This polyploidy, *i.e.* having numerous copies of a gene, could delay the Muller's Ratchet because a deleterious mutation occurring in one copy of a gene can be compensated by other functional copies (Maciver, 2016).

Organisms could also avoid the accumulation of deleterious mutations by a reversion of spontaneous mutations by gene conversion (Maciver, 2016). Gene conversion is a phenomenon during which a homologous chromosome, rather than a sister chromatid, is used as a template in order to perform recombination. During a gene conversion event mutations can get either removed or added to the chromosome, impacting the fitness of individuals (Figure 4) (Butlin, 2002; Flot *et al.*, 2013). Gene conversion can be facilitated by polyploidy. In the genome of *Adineta vaga* signatures of gene conversion were retrieved (Flot *et al.*, 2013).

Finally, Flot *et al.* (2013) also found that around 8% of *Adineta vaga* genome came from non-metazoan genes acquired through horizontal gene transfer. This was recently confirmed by another study on several bdelloid species (Nowell *et al.*, 2018). These horizontal gene transfers may facilitate adaptation if the acquired genes are used. Therefore, high frequencies of gene conversion and horizontal gene transfer could provide bdelloid rotifers with some genetic diversification usually associated to sexual reproduction (Gladyshev *et al.*, 2008).

Resistance to stresses

In addition to their ancient asexuality, bdelloid rotifers are of interest to scientists because of their high resistance to extreme stresses such as complete desiccation or freezing. The semi-terrestrial habitats in which rotifers can be found, often undergo drought periods when water is cued by water evaporation. Bdelloid rotifers manage to survive those stressful desiccation periods by entering a metabolically quiescent state of anhydrobiosis (Ricci & Fontaneto, 2009). Anhydrobiosis is a state during which animals enduring desiccation manage to survive through a stage of "dormancy" in which their metabolisms comes reversibly to a standstill (Wharton, 2015). The ability to survive this type of stress is atypical as most animals and plants do not survive such water losses. In addition to bdelloid rotifers, two other animal phyla, tardigrades and nematodes, are able to survive and reproduce after undergoing complete desiccation at any stage in their life-cycle (Hespeels, Knapen, *et al.*, 2014).

In bdelloid rotifers, anhydrobiosis has been shown to impact individuals at different level causing biochemical, physiological and morphological changes (Ricci & Fontaneto, 2009). When entering anhydrobiosis, morphological changes can be observed in bdelloid rotifers as their body undergoes a contraction resulting into a compact shape called a "tun". Surviving desiccation requires the ability to maintain functional macromolecules (DNA and proteins) and membranes and to counter the action of Reactive Oxygen Species (ROS) (ROS will be further explained in the section ionizing radiation of the introduction). This maintenance can be achieved by preserving the integrity of molecules with antioxidants, sugars and LEA proteins (Late Embryogenesis Abundant protein) or by repairing damages that occurred, e.g. with efficient DNA repair mechanisms (Hespeels, Knapen, *et al.*, 2014). Indeed in most desiccation-tolerant organisms, antioxidants and sugars, such as trehalose, are crucial components for their survival. However, bdelloid rotifers do not seem to synthesise high concentration of trehalose sugar as a protective chemical (Ricci & Caprioli, 2005). However, they seem to possess LEA proteins acting as "molecular shields" by protecting cellular structures, proteins or membranes or by the renaturation of unfolded proteins (Gladyshev & Meselson, 2008; Tunnacliffe *et al.*, 2005).

Furthermore, during prolonged periods of desiccation, organisms can suffer from DNA DSBs. Therefore, over time, such stressful experiences may have reshaped their genome. Indeed, since long periods of desiccation induce DNA DSBs, gene conversion or unfaithful DNA repair might have resulted in genomic changes. Furthermore, desiccation could impact the membrane integrity, such as the gut lining. Therefore, ingested foreign DNA could pass from the digestive system to the oocytes in the germovitellarium, adjacent to the digestive system (Figure 1). This foreign DNA could be integrated into the oocyte DNA through homologous or ectopic recombination during DNA repair, and be duplicated (Gladyshev & Arkhipova, 2010; Hespeels, Flot, *et al.*, 2014).

Unlike other anhydrobionts, bdelloid rotifers are also able to survive long periods of starvation. Starvation could be described as another form of "dormancy" during which bdelloid rotifers manage to survive by suspending any activity and reducing metabolic expenditure.

When fed or hydrated again, bdelloid rotifers continue their life cycle and reproduce. Indeed, when starvation or anhydrobiosis ends, the time spent in dormancy is not impacting their age. This condition during which bdelloid rotifers seem to delete the duration of dormancy from their age has been called the "sleeping beauty" behaviour.
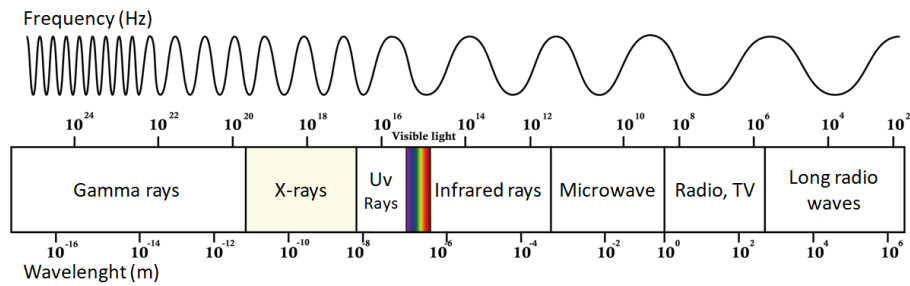
Figure 5 – X-rays wavelength and frequency in comparison to other electromagnetic waves

X-rays ionizing radiations are electromagnetic waves with frequency and wavelength characteristic of electromagnetic waves. For X-Rays their frequency varies between 10^{17} and 10^{20} while the wavelength can vary between 1pm to 10nm. X-rays are therefore energetic waves that can penetrate soft tissues and create lots of impact on the cells.
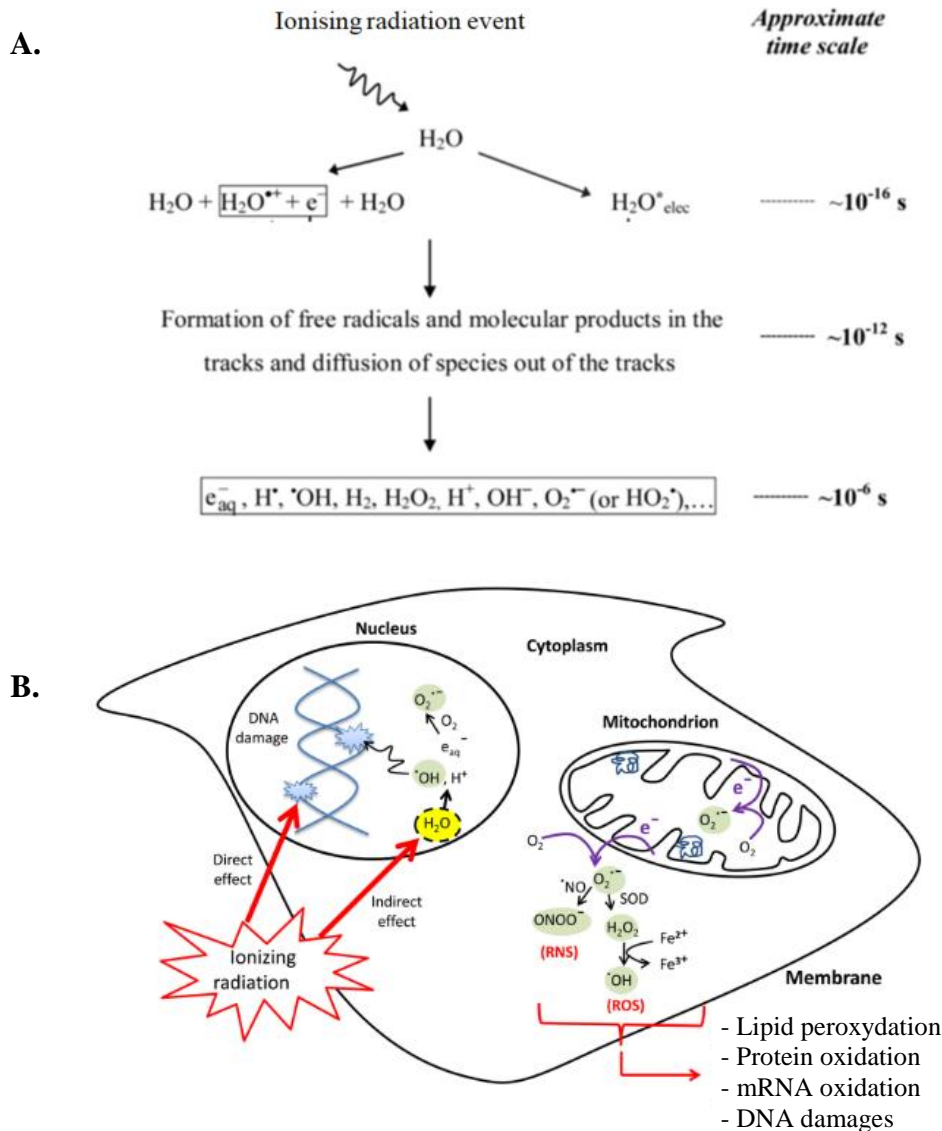
Figure 6 – The direct and indirect cellular effects of ionizing radiation on macromolecules.

(A) Time scale of events during water radiolysis after ionizing radiations. (B) The absorption of ionizing radiation can have direct and indirect impacts on living cells. Direct impacts cause disruption of atomic structures and produce chemical and biological changes. Radiolysis of cellular water, an indirect impact, can cause the generation of reactive chemical species. Finally, ionizing radiations may impact mitochondrial functions causing damages to lipids, proteins, nuclear DNA (nDNA) and mitochondrial DNA (mtDNA) (Azzam *et al.*, 2012).

Even if bdelloid rotifers are not the only animals able to behaves like sleeping beauties (e.g. Tardigrades), other anhydrobionts such as nematodes do not manage to survive starvation period and appear to age during their dormancy period (behaviour called "The Picture of Dorian Gray") (Ricci & Fontaneto, 2009).

It has also been shown that anhydrobiosis could facilitate bdelloid rotifers spatio-temporal movements. Desiccated rotifers, in tun shape, can be easily dispersed by wind and colonize new environments. Their ability to survive stressful environments tend to help their "colonization process". This migration can occur among disconnected microhabitats but also at intercontinental scale (Fontaneto *et al*., 2008; C. G. Wilson, 2011).

Independently to the origin of anhydrobiosis in rotifers, it seems that this capacity might enhance their fitness. It has been shown that constantly hydrated bdelloid populations undergo a decrease of fitness. The cause of this decrease is not understood but it has been observed that after undergoing anhydrobiosis, the fitness of the population is restored. A hypothesis that was suggested to explain this phenomenon is that parthenogenetic reproduction might have some negative impacts on the DNA and the "awakening" from anhydrobiosis might promote DNA repair mechanisms, restoring the integrity and function of the DNA (Ricci & Caprioli, 2005).

Finally, different hypotheses could be suggested concerning the ability of bdelloid rotifers to survive during these stressful environments (i) they have acquired resistance by evolving in those environments, (ii) the resistance was already present and allowed them to conquer these environments (iii) combination of both.

Ionizing radiation

As said earlier, *A. vaga* has the ability to survive to different stresses including high doses of ionizing radiation. Ionizing radiations, such as X-rays, are high energy electromagnetic waves. Those electromagnetic radiations are emitted when excited inner orbital electrons of an atom release energy (Attwood, 2007). X-rays wavelengths vary from 1pm to 10nm and can be divided into two kinds: soft and hard X-rays. Hard X-rays have a shorter wavelength and a higher energy while soft X-rays (Grenz rays) are less energetic and have a longer wavelength (Figure 5) (Attwood, 2007).

Ionizing radiation has tremendous impacts on cells causing numerous direct or indirect damages. The absorption of those radiations can lead to direct damages such as disruption of atomic structures and production of chemical and biological changes.

The indirect damages are due to the radiolysis of water generating, in a short time scale, reactive chemical species, such as reactive oxygen species (ROS) and reactive nitrite species (RNS) (Figure 6A). Three of the main free radicals are the reactive nitrogen species NO• and the oxygen species, superoxide $O_2^{•-}$ and the hydroxyl radical HO• (principal ROS, creating most damages with a half-life time of 10^{-9}s) (Kong & Lin, 2010). In mammalian cells, it has been shown that oxidative changes can arise for days and months after the exposure due to continuous generation of reactive chemical species. ROS exhibit a wide range of oxidative damages on proteins, lipids and nucleic acids by causing protein carbonylation, lipid peroxydation, RNA oxidation and DNA damages (Figure 6B) (Azzam *et al*., 2012). Carbonylation is an irreversible oxidative damage leading to loss of function and protein aggregation. Protein nitration (caused by RNS) can also impact the activity of proteins.
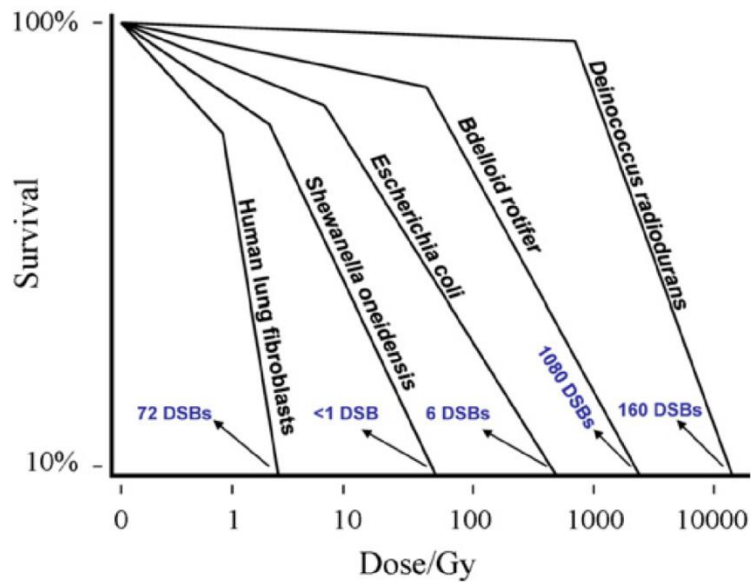
Figure 7 – Survival rates of organisms upon ionizing radiation

The organisms observed are the bacteria *S. oneidensis*, *E. coli*, *D. radiodurans* but also human lung fibroblasts and *A. vaga*. These organisms illustrate a range of resistances to ionizing radiation from 4Gy for the human fibroblast to 12,000Gy for the bacteria *D. radiodurans*. The majority of organisms from prokaryote or eukaryotes are radiation sensitive and killed by doses less than 500 Gy (Daly, 2012).
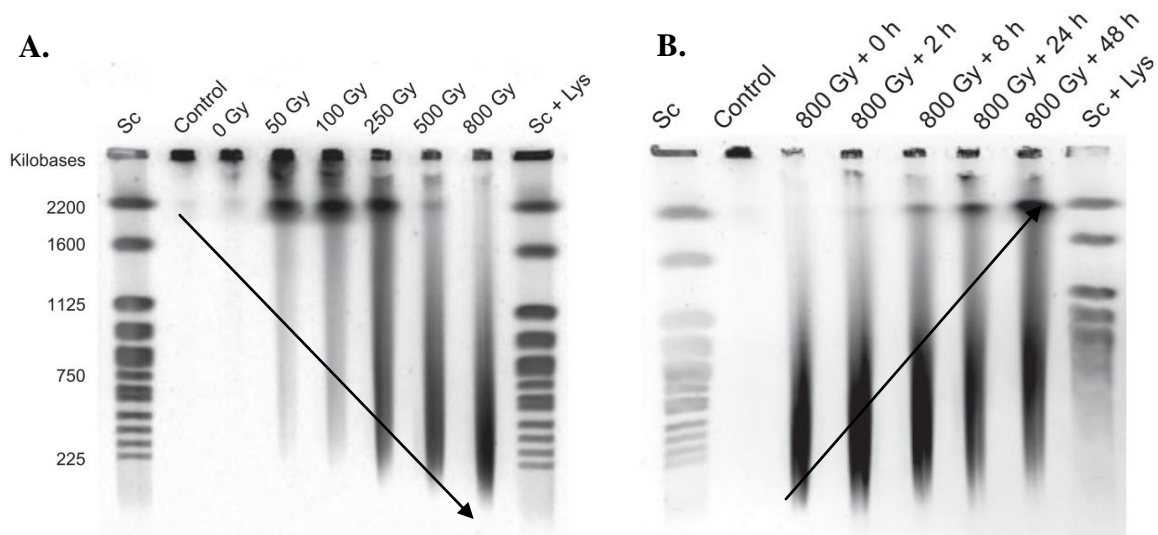
Figure 8 – Ionizing radiation impact bdelloid rotifers by accumulation of "reversible" DSB

Pulse Field Gen Electrophoresis (PFGE) analyses of *Adineta vaga* show the genome integrity upon desiccation and exposure to different doses of ionizing radiation. (A) Accumulation of DNA DSBs appears to be is dose-dependent. (B) Upon rehydration, DNA DSBs are repaired as the small DNA fragments disappear with time (Hespeels, Knapen, *et al.*, 2014).

Lipid peroxydation occurs when free radicals "steal" an electron from lipids affecting poly-unsaturated fatty acids resulting in the degradation of lipids (Kong & Lin, 2010). ROS can also impact nucleic acid resulting in several alterations by enhancing spontaneous gene mutations and causing DNA breaks, base damages, crosslinks, destructions of sugars and telomere dysfunction. If those damages stay unrepaired or mis-repaired it could cause mutations, neoplastic transformation or cell death. Finally, ionizing radiation might impact the function of the mitochondria. Mitochondrial damages can result in lipid, protein, nuclear DNA (nDNA) and mitochondrial DNA (mtDNA) alterations (Azzam *et al.*, 2012).

Resistance of bdelloid rotifers to ionizing radiation

Irradiations have been demonstrated to impact all organisms from unicellular bacteria to pluricellular eukaryotes. The ability of organisms to survive this kind of stress is most often measured by their mortality rate. Indeed, the majority of organisms are radiation sensitive and are killed by doses that are inferior to 500Gy, e.g. human cells cannot survive doses above 4Gy. However, some organisms such as the bdelloid rotifer *A. vaga* or the bacteria *Deinococcus radiodurans* have shown an ability to survive extreme doses, higher than 2,000Gy (Figure 7) (Daly, 2012).

Two main hypotheses have been proposed to explain the resistance to ionizing radiation. Firstly, the aptitude to better resist oxidative stresses; a stress that impacts proteins and decreases their functionality and efficiency (like the ones used for DNA repair (Daly, 2012)). Indeed, bdelloid rotifers and any other radiation resistant organism seem to have developed effective antioxidant protections. *A. vaga* possesses more antioxidant genes than any other model organism studied (Flot *et al.*, 2013). Moreover the essential enzymes, like superoxide dismutase, and non-enzymatic free-radical scavengers, like ROS-scavenging manganese complexes, are upregulated when encountering a stressful environment (Berjak, 2006). In addition to their action as ROS-scavenging complexes, manganese protects proteins from ROS by replacing iron and other divalent cations. Indeed, by using those cations as mononuclear enzymatic cofactors, active sites of proteins can be protected from oxidative damage. Furthermore, the presence of iron can stimulate the production of ROS through Fenton reactions which can enhance oxidative damages. Therefore the presence of manganese, allows a decrease of ROS production (Azzam *et al.*, 2012; Daly, 2012).

$$\text{Fenton reaction: } Fe^{2+} + H_2O_2 \rightarrow Fe^{3+} + OH^- + OH\bullet$$
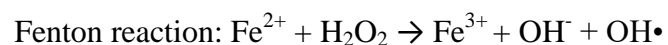
Secondly, cytotoxic studies have often linked the lethality of ionizing radiation to the quantity of DNA DSBs formed. Indeed, accumulation of DSBs can trigger the signalisation pathways leading to apoptosis. In the case of bdelloid rotifers, it has been shown that their DNA suffers from DSBs accumulation like other radiation-sensitive species. However, *A. vaga* still manage to survive, repair their DNA and have viable descendants (Figure 8). This resistance is probably due to the presence of an effective antioxidant machinery that protects the DNA repair proteins that remain active to efficiently repair the incurred damages. Furthermore it has been shown that the inactivation of DNA repair genes can increase the radio-sensitivity (Jackson, 2002).

Double strand breaks DNA repair mechanism

During ionizing radiation numerous damages can be done to the DNA. In the entire DNA damages range, double strand breaks are the more harmful ones. Therefore, the research and experiment realised during the master thesis will focus on them.

DNA DSB are cytotoxic lesions occurring when two complementary strands of DNA helix are broken simultaneously. In addition to ionizing radiation and desiccation, DSBs can have many other origins such as drugs, the encountering of a DNA single strand break and a DNA replication machinery and metabolic ROS. However, DSBs can also occur as intermediates in biological events such as V(D)J recombination (Malu *et al*., 2012). Lack or inaccurate repair of those damages can lead to mutations and genomic instability. Genomic instability can be due to the accumulation of small nucleotide modifications or to chromosomal alterations like translocations or the generation of dicentric or acentric chromosomal fragments. In metazoans, one DSB can be enough to inactivate an essential gene or trigger apoptosis resulting in the death of the cell (Burma *et al*., 2006; Jackson, 2002).

When DSBs occur the DNA-damage-response pathways start with the detection of the damage by DNA-damage binding proteins, triggering a transduction system (protein kinase cascade), amplifying and diversifying the signal. As a result, a series of downstream effectors can be activated leading to the activation of different pathways such as DNA repair, modification of the cell cycle or apoptosis (Figure 9) (Jackson, 2002). When DSBs arise, two major categories of DNA repair mechanisms can restore the duplex structure.
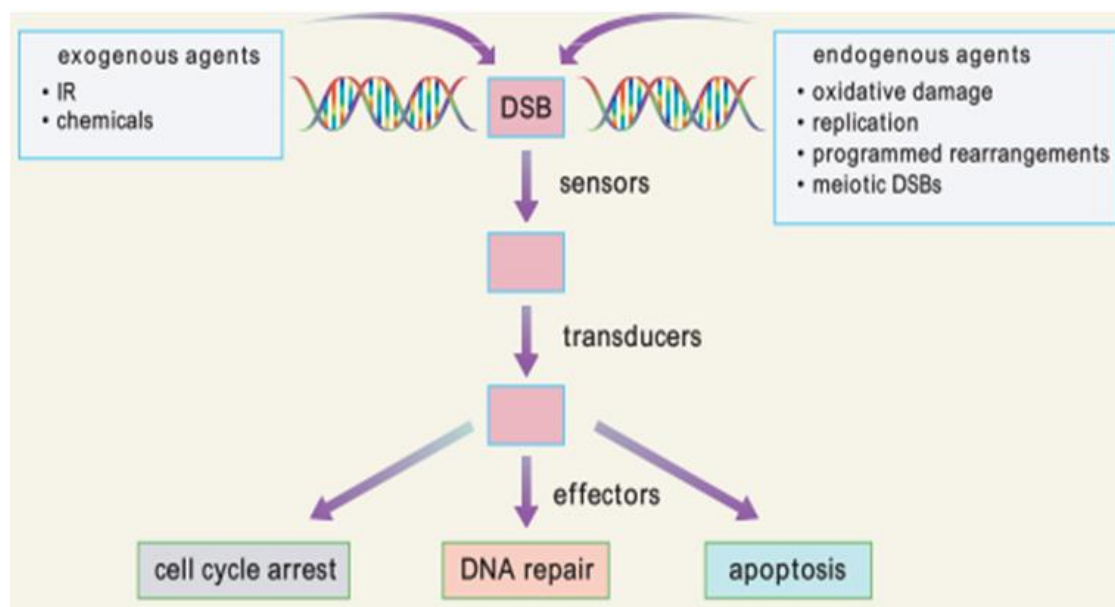
Figure 9 – DNA DSBs and their activation of distinct pathways

DSB can be generated by endogenous and exogenous agents. Once generated, the DSB is detected by sensors (DNA-damage binding proteins), transduction pathways transmit the signal to different pathways such as DNA repair, modification of the cell cycle or apoptosis (Khanna & Jackson, 2001).
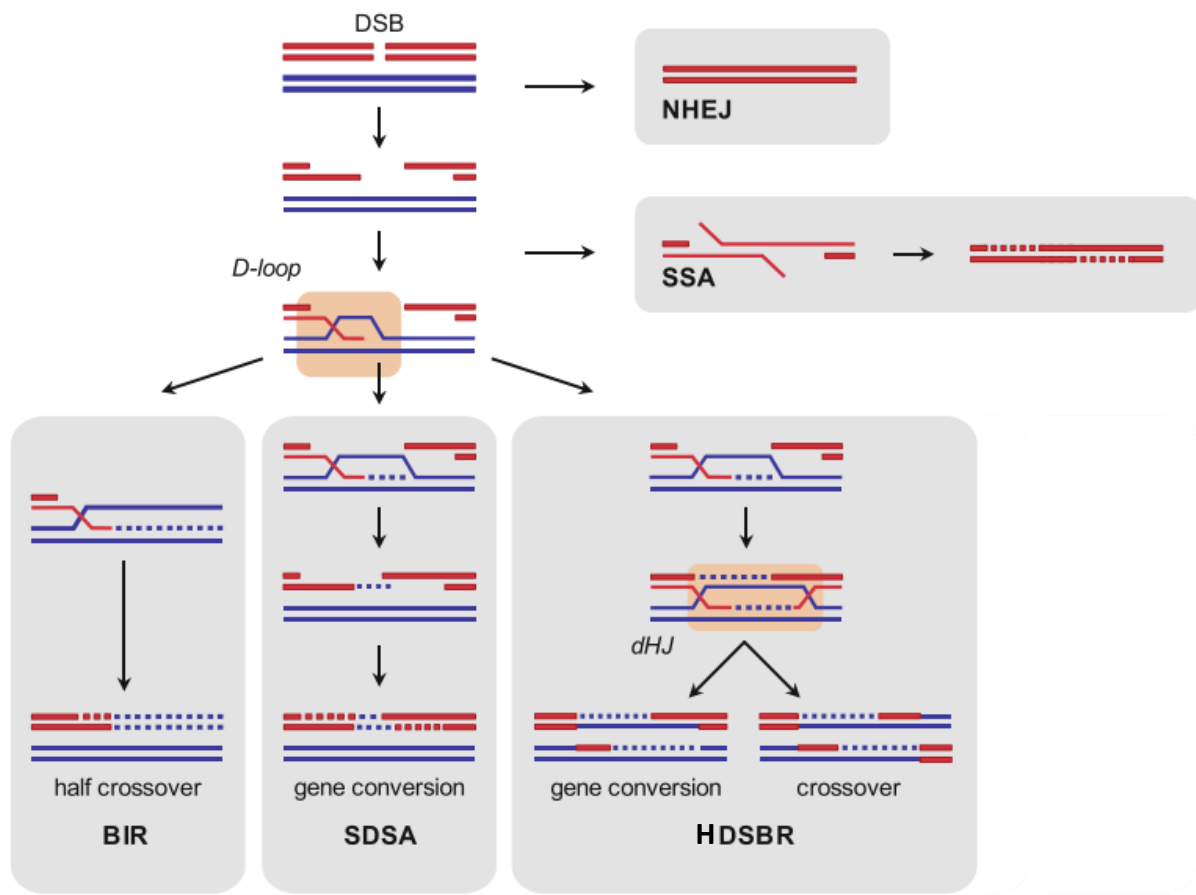
Figure 10 – The different DNA DSB repair mechanisms

When a DSB occur distinct DNA repair mechanisms can restore the DNA duplex structure. Those mechanisms can be divided into two main categories: (i) Non-homology directed DNA repair mechanism and (ii) homology directed DNA repair mechanism. The non-homology DNA repair mechanism is characterised by the NHEJ pathway that ligates the broken DNA ends together. The homology directed repair mechanism includes SSA, BIR, SDSA and HDSBR. In this mechanism the different repair pathways use a homology template to repair the DNA in a faithful way (Sebesta & Krejci, 2016).

When organisms are diploid, even if transient (e.g. replicating bacteria or replicating haploid yeast), during S/G2 phases a sister chromatid is available and therefore a homologous template is present for DNA DSB repair. Those organisms are more likely to perform a homology directed DNA repair mechanism (HR) such as single-strand annealing (SSA), Break-induced replication (BIR), synthesis-dependent strand annealing (SDSA) or Homologous Double-Strand Break Repair (HDSBR). Non-dividing haploid or diploid organisms, outside of S/G2 phases of the cell cycle, do not have homologous sequences nearby and therefore are more likely to perform Non-Homologous End Joining (NHEJ) (Figure 10) (Lieber, 2010; Sebesta & Krejci, 2016).

Homologous recombination

Homologous Recombination (HR) regroups the DNA repair mechanisms during which damaged DNA retrieves genetic information from an undamaged DNA molecule sharing extensive sequence homology (i.e. the sister chromatid) (Jackson, 2002).

Homologous recombination mechanism can be divided in three main steps. First, during the *presynapsis* step a set of heterohexameric nucleases complex, e.g. Mre11-Rad50-Nbs1 (MRN), senses the DNA DSB and resects the DNA ends in the direction 5' to 3' in order to produce 3' single strand tails. This ssDNA is then protected by replication protein A (RPA) from other nucleases. During the second step, the *synapsis,* RAD51 recombinases, with the help of recombination mediators, replace RPA on the ssDNA. The nucleoprotein filament just formed searches for a homologous sequence leading to the formation of a transient D-loop structure. The invading ssDNA is then used as a primer for the replication machinery. DNA polymerase δ will extend the 3' single strand by copying the information of the undamaged homologous DNA. Finally during the *postsynaptic* step, the recombination structure is then resolved to produce a new DNA molecule with a similar sequence to the homologous template (the mechanism is illustrated in figure 11B) (Khanna & Jackson, 2001; Sebesta & Krejci, 2016).

Even though the early stages of HR are similar, the postsynaptic step varies between the SDSA, DSBR or BIR pathways. During the SDSA mechanism, the ssDNA, extended in the D-loop structure, is displaced, annealed with the second end of the DSB and a second DNA synthesis occurs. After ligation by a DNA ligase, the genome integrity is restored and gene conversion products are formed. During HDSBR, in contrast to the SDSA pathway, the D-loop is stabilised and serve as a template for the second end of broken DNA. This results in a double Holliday junction that, when processed, restore the genome integrity resulting in gene conversion or cross over event. Finally, the BIR pathway occurs at single-ended DSB (Figure 10, BIR) (Lieber, 2010; Sebesta & Krejci, 2016)

Furthermore, even though SSA is also a homology directed DNA repair mechanism, the mechanism is different from the other ones. SSA is a pathway during which extensive nucleolytic resection of DSB occurs until homologous sequences are exposed, aligned and annealed to each other, restoring the DNA duplex (Figure 10, SSA) (Sebesta & Krejci, 2016).
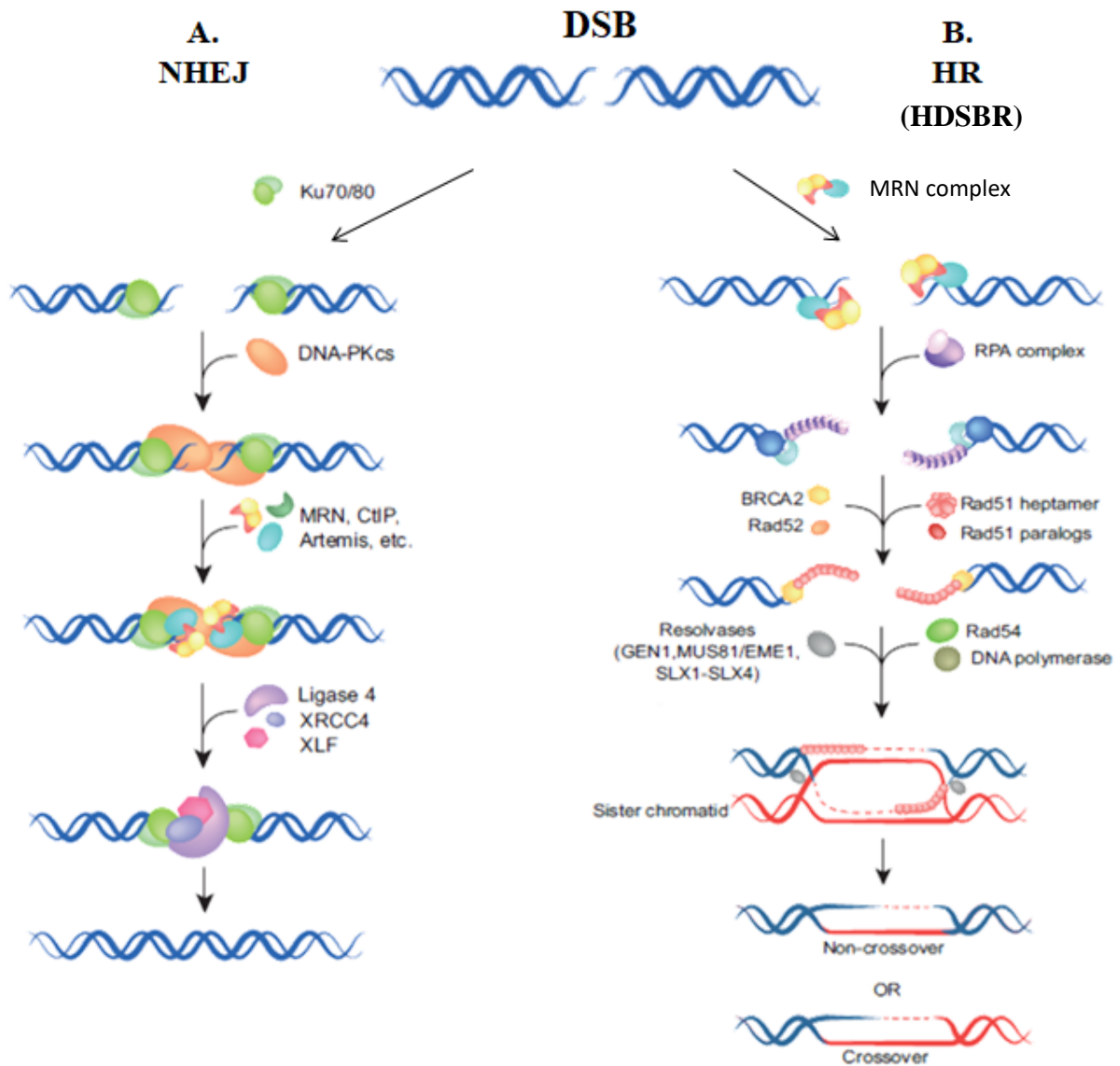
Figure 11 – Homologous Recombination and Non-homologous End Joining pathways

When encountering a DNA DSB, the two main repair pathways occurring are NHEJ and HR. (A) During NHEJ, DSB ends are processed and reassembled in an error-prone mechanism. (B) HR regroups DNA repair mechanisms during which damaged DNA are repaired using the information of an undamaged DNA template from the sister chromatid or homologous chromosome. Here the HDBSR is detailed (Dueva & Iliakis, 2013)

During this master thesis, the different experiments studying HR focused on the RAD51 protein in irradiated *A. vaga* individuals. Therefore, when discussing HR we will only consider the SDSA and HDSBR pathways. Unlike SDSA and HDSBR, the BIR and SSA pathway do not use the RAD51 protein as it does not require an ssDNA homologous sequences invading step. Furthermore, the BIR mechanism repairs mostly single-ended DSBs. This kind of DNA DSBs are not likely to occur during ionizing radiation as they take place when restarting collapsed replication forks and in recombination-dependent telomere lengthening maintaining the chromosome ends in telomerase-deficient cells (Sebesta & Krejci, 2016).

Non-homologous recombination

NHEJ is a process that, unlike HR, does not require a homologous template for the repair. It is an error-prone mechanism leading to mutations or insertions/deletions (indels) at the repair site. Furthermore, even though HR is the predominant DNA repair mechanisms is certain organisms, like *Saccharomyces cerevisiae,* NHEJ seems to be the main DNA DSB repair mechanism present in eukaryotes (Burma *et al.*, 2006).

NHEJ consists of pieces of broken DNA processed and reassembled (the mechanism is illustrated in the figure 11A). It starts with the recognition of the DNA DSB by the DNA-end binding Ku (Ku70 – Ku80) protein complex. The Ku heterodimer binds to the DNA breaks creating a complex that will recruit and stabilize DNA-dependent protein kinases (DNA-PKcs). DNA-PKcs is a serine/threonine kinase activated by phosphorylation that interacts with the DNA end-processing proteins to trim and bridge the DNA ends. DNA-PKcs also signal the presence of a break, move the two DNA breaks closer and recruits DNA-end processing and ligation proteins. DNA-end processing is done by several enzymes, including Artemis. It is a mechanism that can be quite important for IR-induced DSBs as they possess end-blocking groups preventing ligation steps (Lieber, 2010). Once the ends are processed, the complex DNA ligase IV – XRCC4 is recruited for the rejoining step. This complex seems essential in the NHEJ repair mechanism and is present in every eukaryote. In this complex, XRCC4 stabilizes and stimulates the ligase IV activity. Finally, XRCC4 being a crucial protein in the NHEJ mechanism, it will be used during the experiment focusing on the NHEJ (Burma *et al.*, 2006; Lieber, 2010; T. E. Wilson, 2008).

OBJECTIVES

During this master thesis, the main goal was to participate in the research field of resistance to extreme stresses by studying the stress resistance of *Adineta vaga*. Upon ionizing radiation, many damages occur in organisms. Numerous damages impact the DNA, DSBs being the most harmful ones. However, *A. vaga* has the ability to repair these damages and keep on living and reproducing. Therefore main questions can be assessed: is their survival linked to their DNA DSBs repair mechanism(s)? Which DNA DSBs repair mechanism(s) does *A. vaga* use?

In order to start uncovering the secret behind these DNA DSBs repair pathways, we will focus our research on XRCC4 and RAD51, proteins implicated in the NHEJ and HR pathways, respectively. By focusing on XRCC4 and RAD51, three questions will be assessed:

- **Do high doses of ionizing radiations impact the gene and/ or the protein expression profile of XRCC4 and RAD51?**

Modification of gene and protein expression profile of Xrcc4 and Rad51 upon ionizing radiations could give us some lead concerning the potential repair mechanisms occurring.

- **Is the localization of XRCC4 and RAD51 impacted by ionizing radiation and is it cell-dependent (somatic cells or oocytes)?**

It has been shown in multiples experiments that upon ionizing radiation DNA DSBs proteins tend to localize in the nucleus where they actively repair the DNA. Therefore, using antibodies the objective is to see if there is a localization of XRCC4 and/ or RAD51 in bdelloid rotifers nucleus upon ionizing radiation, when DSBs are formed.

Furthermore, *A. vaga* is an eutelic organisms possessing somatic cells in a G0/GI state and oocytes in a G2/S phase. Therefore, it would be interesting to see: (i) if Xrcc4 is mainly present in somatic cells that do not possess a sister chromatid since they are in a G0/G1 cell, (ii) if RAD51 is mainly present in foci into oocytes, letting us think that HR might be occurring.

- **How would bdelloid rotifers reparation mechanisms behave upon deletion of XRCC4 or RAD51 implicated in the DNA DSB repair pathways?**

Creating knock out (KO) organisms would give information concerning the importance of the protein on animal survival and if it is used by the organisms. If Xrcc4 or Rad51 are inactivated and DNA repair is not visible anymore, it would be possible to say that those proteins play a role in the DNA DSB repair mechanisms and speculate that NHEJ or HR are occurring.

MATERIALS AND METHODS

Bdelloid rotifer species: growth conditions

The bdelloid rotifers used are isogenic *Adineta vaga* cloned from a single individual from the Meselson's Laboratory. Rotifers were grown in 150 x 20mm Petri dishes filled with natural mineral water (Spa®), kept in a 25°C incubator, and fed three times a week with salad extract crushed, sterilized by autoclaving in natural mineral water (Spa®).

To work on the different experiments such as Western Blot (WB), Reverse Transcription quantitative Polymerase Chain Reaction (RT-qPCR), Pulse Field Gel Electophoresis (PFGE) and Immunofluorescence (IF) the rotifers needed to be starved in order to reduce all bacteria present both in the medium and constituting their microbiome. The bdelloid rotifers were collected, counted and treated with 1:100 of Penicillin-Streptomycin (10,000U/mL) Gibco™ added to their Spa® water to eliminate most remaining bacteria. After incubation at 25°C overnight with the antibiotics, the rotifers were ready to be manipulated.

Differential mRNA analysis with Reverse Transcription and quantitative Polymerase Chain Reaction

RNA extraction – Around a hundred thousand starved *A. vaga* individuals were centrifugated 10 min at 4°C, at 4,000rpm before snap freezing the pellet by immersing it in liquid nitrogen. The pellet was kept on ice for 10 min to thaw. Under a chemical hood 1mL of TRIzol® Reagent (Invitrogen) was added and left to incubate for 5 min at room temperature. After adding 200µL of chloroform, the tube had to be vigorously shaken for 15 sec and then incubated for 15min at room temperature. After the incubation, the mixture was centrifugated for 15 min at 4°C, at 10,630rpm, creating a separation of phases. Then, on ice, 450µL of the upper aqueous phase was transferred to a fresh 1.5mL DNA LoBind Eppendorf in which 450µL of isopropanol were also added. The mixture was vortexed for 15sec before incubating at room temperature for 10min. After a centrifugation of 10min at 4°C at 10,630rpm, the supernatant was discarded and 1mL of ice-cold 95% ethanol was added. After another centrifugation of 10min at 4°C at 10,630rpm, the supernatant was discarded and 1mL of ice-cold 75% ethanol was added. After a final 10min at 4°C at 10,630rpm centrifugation, the ethanol had to be completely removed and the pellet air dried for 15 min. The pellet was finally resuspended in 20µL of nuclease free water and incubated for 30 min on ice before measuring the Optical Density (OD) using a nanodrop. The extracted RNA can be stored at -80°C.

Before the generation of cDNA through Reverse Transcription (RT), all DNA pieces possibly present after the RNA extraction had to be digested. In a PCR tube, 8µL of the extracted RNA (40ng/µL) was incubated on ice for 15 to 30min. Afterwards, 1µL of 10X buffer of DNase I (Invitrogen) and 1µL of DNase I (Invitrogen) were added in the sample and the mixture was kept for 1h at 37°C. After the incubation, 5µL of 25mM EDTA (Invitrogen) were added and the sample incubated for 10min at 65°C. The digested sample was kept at -80°C until reverse transcription and quantitative Polymerase Chain Reaction.

A.
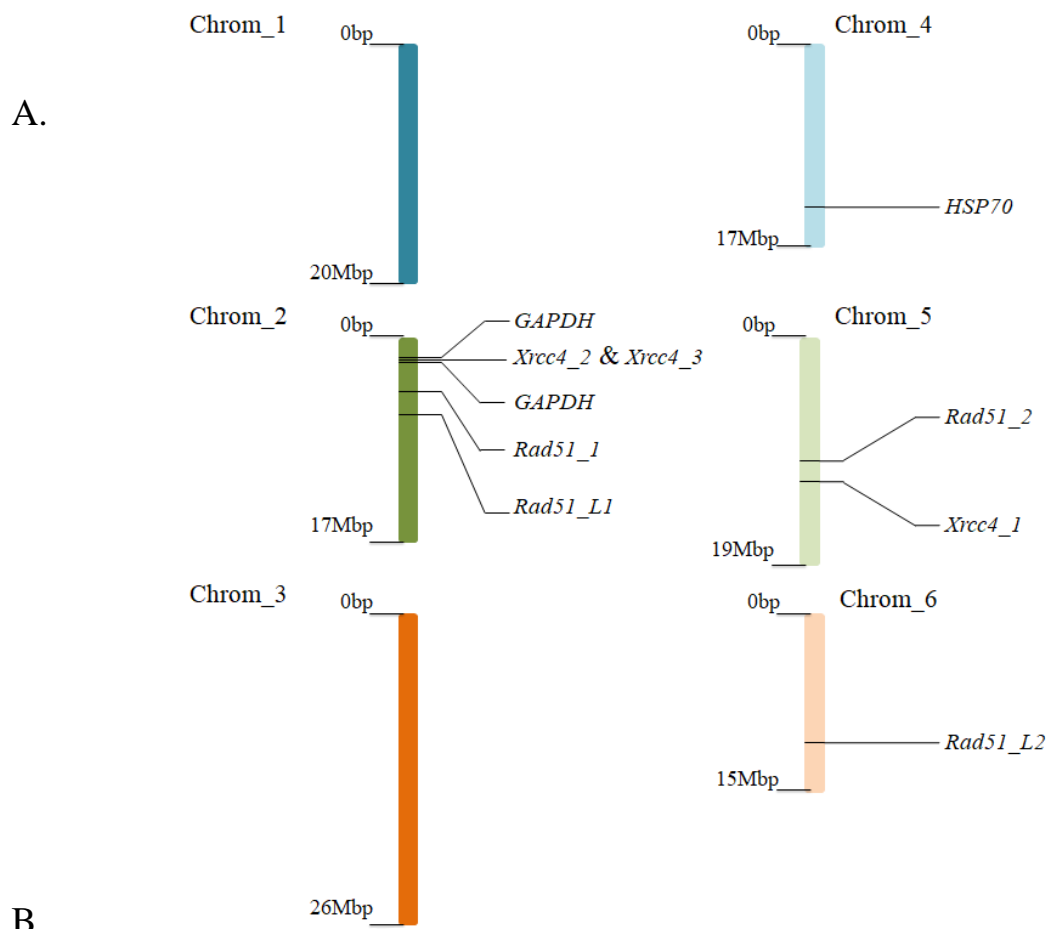
B.

Gene	Chromosome	Query alignment	% similarity	Localization on the genome	Bit-score range
GAPDH	Chrom_2	1 - 1020	99.210	1650302 - 1651713	69.4 - 566
	Chrom_2	375 - 758	92.003	1837586 - 1838076	87.9 - 246
HSP70	Chrom_4	1 - 1780	97.879	13617724 - 13619867	82.4 - 1332
Rad51_1	Chrom_2	1 - 1104	99.745	4444854 - 4446292	246 - 566
Rad51_2	Chrom_5	1 - 1101	98.968	10243964 - 10242600	215 - 551
Rad51_L1	Chrom_2	1 - 1110	97.626	6527866 - 6529092	590 - 713
Rad51_2	Chrom_6	1 - 875	97.626	10600880 - 10602049	132 - 760
Xrcc4_1	Chrom_5	1 - 1065	99.470	12159759 - 12156468	97.1 - 303
Xrcc4_2	Chrom_2	1 - 402	98.438	1765452 - 1762119	106 - 246
Xrcc4_3	Chrom_2	1 - 330	99.583	1761560 - 1765953	99 - 237

Figure 12 – *Xrcc4, Rad51, GAPDH* and *HSP70* localization on *Adineta vaga* genome

(A) Estimation of the localization of the genes of interest on *A. vaga's* 6 assembled homologous chromosomes: chromosome 1 is homeologous to chromosome 4, chromosome 2 is homeologous to chromosome 5 and chromosome 3 homeologous to chromosome 6. The housekeeping *GAPDH* gene can be found twice on chromosome 2 (a complete and a partial version of the gene) while the *HSP70* housekeeping gene is present on chromosome 4. The complete version of the *Xrcc4* gene (*Xrcc4_1*) can be found on chromosome 5 while partial Xrcc4 genes (*Xrcc4_2* & *Xrcc4_3*) are present on chromosome 2. One gene of *Rad51* is present on chromosome 2 (*Rad51_1*) while the other gene (*Rad51_2*) is present on chromosome 5. Finally, *Rad51_L1* is present on chromosome 2 while the *Rad51_L2* seems to be on chromosome 6. (B) The values present in this table were obtained after by blasting the genes sequences on the chromosome-scale haploid genome assembly of *A. vaga* (Narayan *et al*., in prep.). The "localization of the genome column" served as a base of the graphical representation. The bit-score range represents the similarity of the different query alignments. The higher the Bit-score values go, the better is the similarity.

Reverse transcription - The cDNA synthesis was realised with the SuperScript III First-Strand Synthesis System for RT-qPCR from Invitrogen. In a tube were mixed 5μL of DNase-treated RNA (40ng/ μL), 1μL of oligo dT20 primer, 1μL of random hexamer primers, 1μL of 10mM dNTP mix and 2μL of RNase-free water. The mixture was incubated for 5 min at 65°C and then on ice for at least 1min. To the reaction mix were added 2μL of RT buffer, 4μL of 25mM MgCl2, 1μL of RNaseOUT (40U/μL) and 1μL of SuperScript III RT (200U/μL). The reaction was incubated 10min at 25°C for the primer annealing, 50min at 50°C for the cDNA synthesis and 5min at 85°C for the heat inactivation of the reverse transcriptase. After adding 1μL of RNase H the reaction was incubated at 37°C for 20min in order to get rid of any RNA left. Finally, 179μL of nuclease-free water was added to reach a final volume of 200μL. A negative control was made by mixing 5μL of the same DNase-treated RNA (40ng/ μL) with 195μl of nuclease free water (Invitrogen). The samples were then analysed using the nanodrop in order verify the cDNA synthesis, it was then either directly used for a qPCR analysis or stored at -80°C for further use.

qPCR analysis – The qPCR was performed on 8 different targets. The glyceraldehyde-3-phosphate dehydrogenase (*GAPDH*) and the Heat Shock Protein 70 (*HSP70*) were chosen as housekeeping genes as they both are constitutively produced by organisms and often used as housekeeping genes in qPCR (Kozera & Rapacz, 2013). Furthermore, *GAPDH* and *HSP70* were chosen as housekeeping genes since several mass spectrometry analysis previously performed showed that those two genes are highly expressed in *A. vaga*.

As explained in the introduction, bdelloid rotifers are organisms that are degenerate tetraploids with 6 homologous chromosomes. Therefore, they can possess multiple copies of a gene responsible for the production of a protein. In the case of our proteins of interest XRCC4 and RAD51, both proteins can be produced by different genes present throughout the genome. In the case of *Xrcc4*, a complete copy of the gene is present on one chromosome of *A*. vaga (Chromosome 2, Figure 12A) and partial genes are found on his homeologous chromosome 5 (*Xrcc4_2* and *Xrcc4_3*, Figure 12A). These partial genes are separated by 2kbp, it could be speculated that they used to be one complete gene suffering from the insertion of a genetic sequences (sequences alignment illustrated in the figure 13). For Rad51, 2 genes were found throughout the genome. The first one, *Rad51_1*, is located on chromosome 2 and the other one, *Rad51_2*, on chromosome 5 (Figure 12A). Furthermore, two *Rad51-like* genes (*Rad51_L1* and *Rad51_L2*) were also found in the genome, on chromosomes 2 and 6 respectively. *Rad51_L1* and *Rad51_L2* are Rad51 paralogs, those proteins are in the Rad51 protein family. All the members of the *Rad51* protein family, including *Rad51_L1* and *Rad51_L2* are evolutionarily conserved proteins essential for DNA repair by homologous recombination. *Rad51_L1* and *Rad51_L2* form an heterodimer and seems to promote the assembly of the presynaptic *Rad51* nucleoprotein filament (GeneCards, 2016; Renglin Lindh *et al*., 2007).

For those different genes of interest, primers were designed using eprimer3 to generate amplicons varying between 198 to 218bp. Performance of the qPCR assay and primers efficiency were verified by performing calibration curves using tenfold serial dilutions and assessing the PCR efficiency.

```
            1        10        20        30        40        50        60        70        80        90       100       110       120       130
            |--------+---------+---------+---------+---------+---------+---------+---------+---------+---------+---------+---------+---------|
Xrcc4_1     AATAAAACTGAAACAGATGGACGAAGTTATGTATTTAATTGCAAAAAACTTGACAAAAATCGATTGGAATTTGTTTGGAAAGAGAAAATTGAAGCATTGAATTCATTGAAAATTATTGGTAATGTCGAAC
Xrcc4_2
Xrcc4_3
Consensus   ....................................................................................................................................

            131      140       150       160       170       180       190       200       210       220       230       240       250       260
            |--------+---------+---------+---------+---------+---------+---------+---------+---------+---------+---------+---------+---------|
Xrcc4_1     TTGAAGAACGACCTAATGATGAAGTTTTATCGAAGATGATGGACTATACCATCGATGAAATGGACATGTTACGAGCAGCAAATGAACAAAAATTAGTCGAAATCAAATGTACCAATGAACAATTACATAA
Xrcc4_2                                               GATCATTCCATTGAGGAAATGGAAACATTACGATCAGCAAATGAACAAAAAATCTTTGATATTCAACGTATTAATGGACAATTAAATAA
Xrcc4_3
Consensus   .......................................ga...at.ccat.ga.gaaatgga.a..ttacga.cagcaaatgaacaaaaa.t..t.ga.at..aa.gta..aatg.acaatta.ataa

            261      270       280       290       300       310       320       330       340       350       360       370       380       390
            |--------+---------+---------+---------+---------+---------+---------+---------+---------+---------+---------+---------+---------|
Xrcc4_1     AGCTTTAGAAACTGTTAAACGAACAGTTGATATGAAAGAACAACTTGAAACTGATCTATATAGAAAGTTTGTTCTTGTGTTAAATACAAAAAAAAGCAGAATTAGCAAAACTTAAACAACAGATTGAATCT
Xrcc4_2     AGCACTTGAAACAGTCAAACAAACTGTTGACATAAAAGAAAAACTTGAAGCTGATTTATATCGAAAGA-----CATATTTATAA
Xrcc4_3
Consensus   agc..t.gaaac.gt..aaac.aac.gttga.at.aaagaa.aacttgaa.ctgat.tatat.gaaag......c.t.t.t..aa.................................................

            391      400       410       420       430       440       450       460       470       480       490       500       510       520
            |--------+---------+---------+---------+---------+---------+---------+---------+---------+---------+---------+---------+---------|
Xrcc4_1     TATCGTTATGACCATCCGACTACAACCAGAGATGAAGAATCTTATGTAGATTCTCATCCTCGTAGTGTTTCACCAATGGATTCAACATTCAATGAGAGCGAATCTCAAACAAATAAACGACGTCGACATC
Xrcc4_2
Xrcc4_3
Consensus   ....................................................................................................................................

            521      530       540       550       560       570       580       590       600       610       620       630       640       650
            |--------+---------+---------+---------+---------+---------+---------+---------+---------+---------+---------+---------+---------|
Xrcc4_1     AATCGAATGGTACAAGTACAAGTGAAGACGACGATATTCAAGAAATTCAATTGACAAAACCAACAAAATCAAAAACAATGAACAATAGACAAGATAGTTCACTTGATTTAGGTAATGATCAAATGGATTA
Xrcc4_2
Xrcc4_3
Consensus   ....................................................................................................................................

            651      660       670       680       690       700       710       720       730       740       750       760       770       780
            |--------+---------+---------+---------+---------+---------+---------+---------+---------+---------+---------+---------+---------|
Xrcc4_1     TAAAACATCGACGATCGATAAACATCATCAACGACGAAAATTCGTTACCGCAACCAATACAATATCAAAACGTCCATTTGTTAATCATACGGCTACTTCTTCATCAATGACAGTACCTTCATTACCTGAT
Xrcc4_2
Xrcc4_3                                                                                                   GGTGCTGGTATTCCGCCAATATTAGCAACACCGTCATTACCGGAA
Consensus   .............................................................................................t.c.g.ta.t.c..ca..a.t..ca..acc.tcattacc.ga.

            781      790       800       810       819
            |--------+---------+---------+---------+---|
Xrcc4_1     GATTCTCAAACAACCGATGATTTATTGAATAAAATATAA
Xrcc4_2
Xrcc4_3     GAATCTCAAACAACTGATGATTTATTAGATAAAATCTAA
Consensus   ga.tctcaaacaac.gatgatttatt..ataaaat.taa
```

Figure 13 – *Adineta vaga Xrcc4* gene sequences alignement

Alignment of *Xrcc4* genes sequences. The low consensus values (in blue) correspond to around ≤50% of sequences similarity to the complete gene sequence. These sequences alignment was realised using the MultAlin website (Corpet, 1988). More precisely, the mean similarity of the partial sequences to the complete *Xrcc4*_1 is 30% and 25% for *Xrcc4_2* and *Xrcc4_3* respectively. The mean similarity of the partial sequences to their corresponding region on *Xrcc4*_1 corresponds to *76%* for each (for *Xrcc4_2* and *Xrcc4_3*). This homology measurement was measured using NCBI BLAST global alignment.

Table 1 – List of primers used in our qPCR analysis

Genes	Primers Forward	Primers Reverse	Chromosome
GAPDH	TGTGCTGCAATCAAAGAAGC	CGACACGGTTTGAATAACCA	Chrom. 2
HSP70	TGTACAGCAGCACCATAGGC	CAACACTTGAGCCTGTCGAA	Chrom. 4
Xrcc4_1	CGAGCAGCAAATGAACAAAA	TCTGGTTGTAGTCGGATGGTC	Chrom. 2
Xrcc4_2	ACCGGAACAACAGGACACAT	AGGTCGTTCTTGAAGTTCAGC	Chrom. 5
Rad51_1	AGGCACATTTCGACCTGAAC	CCACGGCCAGAATAATCAGT	Chrom. 2
Rad51_2	GAATATCGTTGCGGCAAATC	AAGCACGTGCATAGGCAATA	Chrom. 5
Rad51_L1	TCAGTGAATGTTCGTCTTGC	CCGCTTGAATTAAACGTGGT	Chrom. 2
Rad51_L2	GGTGGTATTCGTTTGGGTGT	GATTCTCAGCTGCCATAGCC	Chrom. 6

The standard curves showed an R^2 of 0.967 or more with an efficiency varying between 84 and 135% (Details annex A.A.). The different primers used are listed in table 1. Additionally, the negative control exhibited either no amplification curve or really late amplifications.

The qPCR was realised with the SsoAdvanced Universal SYBR® Green Supermix from Bio-Rad. For one sample a mix was made with: Supermix 1X, 0.25µM of forward primers, 0.25µM of reverse primer and nuclease-free water to reach 15µL. In a 96 wells qPCR plate the 15µL mixture was loaded and 5µL of cDNA were added, containing around 4ng of cDNA. After making samples for the different conditions and loading the qPCR plate, the plate was sealed with a transparent plastic film. The plate was centrifugated at 2500rpm to ensure that the samples were at the bottom of the wells. Finally, the plate was loaded in a StepOne Plus qPCR machine. The running program of the machine is described in table 2.

The detection of the qPCR amplicons is based on the use of a non-specific fluorescent dye (e.g. SYBR GREEN) that intercalate in dsDNA. The amplification of the cDNA, and therefore its quantification, depends on the quantity of cDNA present in the sample.

The qPCR results were analysed using the $2^{-\Delta\Delta CT}$ method, a way to measure relative gene expression levels between samples (Rao *et al*., 2013). The $2^{-\Delta\Delta CT}$ method assumes that the efficiency of the amplification is 100%. However, in our case, the efficiency of our primers was measured and therefore will be used for our calculation. Furthermore, statistical analyses were applied on our qPCR analyses. In this case, a two tailed Student's t-test was used after verification of the variance homogeneity using a Hartley test.

Table 2 – qPCR settings

Run stages	Cycle Step	Temperature	Time	Cycle
Holding stage	Initial denaturation	95°C	30sec	1
Cycling stage	Denaturation	95°C	15sec	40
	Extension	60°C	60sec (+ plate read)	
Melt Curve Stage	Melt Curve	95°C	15sec	1
		60°C	60sec	
		95°C	15sec	

RT-qPCR sequences verification by cloning and sequencing

Following the amplification of the cDNA through qPCR, the specificity of the amplification was verified to ensure that the sequences analysed with the RT-qPCR were the sequences of interest. Therefore the qPCR products were cloned into a PCR cloning vector, transformed into *Escherichia coli,* and clones were chosen, underwent plasmid purifications and were analysed by DNA sequencing.

DNA purification – The DNA purification was realised with the Monarch® PCR & DNA clean-up kit (BioLabs). The first step of the sequence analysis was the purification of the PCR amplicons present in the qPCR samples. The 20μL of samples were recovered and diluted with milliQ water to reach a total volume of 50μL. Binding buffer was added, its volume being 5 times the volume of the sample, before performing a 1 min 13,000rpm centrifugation. The column was then washed 2 times with 200μL of wash buffer and 1 min 13,000rpm centrifugation before going through a 2 min 13,000rpm centrifugation with an empty tube to get rid of any ethanol that could be left after the washes. Before recovering the DNA present on the column, the washed column was loaded on a 1.5mL DNA LoBind tubes (Eppendorf). Finally, 20μL of elution buffer were added on the column, a centrifugation of 13,000rpm during 1 min allowed the elution of the DNA from the column to the Eppendorf. The DNA content present in the Eppendorf was finally measured using the nanodrop.

Amplicon ligation within a plasmid – The cloning made by the ligation of the amplicon in a plasmid and the transformation of bacteria was done using the NEB® PCR Cloning Kit.

For the ligation 1μl Linearized pMiniT 2.0 Vector (25ng/μL), 1μL of purified DNA (concentration between 30 and 50ng/μL) and milliQ water were added to reach a total volume of 5μL. In another tube was prepared a mixture of 4μL of Cloning Mix 1 and 1μL of Cloning Mix 2. Both were reassembled in one tube and incubated for 15min at 25°C and 2min on ice. The ligation mixture was then stored at -20°C.

Bacteria transformation - For the transformation, NEB 10-beta competent *E. coli*, stored at -80°C, were used. After thawing on ice, 50μL of the competent bacteria and 2μL of the ligation mixture were mixed. After 20min of incubation on ice, the tube incubated for 30sec at 42°C, creating a heating shock for the bacteria, and finally for 5min on ice. Afterwards, 950μL of NEB® 10-beta/Stable Outgrowth Medium were added and the mixture incubated for 1h at 37°C at 250rpm. Finally, 50μL of transformed bacteria were spread out on a petri dish filled with a medium of autoclaved LB-agar (35g/L) containing ampicillin at a concentration of 100μg/mL. If needed, a 10X dilution can be made in order to obtain isolated colonies on the petri dishes. After growing over night at 37°C colonies were visible. Isolated colonies were chosen and resuspended in 5mL liquid LB Broth Base Ultrapure (20g/L) with a concentration of ampicillin at 200μG/mL. Finally, the tubes incubated overnight at 37°C at 250rpm.

Plasmid purification - In order to purify the plasmids from the bacteria, purifications were made with the QIAprep® Miniprep from Qiagen.

Bacteria were pelleted by centrifugating the 15mL tubes at 4000rpm during 10 min and transferred in a 1.5mL Eppendorf before being centrifugated for 3min at 13 000rpm. The pellet was resuspended in 250μL of resuspension buffer and 250μL of NaOH/SDS lysate buffer were added in the tube before being mixed by inversion 5 to 6 times.

Once every tube had been filled with lysate buffer, the tubes had to be filled with 350μL of neutralization buffer and were also mixed by inversion. The tubes were centrifugated at 13,000rpm for 10min and 800μL of supernatant were loaded on a column. After 1min of centrifugation at 13,000rpm the collecting tubes were emptied and 750μL of wash buffer containing ethanol were added. The columns were centrifuged two times for 1min at 13,000rpm, once filled and once emptied, to ensure that no buffer was left. The dry columns were placed in a 1.5mL LoBind Eppendorf tubes, 50μL of elution buffer were loaded on the columns. The columns incubated for 1min at room temperature before being centrifuged for 1min at 13,000rpm. The DNA concentration was then determined using a nanodrop.

Insert size verification - In order to check if the insert of the bacteria corresponded to the qPCR amplicon, insert size was checked using PCR amplification and gel migration. PCR were performed using the GoTaq® Green Master Mix from Promega. The samples were made with the mixture described in table 3. The plate can be kept at 4°C until performing the PCR (settings in table 4).

Table 3 - PCR mixture

PCR mixture	
Reagent	**Final concentration**
5X Green GoTaq® Reaction Buffer	1X
dNTPs	0.2mM
Cloning Forward	0.5μM
Cloning Reverse	0.5μM
GoTaq®G2 DNA Polymerase (5u/μl)	0.25μL
Plasmid	200ng
MilliQ Water	Up to 50μL

Table 4 – PCR settings

Cycle Step	Temperature	Time	Cycle
Denaturation	95°C	2min	
	95°C	30sec	
Annealing	52°C	30sec	
Extension	72°C	1min	30 cycles
	72°C	5min	
Soak	4°C	∞	

Table 5 – Composition of the CHAPS-Glycerol buffer

CHAPS-Glycerol buffer	
Reagent	**Final concentration**
Tris-HCl pH7.5	15 mM
MgCl2	5 mM
KCl	60 mM
Sucrose	0.32 M
Glycerol	10%
DTT	1 mM
PMSF	1 mM
CHAPS	1%
MQ water	Depend on final volume
Protease Inhibitor tablet	1 tablet/ 10mL

Table 6 – Composition of the RIPA buffer

RIPA buffer	
Reagent	**Final concentration**
Tris-HCl pH8.0	10 mM
NaCl	140 mM
SDS	0.1%
Deoxycholate	0.1%
Triton X-100	1%
EDTA	1 mM
PMSF	1 mM
MQ water	Depend on final volume
Protease Inhibitor tablet	1 tablet/ 10mL

Table 7 – Composition of the High Salt Buffer (HSB)

High Salt Buffer	
Reagent	**Final concentration**
Tris-HCl pH8.0	10 mM
EDTA	1 mM
DTT	5 mM
PMSF	1 mM
KCl	1 M
CHAPS	1%
MQ water	Depend on final volume
Protease Inhibitor tablet	1 tablet/ 10mL

To verify the size of the PCR product migrations were performed on 1% agarose gel. Therefore the gels were made by mixing and boiling agarose in TAE 0.5X. In the mixture 5µL of SYBRSAFE were added before casting the gel. The agarose was left to polymerize for 30 min. The gel was then placed in a migration tank filled with TAE 0,5X buffer before being loaded with 7µL of BenchTop 100bp DNA Ladder (Promega) and with 20µL of PCR samples. The migration occurred for 45 min at 69V. The gel was then imaged with a BioRad Chemidoc XRS camera.

Sequencing - Once the verification of the amplicon size, the samples are selected to be sent to the industry Genewiz for sequencing. The sequencing results were blasted against the chromosome-scale haploid genome assembly of *A. vaga* (Narayan *et al*., in prep.) to verify that the sequenced DNA fragments corresponded to the expected sequences.

Protein expression analysis using whole cell extract

Protein extraction – Starved rotifers (150,000 individuals) were washed twice with 10mL of phosphate-buffered saline (PBS) and centrifuged 10 min at 4°C, at 4,000rpm before and after each wash. The rotifers were then dounced 1,000 times with a Pestle B dounce in 300µL of lysis buffer (see composition below) followed by 15min at 4°C, at 14,000rpm centrifugation. The supernatant was collected and the concentration of the proteins was determined using a standard Pierce assay using BSA dilutions as standard curve. The collected proteins were then used for western blotting. The different buffers used in this study are described in the Tables 5 – 7.

Western blot - Samples were composed of 10µg of proteins, Lithium Dodecyl Sulfate sample Buffer containing bromophenol blue as loading dye, sample reducing agent (Invitrogen) and milliQ water. Before being loaded, the samples were heated for 5 min at 95°C allowing the denaturation of proteins. Migrations took place in Invitrogen 4-12% Bis-Tris Plus Gels in 1X MES Running Buffer (Invitrogen) during 1h15 at 120V. The ladder used was the SeeBlue™ Plus2 ladder (Invitrogen).

For the Western Blot, a polyvinylidene fluoride (PVDF) membrane was used and activated in methanol (MeOH). Transfers occurred in a transfer buffer (Invitrogen Transfer Buffer, 10% MeOH & 1:1,000 Invitrogen anti-oxidant) during 1h at 20V.

Membranes were blocked during 1h in Tris-buffered saline, 0.5% Tween 20 (TBST) and 5% of blocking agent non-fat dry milk (NFDM) at room temperature. The primary antibody was diluted in a solution of TBST and 1% blocking agent. The incubation occurring for 1h at room temperature was followed by 3 washes in TBST for 5 min. The same process was used for the secondary antibody. The concentration of the antibodies were 1:1,000 for the rabbit anti-histone H3 (Bethyl), 1:2,000 for the mouse anti-α-Tubulin (Sigma-Aldrich), 1:2500 for the guinea-pig anti-rad51 (Proteogenix), 1:2500 for the guinea-pig anti-Xrcc4 (Proteogenix) and 1:5,000 for the goat anti-mouse HRP conjugated (Invitrogen), the goat anti-rabbit HRP conjugated (Invitrogen) and the goat anti-guinea pig (Invitrogen). After the 3 washes that followed the secondary antibody, membranes were incubated for 10 minutes in a horseradish peroxidase (HRP) substrate for enhanced chemiluminescence (Thermo scientific). The western blots were finally revealed using an AI600 Imager.

The antibodies anti-α-tubulin and anti-histone H3 are respectively monoclonal and polyclonal antibodies commercially produced to target the human proteins. However the homology between the human and the *A. vaga* proteins are close enough for the antibody to work with *A. vaga* (Table 8). The degree of homology is lower between any XRCC4 and RAD51 for which a commercial antibody is available, demanding a custom production. Polyclonal antibodies directed against the proteins XRCC4 and RAD51 were produced by the Proteogenix firm. They injected guinea pigs with synthetic proteins purified in *Escherichia coli* from given bdelloid rotifers sequences extracted from the genome of *Adineta vaga*.

WB was performed using biological replicates and technical replicates. The biological replicates consist of WB made with proteins extract realised with different batches of irradiated rotifers. The technical replicates consist of WB realised with the same protein extracts but loaded several times on different gels.

The quantification of the WB is made using the AI600 imager machinery that calculate the intensity of the bands.

Table 8 - **Homology between *Adineta vaga* and *Homo sapiens* protein and gene sequences**

Analysis	*Adineta vaga*	*Homo sapiens*	Query cover	E value	% of similarity
BlastP	>AFR46097.1 **α-tubulin**, partial	**Tubulin**	100%	0.0	97,16%
BlastP	>ACF75493.1 **Histone H3**	**Histone H3.1**	100%	1e-94	97.06%
BlastN	**Xrcc4_1** sequence	/	/	/	/
BlastN	**Rad51_1** sequence	**RAD51** recombinase, mRNA	70%	1e-79	68.83%
BlastN	**Rad51_2** sequence	**RAD51** recombinase, mRNA	73%	3e-93	69.89%

Coomassie blue and silver staining – Coomassie and silver staining enable the visualisation of proteins migration profiles. For the Coomassie blue staining the proteins separated on acrylamide gel were treated with the following solutions: a fixation solution (50% MeOH & 10% glacial acetic acid) for 1h, a Coomassie blue staining solution (50% MeOH, 10% glacial acetic acid & 0,1% Coomassie Brilliant Blue) for 30 min and a destaining solution (40% MeOH & 10% glacial acetic acid) for 3 x 15 min.

The Silver staining of the proteins were performed using SilverQuest™ Silver Staining Kit from Invitrogen.
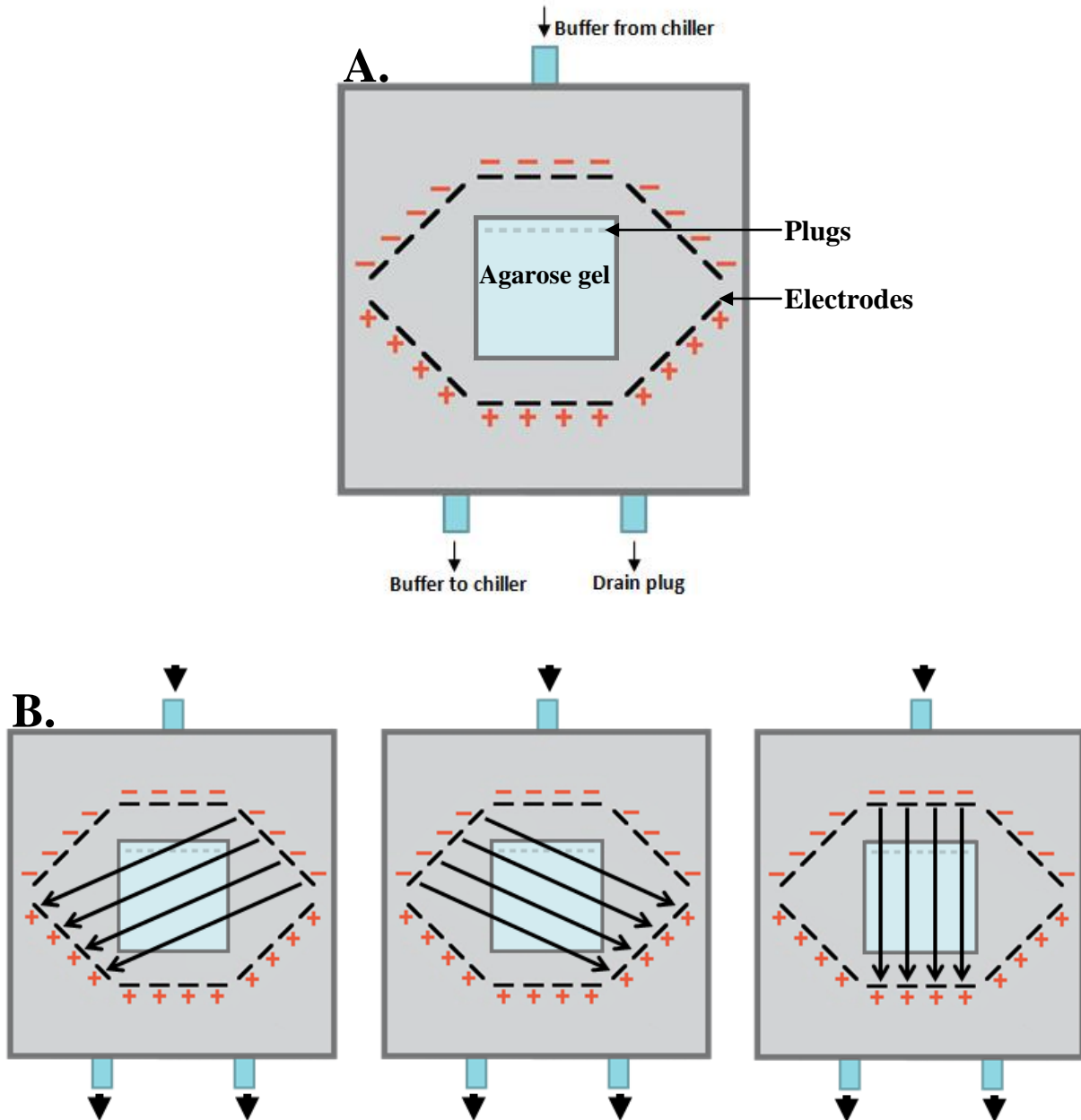
Figure 14 – Illustration of a PFGE and its operation

(A) An agarose gel with plugs at the top is placed at the centre of the machine surrounded by positive and negative electrodes. Buffer that has been cooled to 14°C is circulating. The drain plug is used when the machine is washed after the run to get rid of the buffer left in the machine. (B) On top of the agarose gel the plugs contain digested *Adineta vaga* "freeing" their DNA. Due to the positions of the positive and negative electrodes in the PFGE, large fragments of DNA can be resolved. The angle of the electric current switches every few minutes (depending on the operating parameters). The permanent change of the current angle allows migration and separation of large DNA fragments by moving them from side to side.

DNA repair kinetics analysis with Pulse Field Gel Electrophoresis after irradiation

Irradiation - Starved *A. vaga* individuals in Spa® water were transported to the X-RAD 225 (Precision) in the LARN laboratories. The samples were kept on ice or on an ice tray to avoid heating of the samples during the irradiation. The non-irradiated control is kept on ice for the time of the irradiation. After pre-heating the machine and measuring the irradiation (in Gy/min), bdelloid rotifers (~150,000 individuals/ condition) were placed in the middle of the machine on the ice tray and were irradiated at 800Gy (X-rays). The machine parameters were: 225kV, 19mA, filter 1, SSD 30/3.0.

Pulse Field Gel Electrophoresis - A thousand *A. vaga* individuals were washed two times at 14,680rpm for 3min in 1mL of solution A (50mM EDTA, 10mM Tris HCl pH 8.0) and resuspended with 30μL of solution A. Then, 2% agarose was heated to 95°C and kept at 56°C, 30μL of 56°C agarose was added to the suspended rotifers to reach a final concentration of 1% agarose. The mix went into a PFGE plug mold.

After hardening at 4°C the plugs were placed in 500μL of digestion solution (200mM of EDTA, 100mM of Tris HCl pH 8.0, 1mg/mL Proteinase K (ThermoFisher Scientific) and 1% Lauroylsarcosine sodium salt solution (Sigma)) and incubated for 18h at 56°C. The plugs were then washed two times in solution A and two times in TAE 1X. The plugs were loaded in a 1% agarose gel and as a ladder *Saccharomyces cerevisiae* chromosomal DNA (BioRad) was used.

The BioRad Chef Mapper™ was filled with 3L of TAE 1X, cooled to 14°C, the gel was placed in the centre and the electrophoresis started. The machine parameters were: Voltage 5.5V/cm, run 24h, angle of 120°, initial switch time 60s, final switch time 180s and Coefficient linear. After the run, the PFGE gel was labelled in a SYBR Gold (Invitrogen) and TAE 1X solution for 20min. The gel was then scanned with a BioRad Chemidoc XRS camera. The machine operation is explained in the figure 14 A & B.

Differential protein expression analysis by immunofluorescence

Immunofluorescence - In order to see the impact of irradiation on the localization and behaviour of proteins, immunofluorescence was performed. Bdelloid rotifers possess a thick cuticle, in order for the antibodies to reach their target proteins, rotifers needed to be permeabilized. Around 500 rotifers were placed on a Super frost Plus™ slides (ThermoFisher Scientific) and squashed by pressing down a cover slip on the rotifers. They were then submitted to freeze crack. Freeze cracking is performed by immersing the slide with rotifers squeezed under a coverslip in liquid nitrogen and cracking the coverslip open with a scalpel blade as illustrated in figure 15. Proteins were then fixed by cross-linking them with 1% of formaldehyde for 10min. The rotifers were then washed 3 times with PBS and blocked with a solution of 3% BSA, 0,3% Triton X-100 and PBS. After one hour of blocking, the primary antibody was added on the slide at a concentration of 1:150. Slides were incubated overnight in a humid chamber at 4°C. After the incubation, they were washed 3 times with PBS for 5 min. The secondary antibody, diluted in the blocking solution, is added on the slide at a concentration of 1:150 and incubated for 1h at room temperature in a dark chamber. The slides were then washed 3 times with PBS for 5min.
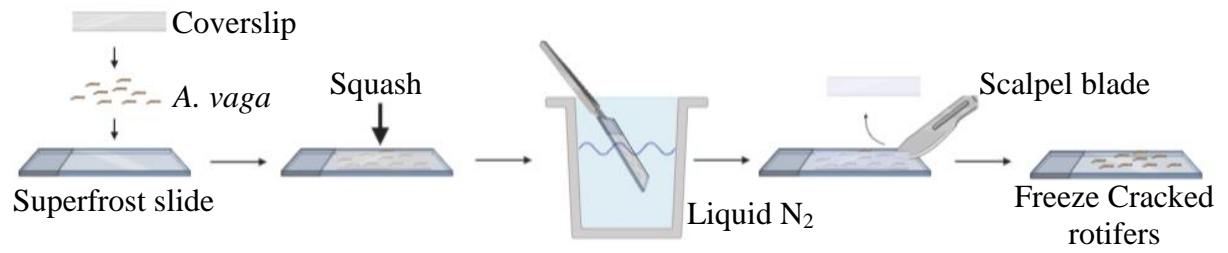
Figure 15 – Illustration of a Freeze crack

A few hundred rotifers are placed on a Superfrost slide and squashed by pressing down a coverslip. The squashed rotifers are immersed in liquid nitrogen. The coverslip is removed with the help of a scalpel blade, cracking open the rotifers.

Slides mounting - The slides were either mounted with SlowFade™ Diamond Antifade Mountant (Invitrogen) containing DAPI or with DAPI incubation and mowiol adhesive mounting medium. The DAPI binds to adenine–thymine regions in DNA fluorescently staining the DNA and therefore allowing a localization of the nuclei.

When mounting a slide with SlowFade, a drop of the product was placed on a coverslip and the slide was placed on the drop. Pressure was applied on the slide and the coverslip to ensure a good repartition of the product and to get rid of bubbles that could be encaptured within the SlowFade. Finally, the slide was sealed with the help of transparent nail polish and stored at 4°C until visualisation with a microscope.

When mounting a slide with mowiol, the slide has to be washed two times 5min with PBS before and afterwards 20min of incubation in 1:1000 DAPI (diluted in PBS). Mowiol was warmed up to 60°C and applied on a coverslip before being put on the slide. Pressure was applied on the slide and the coverslip to ensure a good repartition of the product and to get rid of bubbles that could be left within the mowiol.

The slide was stored at 4°C for a good solidification of the mowiol. The slide was finally observed with a microscope (Settings in table 9).

Table 9 – Microscope settings

Microscope	Camera
Confocal Leica TCS SP5	
Wide field Zeiss Axioimager Z.1	Hamamatsu ORCA-flash4.0
Wide field Olympus fluorescent microscope	Hamamatsu ORCA-flash4.0

Antibodies - The different antibodies used were mouse anti-α-Tubulin (Sigma-Aldrich), rabbit anti-Histone H3 (Bethyl), guinea pig anti-Xrcc4 (Proteogenix), guinea pig anti-Rad51 (Proteogenix), goat anti-guinea pig alexa fluor 488 (Bethyl), goat anti-mouse alexa fluor 569 (Invitrogen) and goat anti-rabbit alexa fluor 488 (Invitrogen).

First step to protein inactivation

Neomycin sensitivity assay - Rotifers were isolated in 96-well cell culture plate U-bottom, to test the lethal concentration of neomycin (G-418 Sigma-Aldrich). The concentrations were tested from 0 to 2500µg/mL. Every day for 7 days, the survival rate of the rotifers was measured.

RESULTS AND DISCUSSIONS

Bdelloid rotifers are organisms that possess an ability to resist extreme stresses. One of those stresses is ionizing radiation (IR) creating lots of damages to living systems. Considered as the most lethal, DNA DSB damages also occur in bdelloid rotifers after exposure to IR. But bdelloid rotifers can repair the DNA DSBs, suggesting that bdelloid rotifers possess efficient DNA repair mechanisms or at least the repair proteins are still active after exposure to IR. The research on DNA repair mechanisms within this Master thesis started by looking at the gene expression of genes implicated in the most important DNA DSB repair mechanisms, HR and NHEJ.

1. Analysis of the differential expression of *Xrcc4* and *Rad51* genes upon ionizing radiation using a transcriptomic approach

RT-qPCR is a method commonly used for gene expression analysis due to its accuracy, sensitivity and speed. Using probes designed against our genes of interest, RT-qPCR analysis has been used to discover the impact of ionizing radiation on bdelloid rotifer gene expression.

When exposed to ionizing radiation, bdelloid rotifers suffer from numerous stresses. The radiations can create damages but also initiate signals responsible for immediate transcriptional response impacting DNA repair and cell signalling (Snyder & Morgan, 2004). Previous work suggested that the expression of genes involved in DNA DSB repair could vary after irradiation. Therefore, we choose to look upon the gene expression of the proteins XRCC4 and RAD51, two essential actors implicated in DNA DSB repair, respectively NHEJ and HR, at different time-points after an 800Gy X-ray irradiation of hydrated A. vaga individuals. Furthermore a PFGE experiment was realised using the same bdelloid rotifers illustrating the impact of ionizing radiation on *A. vaga* DNA integrity upon ionizing radiation (Annex A B).
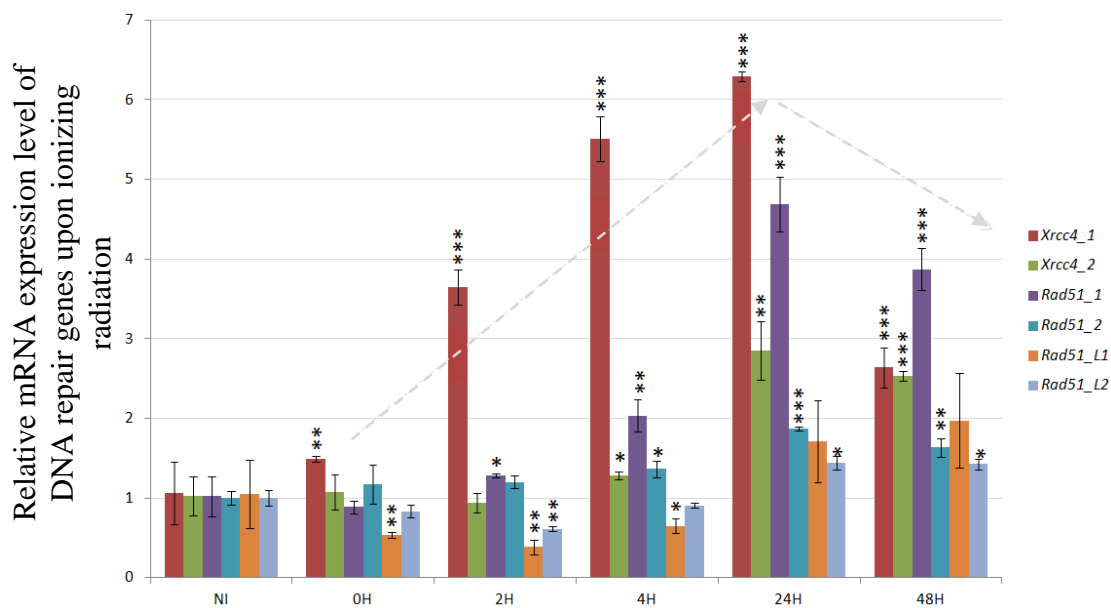
RT-qPCR was performed on RNA extracts obtained from irradiated *A. vaga* (800Gy). The analyses were performed on 8 different targets (listed in the Table 4). Bdelloid rotifers being degenerate tetraploids, proteins can be expressed from more than one gene copy. For XRCC4, the protein could originate from one gene present on chromosome 5 and another present on chromosome 2 that seems to have been separated into two parts. The protein RAD51 could be translated from two different genes (present on chromosomes 2 and 5). Finally, the RAD51_Like 1 protein can be expressed by a gene located on chromosome 2 while the *Rad51_Like 2* gene is located on chromosome 6. *Rad51_L1* and *Rad51_L2* are Rad51 paralogs, those proteins are in the Rad51 protein family. All the member of the *Rad51* proteins family, including *Rad51_L1* and *Rad51_L2* members are evolutionarily conserved proteins essential for DNA repair by homologous recombination in certain organisms.

Xrcc4_1 corresponds to the complete version of the protein while *Xrcc4_2* corresponds to a partial version corresponding to the C-terminal of the protein (figure 13). The second partial gene (*Xrcc4_3*) expression is not measured here as we could not design specific primers, every primer would also detect *Xrcc4_1*. *Rad51_1* corresponds to the genes expressing *Rad51* present on homologous chromosomes 2a and 2b, while *Rad51_2* corresponds to the genes present on homologous chromosomes 5a and 5b (Sequences alignment in the Annex A).
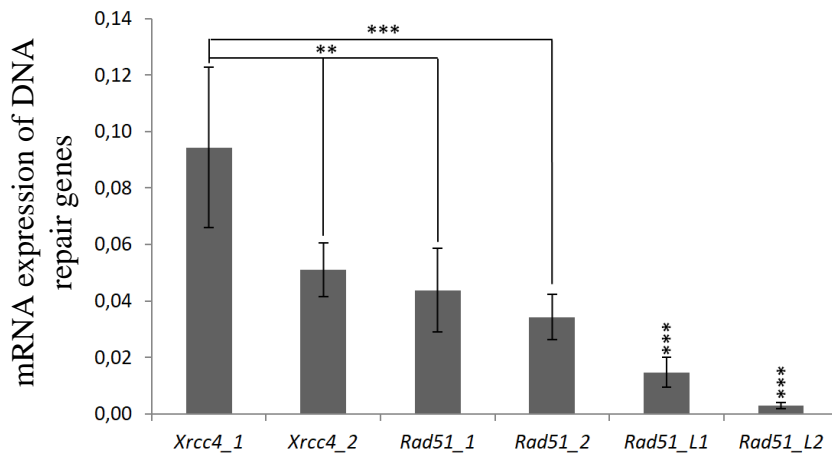
Figure 16 – *Adineta vaga* DNA repair mechanism gene expression. Gene expression profile of specific proteins in non-irradiated biological duplicates (technical triplicates). The expression was measured using RT-qPCR analyses of RNA extracts coming from non-irradiated *A. vaga*. The analyses were performed on 8 different targets: *Xrcc4_1*, *Xrcc4_2*, *Rad51_1*, *Rad51_2*, *Rad51_L1* and *Rad51_L2*. The relative expression levels were referred to the expression of *GAPDH*. The data represent the mean of 2^Delta Ct measures ± standard deviations. Two-tailed P values were calculated using a two tailed Student's t-test (*, P<0.05; **, P<0.01; ***, P<0.001). The gene expression for *Xrcc4_2*, *Rad51_1* and *Rad51_2* were analysed regarding the *Xrcc4_1* gene expression. Furthermore, the expression of *Rad51_L1* and *Rad51_L2* were statistically analysed in comparison to every other gene expression showing a statistically less important expression than the other DNA repair genes.

Figure 17 – *Adineta vaga* mRNA kinetics after 800Gy X-ray irradiation. Gene expression of DNA repair mechanism proteins upon 800Gy ionizing radiation realised in technical triplicates. The expression was measured using RT-qPCR analyses on RNA from *A. vaga* individuals exposed to X-ray IR. The analyses were performed on 8 different targets: *Xrcc4_1*, *Xrcc4_2*, *Rad51_1*, *Rad51_2*, *Rad51_L1* and *Rad51_L2*. The relative expression levels were referred to the expression of GAPDH. The Data represent the mean ± standard deviation. Two-tailed P values were calculated between indicated column and its left adjacent column using Student's t-test (*, P<0.05; **, P<0.01; ***, P<0.001). This statistical analysis allows us to see the variation of gene expression at different time-points post irradiation in comparison to the non-irradiated (NI) gene expression level.

Rad51_L1 and *Rad51_L2* correspond to the two genes expressing the RAD51-Like proteins. Finally, *GAPDH* and the *HSP70* were used as housekeeping genes.

Before analysing the impact of irradiation on gene expression, the basal expression of the genes was measured by performing a RT-qPCR analysis using non-irradiated bdelloid rotifers (Figure 16). The gene expression profile shows that the genes are expressed. *Xrcc4* genes seem to be significantly (** P<0.01 and ***P<0.001) more expressed that the *Rad51* genes. Both *Rad51_like* genes are significantly (***P<0.001) less expressed than the other DNA repair mechanism genes studied.

The gene expression profile that was obtained after exposing *A. vaga* to 800Gy of ionizing radiation shows variation in gene expression (Figure 17). The complete gene of *Xrcc4*, *Xrcc4_1*, shows a significant increase in expression with time, reaching a peak at 24h while *Xrcc4_2* seems to be only slightly increasing at 24h. *Rad51_1* also shows an increase of gene expression even though less important than *Xrcc4_1* and at later time-points post-irradiation. *Rad51_2*, *Rad51_L1* and *Rad51_L2* do not show an increase of expression upon irradiation, the like proteins expression even decreases upon irradiation. Finally, every gene expression seems to show a general augmentation occuring at 24h and decrease at 48h (as illustrated by the arrows on the figure 17). This expression profile was reproducible among the technical triplicates. Finally, the specificity and efficiency of primers was measured (Annex A A.) and the gene amplificated with the RT-qPCR were verified using cloning and sequencing (Annex A C.). The efficiency of Rad52_L2 was of 135% therefore, analyses made concerning this gene have to be taken with caution.

Those gene expression profiles suggest that in non-irradiated conditions there is a constitutive production of the genes involved in NHEJ and HR with Xrcc4 being highly expressed. Irradiation has an effect on gene expression as significant variations between time-points were observed with an increase of expression, especially for *Xrcc4_1* and *Rad5_1*, at 24h post-irradiation. It also suggests that the transcriptional response to this stressful event is specific to some specific genes. Furthermore, *Xrcc4_1* seems significantly more expressed than the other genes and at an earlier time-point, suggesting that *A. vaga* might activate NHEJ upon irradiation. However, *Rad51_1* is also expressed upon irradiation, but at a later time-point. Therefore, it seems that both *Xrcc4* and *Rad51* are over-expressed upon radiation. However, no affirmation can be drawn concerning which DNA DSB repair mechanism is preferentially used by the cell. Finally, these analyses were also made using the *HSP70* as housekeeping gene and the results show the same kind of profile (Annex A. - C. & D.).

Further proteomic and specific location analyses of the proteins after irradiation using proteomic approaches and IF, will be needed to decipher which DNA repair mechanism is used in *A.vaga* and whether there are differences between the somatic and germinal cells.

2. Analyses of the differential protein expression of XRCC4 and RAD51 upon ionizing radiation using a proteomic approach

Gene expression analyses showed an impact of irradiation on *Xrcc4* and *Rad51*. Therefore, proteomic analyses were done to see if the proteome would show differences upon exposure to ionizing radiation. Those proteomic researches started with the acquisition of polyclonal antibodies directed against *Xrcc4_1* and *Rad51_2*. These genes were chosen based on previous RNA-seq analyses.

Even though our RT-qPCR analyses seem to suggest that *Rad51_1* is more expressed than *Rad51_2*, the sequences are homologous enough for polyclonal antibody to detect proteins produced by both genes (Gene homology illustrated in the Annex B). Antibodies are commonly used in research to track proteins of interest thanks to their ability to bind to specific targets (Bordeaux *et al.*, 2010; Bradbury & Plückthun, 2015). These antibodies will be crucial here to study the DNA repair mechanisms of bdelloid rotifers as they will be used to discover what occurs inside rotifer nuclei when their DNA suffers DSBs.

2.1. Development of whole cell extraction procedure to study differential protein expression in *A. vaga*

When working with nuclear proteins, like the DNA repair proteins XRCC4 and RAD51, the first objective is to make sure that the nuclear fraction is reached when doing protein extractions. Even though transcriptomic analyses show a constitutive expression of XRCC4 and RAD51, we did not know if these proteins were sufficiently expressed in non-irradiated rotifers. Western blotting detections were therefore first performed with histone H3 and α-tubulin proteins, proteins highly expressed in bdelloid rotifers as shown during previous mass spectrometry analyses. The α-tubulin serves as a control as it is an abundant protein of the cytoplasmic fraction. Histone H3 is a nuclear protein implicated in the condensation of the chromatin and is a good control for nuclear protein extractions (Bártová *et al.*, 2008). Both commercial α-tubulin and histone H3 antibodies designed initially to target human proteins were previously shown to detect the corresponding proteins in the bdelloid rotifers. However, previous experiments showed really faint signals for the histone H3 detection which could be due to the protein extraction itself as the nuclear fraction might not have been efficiently reached.

To perform new protein extractions, starved rotifers were washed, centrifuged and underwent 1,000 dounces in lysis buffer which breaks rotifers and nuclei. In order to optimize the extraction, different buffer compositions were tested and the quality of the extraction was determined by probing α-tubulin and histone H3 (see Materials & Methods). A CHAPS-Glycerol buffer was used, the non-ionic detergent power of the CHAPS could permeabilize cells by solubilising membrane proteins and therefore improve the protein extraction while the glycerol helps maintaining the native conformation of proteins, preventing protein aggregations (Vagenende *et al.*, 2009). A RIPA buffer and a High Salt Buffer (HSB) were also tested. RIPA buffer is commonly used for whole protein extract and is efficient for solubilisation and extraction of cytoplasmic, nuclear and membrane proteins. The high salt buffer, is tested as high concentration of salt improves nuclei lysis and solubilisation of proteins bound to DNA. However, when the salt concentration is too important it can cause protein precipitation, therefore a product improving solubilisation could be added (i.e. CHAPS detergent).
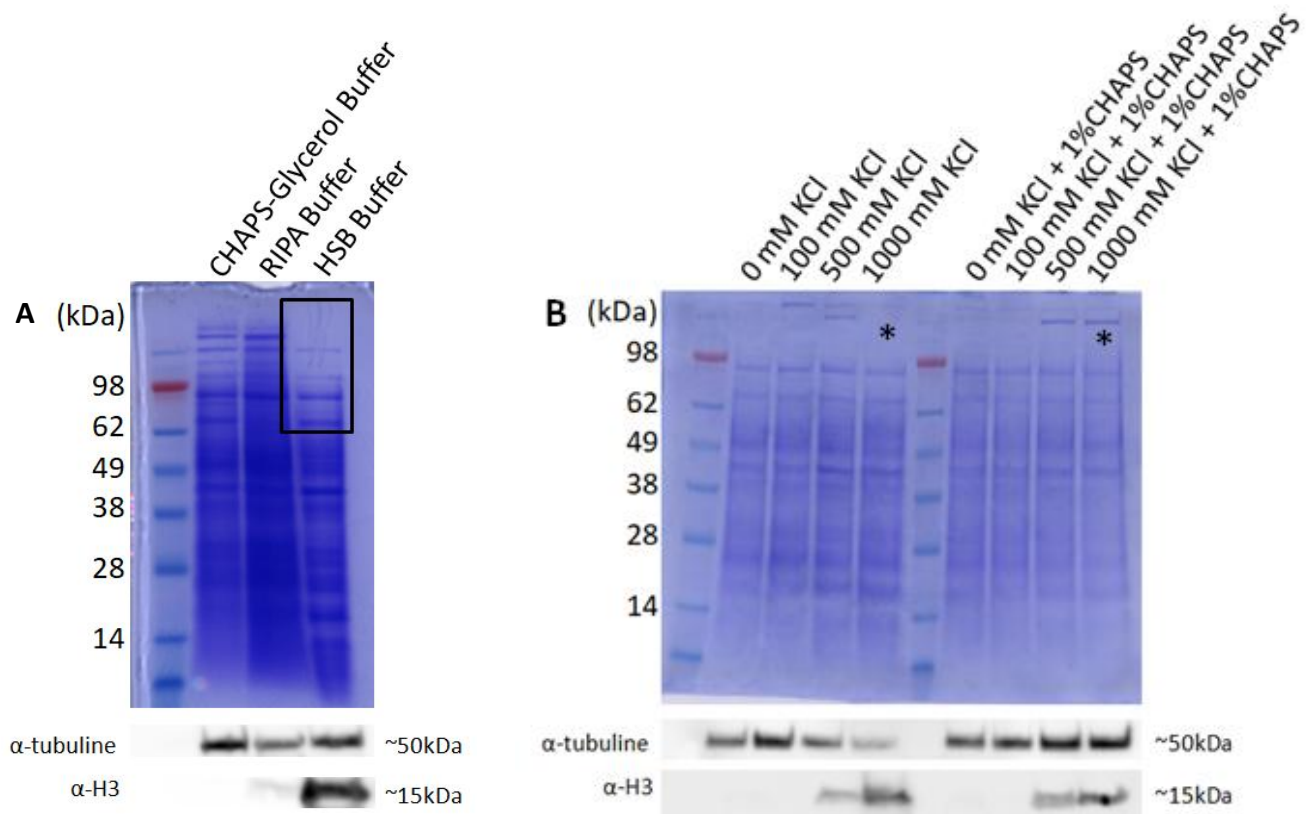
Figure 18 – Extraction buffer optimization. (A) Coomassie blue stained gel charged with 5µg of whole protein extract made with three different buffers: CHAPS-Glycerol, RIPA & HSB. Western blotting of α-tubulin and histone H3 were made with the same protein extractions as the Coomassie blue. The black square present shows the deficit of high molecular weight proteins in HSB buffer. (B) Coomassie blue stained gel charged with 5µg of whole protein extract made with three HSB with different concentrations of KCl without or with 1% of CHAPS detergent. Western blotting of α-tubulin and histone H3 were made with the same protein extracts as the Coomassie blue gel. The WB were made with the same parameters as the one in figure 18A. Asterisks show the recovery of high molecular weight proteins after adding 1% of CHAPS in the HSB buffer.
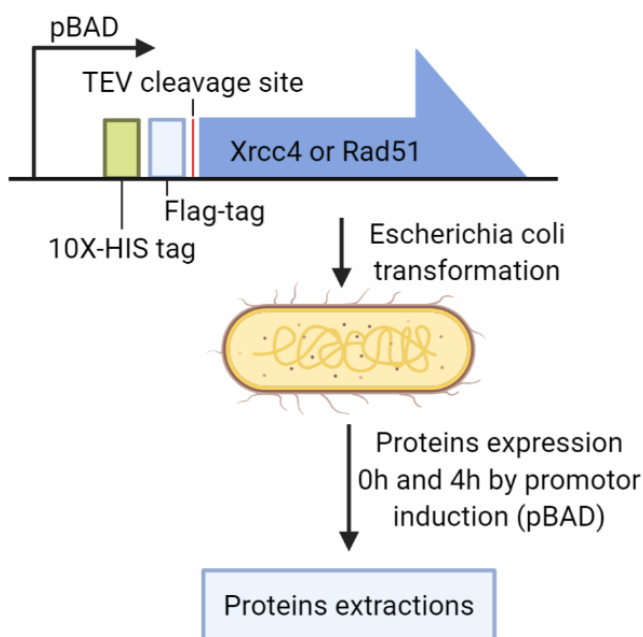
Figure 19 – Illustration of *E. coli* modification with a modified plasmid expressing XRCC4 or RAD51 prior to protein extraction. Illustration of *E. coli* transformation with plasmids containing XRCC4 or RAD51 sequences tagged with a 10X-histidine a Flag-tag, a TEV cleavage site and under an inductive pBAD promoter. The expression of the proteins was controlled by addition of L-Arabinose. Extractions were performed at different times post induction of the pBAD promoter (0H & 4H).

The bacteria transformation and proteins expression and purification were realised during a previous Master thesis. Therefore the protocol cannot be found in this Materials and methods.

As observed on figure 18A, even though the α-tubulin has been properly extracted with the three buffers, it is not the case for the histone H3. WB showed that the HSB extracted more nuclear proteins. However, with the high quantity of salt present in this buffer the lithium dodecyl sulphate (LDS), i.e. a detergent, present in the preparation of the sample underwent a phenomenon of salting out. The resulting precipitation varied from sample to sample making it hard to have reproducible results. Furthermore, the high molecular weight proteins, seemingly extracted with the RIPA and CHAPS-Glycerol extractions, are not present with the HSB extraction (Square Figure 18A).

To decrease the phenomenon of salting out and increase high molecular weight protein extraction, different concentrations of KCl with or without 1% CHAPS were tested. CHAPS could help reaching the high molecular weight proteins. As visible on figure 18B (left) for histone H3, it seems that 1M of KCl is optimal for nuclear protein extraction. However, in the absence of CHAPS, the α-tubulin, a "heavier" protein, saw its intensity decrease with the increase of salt (Figure 18B, leftt). Coomassie blue staining shows that high molecular weight proteins, lost with 1M of KCl, are recovered when 1% of CHAPS is added. Indeed, the α-tubulin profile is constant and the nuclear proteins are still extracted on the WB 1M KCl and 1% CHAPS (Figure 18B, right). Moreover, the CHAPS enhanced the quantity of proteins extracted. Therefore, a smaller quantity of protein extract is needed for the sample preparation, decreasing the quantity of salt in the sample. With a decreased quantity of salt in the sample the LDS would not precipitate at ambient temperature.

From these results, the HSB with 1M KCl and 1% of CHAPS will be used for further experiments. The extraction buffer being optimized, the antibodies against RAD51 and XRCC4 need to be tested and "validated".

2.2. Validation of polyclonal antibodies developed against the proteins XRCC4 and RAD51

When working with antibodies, validation of their specificity and their reproducibility in different experimental conditions is crucial. Common ways to check the specificity of antibodies would be by gene inactivation using siRNA depletion or gene deletion/inactivation using for example CRISPR-cas9. In addition, immunoprecipitation (IP) experiment can also be used to confirm the antigen detected by the antibody. However, in the case of bdelloid rotifers gene inactivation or IP methods are not available. Therefore, another experiment using transformed bacteria expressing the proteins of interest was performed to showcase the specificity of the antibodies.

Escherichia coli bacteria were transformed with arabinose-inducible vectors expressing XRCC4 and RAD51 proteins modified with a 10X-His-tag, a protease TEV cleavage site and a flag-tag (Figure 19). Protein extractions were performed on those bacteria before (t0h) and after 4h of expression with L-arabinose (t4h). Those protein extracts were used during western blotting experiments. The immunodetection of the WB membranes were realised with our polyclonal antibodies and with a monoclonal antibody directed against 10X-HIS-tag. The purpose of this experiment was to confirm the detection of XRCC4 and RAD51 by our polyclonal antibodies. This confirmation was made through the comparison of band localization between the different expression timings of the vector using the antibodies directed against XRCC4, RAD51 and against their 10X-HIS-tag. Furthermore, a cross immunodetection was made where the antibody against XRCC4 was used on a western blot of RAD51 producing bacteria extract and vice versa.
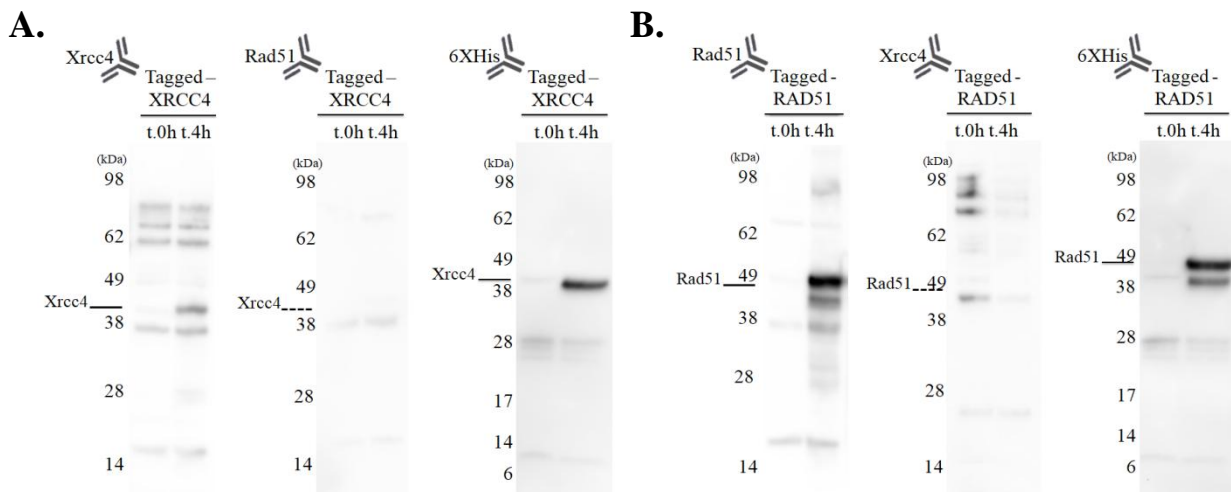
Figure 20 – Confirmation of the target protein detection by our polyclonal antibodies against XRCC4 and RAD51 proteins. Western blotting of bacteria protein extracts at different time-points of protein induction: before induction (t.0h) and 4hours post induction (t.4h). (A) Western Blots of 10XHis-tagged-Xrcc4 induced total *E. coli* proteins extract. Primary antibody against XRCC4 and secondary antibody against guinea-pig were concentrated at 1:2,500 and 1:5,000 respectively. Primary anti-6XHis-tag antibody and secondary antibody against mouse were concentrated at 1:1,000 and 1:1,000 respectively diluted in TBST with 1% NFDM. The extract was detected first with their specific antibody and secondly with the opposite antibody and finally with an anti-6XHis-tag antibody. (B) Western Blots were performed with the same conditions but focusing on the protein RAD51.
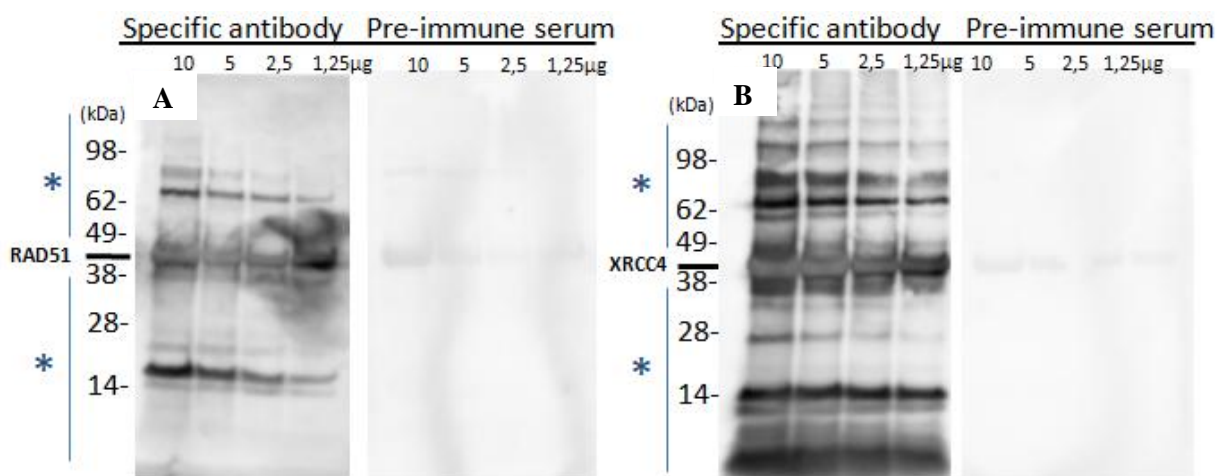
Figure 21 – Antibodies validation and WB optimization using purified antigens. Western blotting of purified antigen in *E. coli* with a decreasing quantity from 10 to 1.25µg. (A) Western Blot of RAD51 purified antigen on a PVDF membrane blocked with 5% NFDM TBST (0.1% Tween 20). Primary antibody and secondary antibodies are concentrated at 1:1,000 and 1:2,500 respectively and diluted in TBST with 1% NFDM. The antigen was detected first with their specific antibodies and secondly with their pre-immune serum. Western blotting A and B were performed with the same conditions. The asterisks (*) correspond to non-specific bands.

After performing the WB, we saw that the antibodies detected our proteins of interest as a band after 4h of protein expression, while no band was present when the vector is not expressed (t0H). Furthermore, this band migrated at a size corresponding to the expected size of these two proteins. This observation was done for both proteins XRCC4 and RAD51 (as visible on Figure 20). Additionally, a cross immunodetection also showed that the antibodies did not detect the other protein of interest. Finally, the detection of proteins with the antibody directed against the 10X-His-Tag shows a band at the same localization as our polyclonal antibody, suggesting that the polyclonal antibodies detect the expected proteins.

The fact that the protein bands are a little higher than the expected size of these proteins can be explained by the presence of the tag making the proteins heavier. The corresponding localization of the band enhances the hypothesis that our antibodies can detect the proteins XRCC4 and RAD51. However, even though our antibodies are directed against eukaryotic proteins, they show some non-specificity as other bands can be seen on the WB (asterisks in Figures 21). These non-specific bands could originate from the antibody production process. During the immunization process, guinea pigs were injected with proteins of interest purified from *E. coli*. If the proteins were not perfectly purified, the guinea pigs created antibodies against the protein of interest and against proteins co-injected with the protein of interest. Therefore, the non-specific bands might not come from the non-specificity of the antibody targeting XRCC4 and RAD51 but from the non-purity of the protein injected for immunization.

Furthermore, when receiving the polyclonal antibodies against XRCC4 and RAD51, their purified antigens and their pre-immune serum were also delivered. Therefore, the purity of the "purified" antigens was checked, as it could give some indications about the non-specificity of the antibodies. Western blots A and B on figure 21 were performed on the purified antigens at a decreasing concentration from 10 to 1.25µg with a concentration of primary and secondary antibodies of 1:2,500 and 1:5,000, respectively. The results show that bands were present at the expected molecular weight for both XRCC4 and RAD51, respectively 40,94kDa and 40,33kDa, whereas the signal was clearly less intense with pre-immune sera (Figures 21A-B). WB were also filled with non-specific bands showing that the antigen used for the immunization was not perfectly pure (asterisks in Figures 21A-B).

To conclude, our polyclonal antibodies showed their ability to detect their target proteins, XRCC4 and RAD51. Therefore, WB experiment using *A. vaga* whole protein extract can be optimized and the antibodies can be used to see the impact of ionizing radiation on bdelloid rotifers and on their DNA DSB repair mechanism.

2.3. Experimental set up of western blot against XRCC4 and RAD51 with *A. vaga* whole cell extract

The non-specificity linked to the co-purification of *E. coli* proteins with our proteins of interest should not be present on WB using whole protein extract from bdelloid rotifers. Indeed the co-purified *E. coli* proteins are not expected in an eukaryotic, bdelloid rotifer, protein extract.

Our antibodies were therefore tested against whole protein extracts of *A. vaga* using different methods of blocking agent (BSA or non-fat dry milk). The results show that the "specific bands" were still present but also some non-specific bands (asterisks in Figures 22A-B).
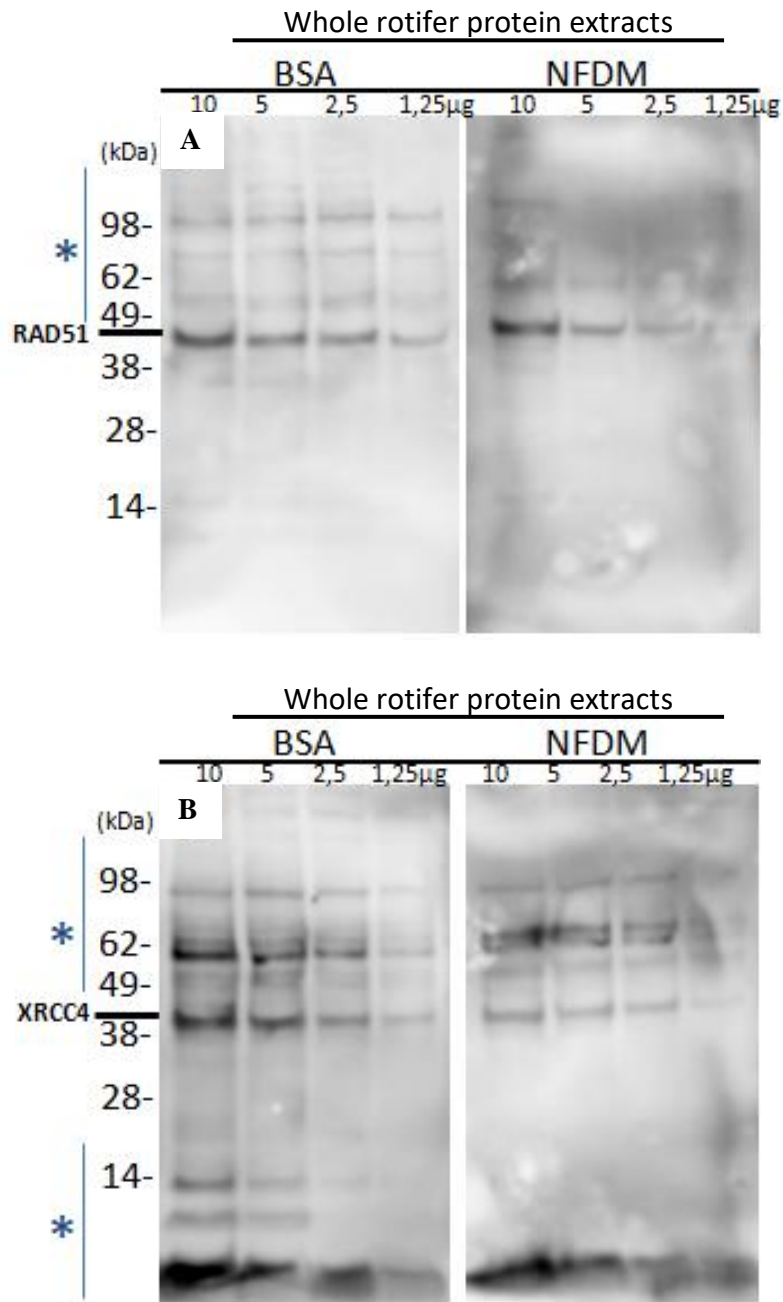
Figure 22 – Antibodies validation and WB optimization. Western blotting of whole rotifer protein extract with a decreasing quantity from 10 to 1.25μg. (A) Western Blots of bdelloid rotifers whole protein extracts on a PVDF membrane blocked either with 5% BSA TBST (0.1% Tween 20) or 5% NFDM TBST (0.1% Tween 20). Primary antibody and secondary antibodies against RAD51 or (B) XRCC4 were concentrated at 1:2,500 and 1:5,000 respectively is diluted in 1% BSA.

This non-specificity in WB can originate from the production of the antibody itself. In this case, the polyclonal antibodies were produced against a protein coming from the given sequences *Xrcc4_1* and *Rad51_2* from *A. vaga*: so they recognize a synthetic peptide produced in *E. coli*. As a consequence, our polyclonal antibody was not directed against the proteins in their native conformation or with their post translational modifications (PTM) which could result in specificity troubles. Furthermore, polyclonal antibodies can recognize a pool of epitopes that might be present in other proteins or on degraded parts of proteins (Bordeaux *et al.*, 2010). Deepti and Dinakar said that "[...] *antibodies are often functionally promiscuous or multi-specific which can lead to their binding to more than one antigen. An important cause of antibody cross-reactivity is molecular mimicry* [...]". Molecular mimicry occurs when there are structural, chemical or immunological similarities between different epitopes resulting in interactions with the same paratope, i.e. the antibody antigen-binding site (Deepti & Dinakar, 2019). In our case, RAD51 possess different paralogs or RAD51-like proteins that could have similar epitopes with the target protein. XRCC4 suffer also from "gene redundancy" (Hecox-Lea & Mark Welch, 2018). Proteins from these redundant genes could possess similar epitopes while being sufficiently different to produce bands at different molecular weights.

In the end, the non-specific bands could be due to some degradation of the proteins, some PTM impacting molecular weight or, as said earlier, other proteins that share similar epitopes. Finally, the presence of non-specific bands should not impact the analysis of our protein of interest and this is the reason why they will be used in the next experiment to analyze the differential expression of XRCC4 or RAD51 proteins upon irradiation of *A. vaga*.

2.4. Differential expression of XRCC4 and RAD51 proteins at different time-points after 800Gy of ionizing radiation

Using the polyclonal antibodies, there is a possibility to observe potential modifications in protein production at different time-points after irradiation of *A. vaga*. This could give some hint on the "behaviour" of proteins and, therefore, provide some clues about the active DNA DSB repair mechanism(s) in rotifers after stressful ionizing radiation.

Whole protein extractions were performed on biological quadruplicates and technical triplicates on irradiated *A. vaga* (800Gy) at different time-points after irradiation in order to see the impact on protein expression. Silver staining, Coomassie blue staining and western blots were performed. Silver staining and Coomassie blue staining are both protein staining methods with different sensitivity. Silver staining is more sensitive, detecting protein at nanogram level (>1ng), while Coomassie blue staining, also sensitive (10ng) is easier to perform. Since we wanted to use the same samples as our WB experiment gels were loaded with micrograms of proteins. Therefore, silver and Coomassie stainings showed the same kind of profiles. Coomassie blue staining being less constraining was chosen (Dong *et al.*, 2011). These staining experiments allowed us to see the complete proteome and check whether IR had important impacts on its profile, while western blotting allowed us to focus on XRCC4 and RAD51 protein expression.

The irradiation efficiencies were confirmed by Pulsed-field gel electrophoresis (PFGE) showing the integrity of DNA at different time-points. The results clearly showed that at 0h, the DNA is fragmented into pieces of 225 kb on average and that higher molecular weight DNA fragments are reassembled progressively to reach a plateau at 48h and 72h post irradiation (Figure 23A).
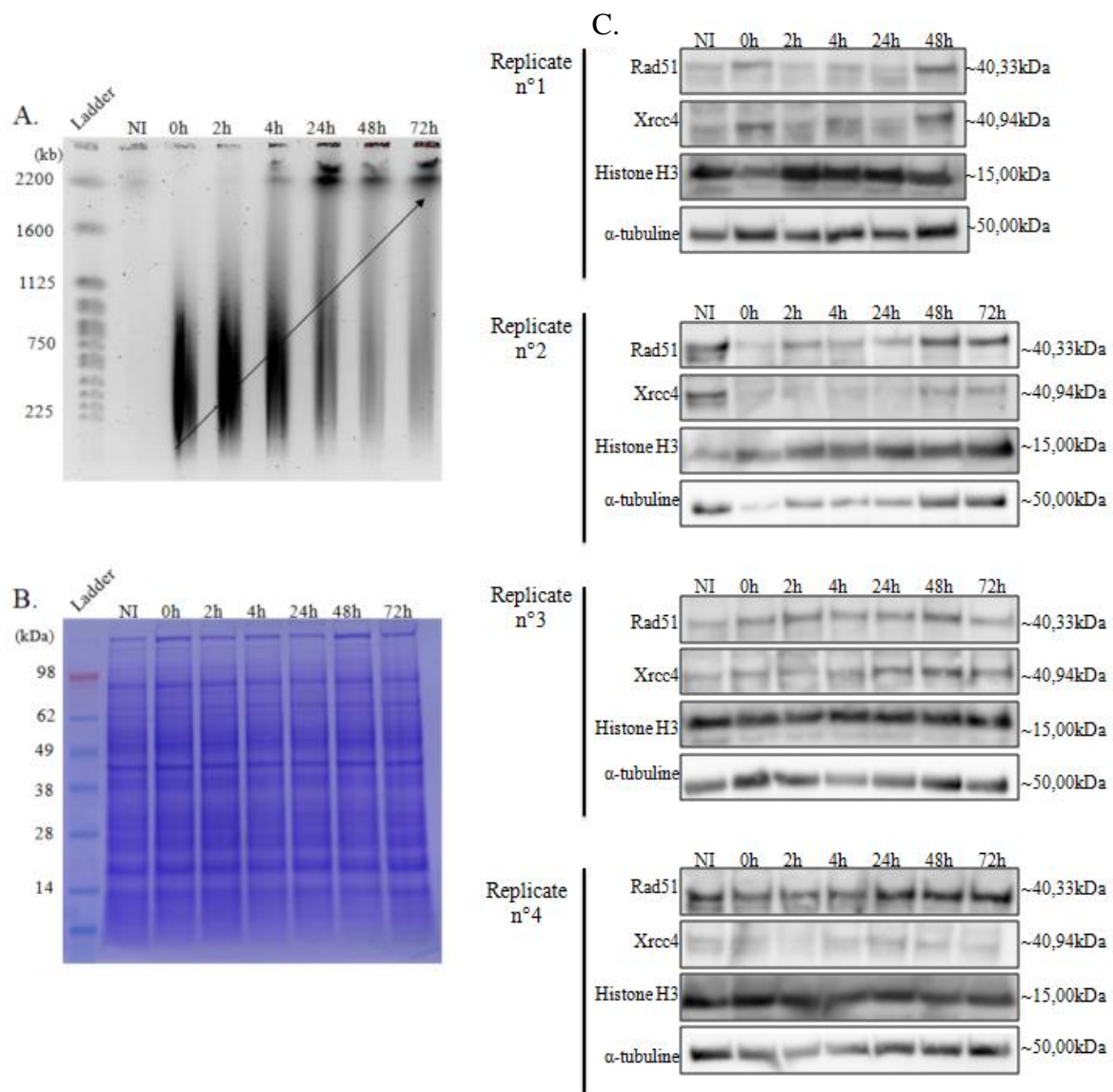
Figure 23 – 800Gy irradiation impact on whole protein extract and on *Adineta vaga* DNA DSB at different time-points. (A) PFGE analysis of the effect of ionizing irradiation on the genome. The different lanes of the gel contained the DNA profile of 1,000 individuals showing that with time bigger DNA fragments are formed suggesting an active DNA DSB repair mechanism such as NHEJ or HR. (B) Coomassie blue staining charged with 10µg of whole protein extract at different time-points post 800Gy irradiation with a non-irradiated (NI) control. (C) Western blotting detected with antibodies against α-tubulin, Histone H3, RAD51 & XRCC4 made with the same sample as the Coomassie blue staining. The replicate n°1 was loaded with 5µg of proteins and blocked with BSA while the other replicates were realised according to the Materials &Methods.

This result suggested that DNA was actively repaired upon irradiation. This PFGE experiment was representative for every PFGE profile obtained for the biological replicates.

The Coomassie blue staining on figure 23B was made with the same quantity of proteins for each condition to analyze the integrity of the proteome profile after irradiation. When looking at the Coomassie blue gel, no major differences can be seen between the different time-points. This could lead us to speculate that irradiation might not have a huge impact on the general aspects of the proteome. Furthermore, protein extractions were performed on approximatively 150,000 rotifers per condition. When undergoing ionizing radiation each rotifer is impacted differently. Therefore analysis of the general proteome profile might not reflect the impact that it could have on one individual. This results in profiles that seem similar with "invisible" impacts. Furthermore, if some proteins were impacted, they might be hidden behind bands of proteins of the same molecular weight that were not impacted.

While the Coomassie staining and the PFGE showed consistent results between the different replicates, the profile observed by western blotting varied between replicates. First and foremost, when looking at the non-irradiated conditions, rotifers seem to be expressing both XRCC4 and RAD51 in every biological replicate (Figure 23C). This result suggests that both proteins are constitutively expressed in *A. vaga* as already suggested by our RT-qPCR experiments. This correlates with the literature showing a constitutive expression of these proteins in both radio-resistant and radio-sensitive organisms (Beltrán-Pardo *et al*., 2013; Choi *et al*., 2017). However, when looking at the different time-points different profiles can be seen (Figure 23C). The α-tubulin and histone H3 signals seem to be relatively stable over the different time-points analyzed. However, some variability is present among the replicates of the experiment, e.g. t0H, H3 replicate n°1 or t0H, α-tubulin replicate n°2. However, those variations are probably due to technical issues.

As visible on replicate n°1, it seemed that both XRCC4 and RAD51 decrease at time-points 0h-2h-4h and 24h and increase back until time-point 48h. These results suggested that the expressions of these proteins might be affected at early time-points following ionizing irradiation. To confirm these results, 3 other biological replicates of the experiment were performed. Unfortunately, these experiments did not show the same profile of decrease and subsequent increase of XRCC4 and RAD51 expression upon radiation. This suggests that the variability seen in replicate 1 might be a technical issue rather than a real biological result. The variability of those WB can be further confirmed with our quantification analyses (Figure 24). Even though some differences are present between time-points, the standard deviations clearly show that no conclusion can be drawn due to the apparent high variability.

As a result, western blotting analyses show lots of variations between biological replicates and the quantifications are not consistent. Therefore, no real conclusion can be drawn concerning the evolution of XRCC4 and RAD51 at the different time-points post-irradiation using this method. The results obtained here may suggest that the variation could be due to technical issues with the rotifer manipulations, which will be addressed in the next section. The only preliminary conclusion that can be taken here is a constitutive expression of the proteins which supports our RT-qPCR analyses.
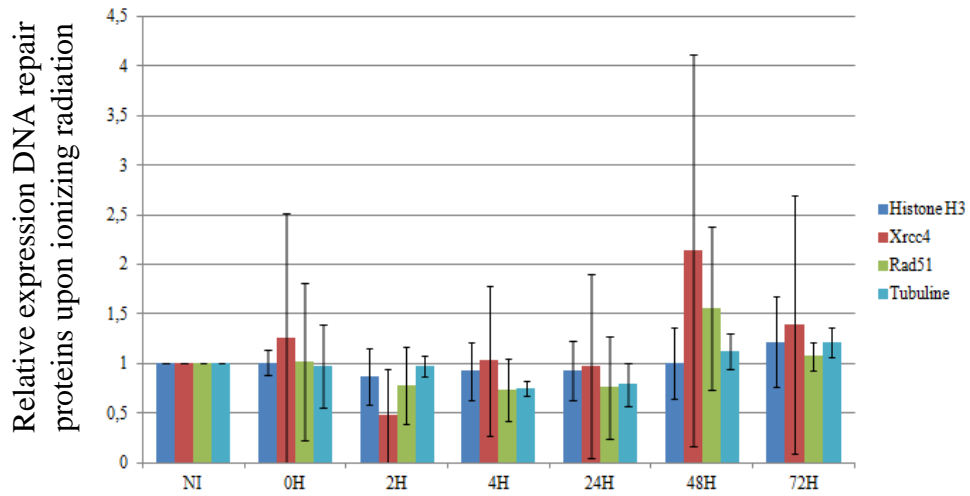
Figure 24 – Impact of ionizing radiation on the proteins XRCC4, RAD51, the histone H3 and the α-tubulin expression profile. Quantification of the X-ray irradiation impact on whole proteins, the quantification analyses were made using the WB of figure 23. The scale bar represents the mean expression signal ± its standard deviation of the different replicates. The quantification was made using the WB band intensities measured using the AI600 imager.
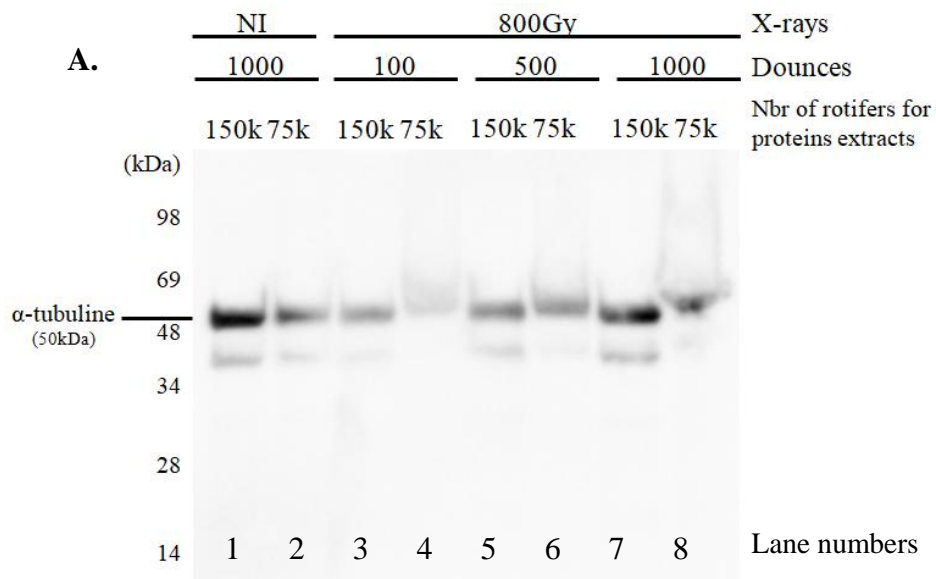
NI		800Gy					
1000		100		500		1000	
150k	75k	150k	75k	150k	75k	150k	75k
9,1µl	21,2µl	14,6µl	32µl	10µl	21µl	9,3µl	23µl

Figure 25 – Impact of the mechanical lysis and high salt concentration on protein integrity, migration and detection. Western blotting of *A. vaga* whole protein extracts on Non-irradiated (NI) and 800Gy irradiated individuals. The extracts were obtained with different rounds of dounce and starting with different quantities of bdelloid rotifers (75,000 and 150,000). WB were detected using antibodies directed against α-tubulin (see M.&M. for more details).
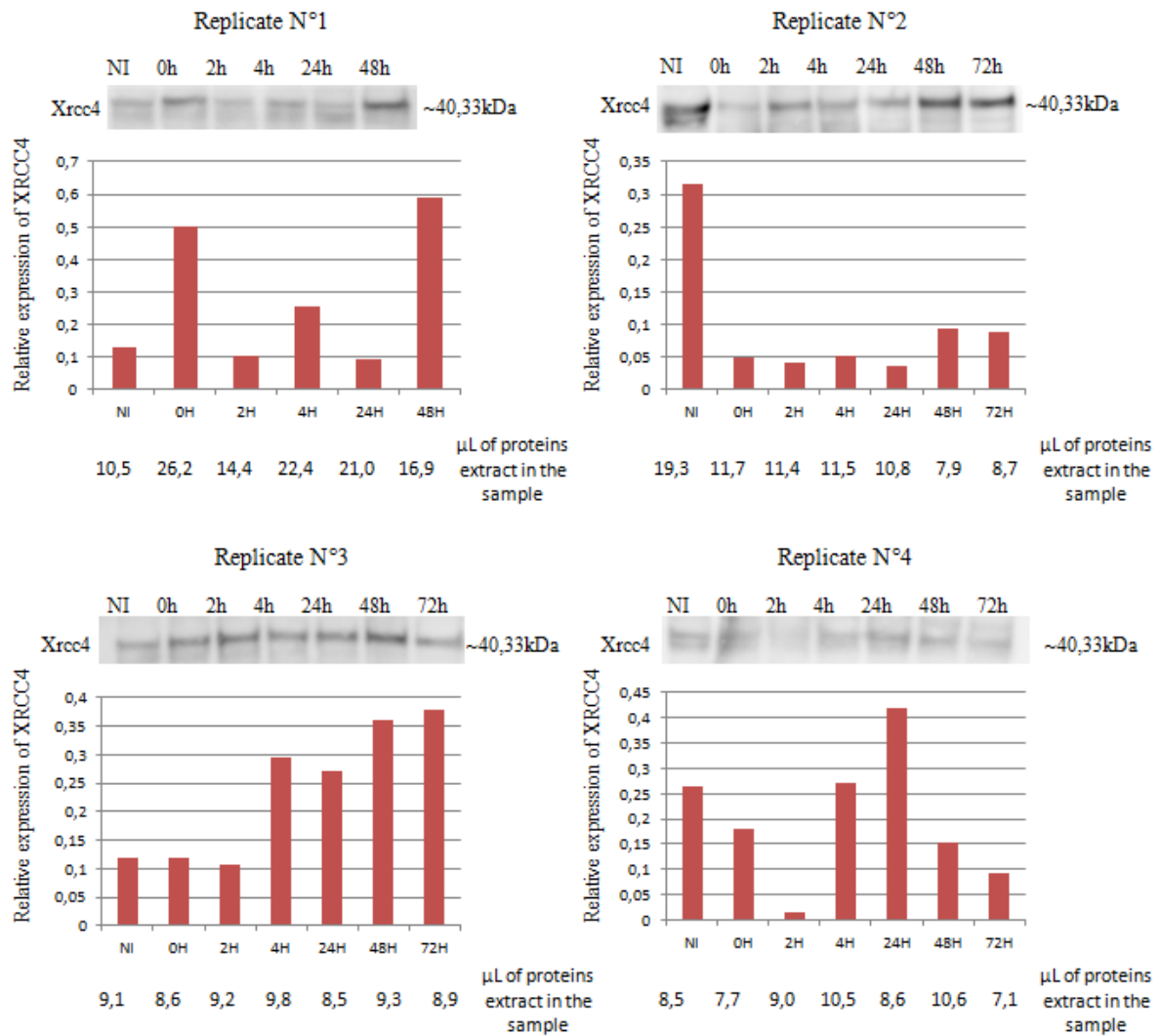
2.5.   Impact of bdelloid rotifer manipulation on western blotting analyses

When undergoing ionizing radiation such as X-rays, bdelloid rotifers do not only suffer from the formation of DNA DSBs. The radiation could also weaken the cuticle making rotifers more sensitive to manipulations. If the cuticle is weakened, for the same quantity of dounces irradiated rotifers will undergo the mechanical lysis faster and the high quantity of dounces (1,000) may impact the integrity of the proteins in addition to the lysis itself. Furthermore, the WB samples contain a high quantity of salt which could impact protein migration and detection by the antibody. Therefore, the variable results obtained in our WB experiment could be linked to differences in sample preparations and not reflect the biological effect of irradiation. We are focusing here first on the impact of the mechanical lysis by changing the numbers of dounces used.

Whole protein extractions were performed on irradiated *A. vaga* individuals (800Gy) at different time-points post-irradiation. Different numbers of dounces were tested to compare the impact of mechanical lysis on protein integrity of irradiated and non-irradiated rotifers, with the same number of rotifers per replicate. The protein tested to see the impact of the mechanical lysis was α-tubuline because it is present in high quantities in rotifers. We observed a positive correlation between the number of dounces and band intensity (Figure 25, lane 3, 5, 7). This could be explained by the fact that a lower number of dounces does not allow an extraction of intracellular proteins as efficiently as 1,000 dounces, or it could be due to salt differences in the samples (explained below). The integrity of the proteins was not different when comparing the 1,000 dounces in the irradiated (Figure 25, lane 3, 5, 7) or non-irradiated conditions (Figure 25, lane 1).

WB experiment was also done to see the impact of salt concentration on the WB analyses (migration and detection) since the extraction lysis buffer used contains 1M of KCl. Protein extractions were performed on different quantities of bdelloid rotifers as the salt ratio changes with the ratio of rotifers quantity/volume. Therefore, extractions were performed on batches of 75,000 and 150,000 *A. vaga* individuals in 300μL volume. Accordingly, the different protein extracts will not contain the same concentration of proteins. Therefore, in order to reach the same quantity of proteins in the samples that will be loaded on the gel (i.e. 10μg), different quantity of proteins extract were used (Figure 25B).

High concentration of salt in samples can cause inconsistent/ unpredictable proteins migrations resulting in non- straight bands (BioRad, 2019; Uppsala, 2016). This information can be confirmed with our WB result using 75k rotifers proteins extract aspect and the correlation with protein extract present in the sample (figure 25 A lanes 4, 6 and 8 and B). Even though the KCl impact on migration is clearly explained in the literature, the impact it could have on protein detections on a WB membrane is rarely mentioned. However, looking at the variability in WB results throughout the replicates (Figure 23C), the impact of salt on protein detections was still evocated and looked upon. In the non-irradiated condition, even though the same quantity of proteins was loaded on the gel, the 75k lane shows a band with a lower intensity which correlate with a higher quantity of protein extract in the sample (Figure 25 A lanes 1 and 2). However, when looking at the impact salt quantity in comparison to our quadruplicates results, no correlation could be clearly seen. Indeed, protein signals did not decrease in conditions where the volume of loaded sample was higher (Figure 26, Replicate n°1 t(0H) and t(2H)).

Figure 26 – Impact of salt concentration on the biological quadruplicate of whole rotifers protein extract at different time-point upon ionizing radiation focusing on Xrcc4. Western blotting and quantification of bdelloid rotifers whole protein extracts on Non-irradiated (NI) and at different time-points post 800Gy of X-rays ionizing radiation. WB were detected using antibodies directed against XRCC4 (see M.&M. for more details). The scale bars represent the expression signal. The quantification was made using the WB bands intensities measured using the AI600 imager.

These experiments had for objectives to understand the origin of the WB variability. The experiment on mechanical lysis of rotifers shows that the number of dounces did not impact the integrity of the proteins as no degradation was observed in the irradiated and non-irradiated condition at 500 and 1000 dounces. However, another experiment realised in the lab showed an impact on the proteins integrity when extraction were made with 2,000 dounces. Therefore, even though not visible here, mechanical lysis might participate in the variability.

Furthermore, the second hypothesis for the variability was the impact of salt concentration in our samples. However, even though high concentration of salt clearly have an impact on the protein migration, the result using the biological triplicate do not seem correlated to the salt.

Finally, it is still unclear what could be at the origin of this variability. However, it would be interesting to harmonize the quantity of salt in samples final volumes between the samples of or it dialysed in order to get rid of the salt in the sample. This could remove any potential impact KCl might have on the detection of the membranes by the antibodies.

3. Impact of ionizing radiation on XRCC4, RAD51, the Histone H3 and the α-tubulin localizations using an immunofluorescence approach

Another method to study the impact of radiation on *A. vaga* proteins is immunofluorescence (IF). Indeed, IF can provide information on the localization and the structure of the assembled fluorescent foci/signals of the proteins of interest and whether modifications are observed upon irradiation. Indeed, DNA DSB repair proteins foci have already been shown in damaged nuclei (Choi *et al*., 2017).

3.1. Optimizing the fixation and permeabilization methods in order to observe differential localization of nuclear proteins *in situ*

In order to be able to localize XRCC4 and RAD51 in rotifers in different conditions by IF, organisms need to be homogeneously permeabilized for the antibodies to reach the nuclei. Immunofluorescence experiments on nuclear proteins had yet to be developed as it was never done on bdelloid rotifers. Therefore, as for the protein extraction procedure, an adapted IF method is developed and optimized here.

When performing IF, fixation methods using formaldehyde (FA) and methanol (MeOH) are commonly used in *Caenorhabditis elegans* that, like rotifers, possess a cuticle making it hard to stain cells and nuclei. Fixation is a necessary step in IF to fix the antigen. There is light fixation, precipitation of the antigen that can be done with MeOH or acetone (Ac), and hard fixation with FA that cross-links the antigen (Duerr, 2013). Furthermore, in order to detect intracellular, especially intranuclear, antigens rotifers need to be permeabilized using specific permeabilizing reagents. Detergents like saponin or Triton X-100 interact with lipids specifically or non-specifically, respectively, permeabilizing membranes (Krisko & Radman, 2010). Another crucial step when permeabilizing an organism with a cuticle is a freeze crack step (FC). It consists of cracking open the cuticle of individuals after sinking them in liquid nitrogen (Figure 15). Opening the cuticle gives an easier access to the cells and plays an important role in IF (Duerr, 2013).
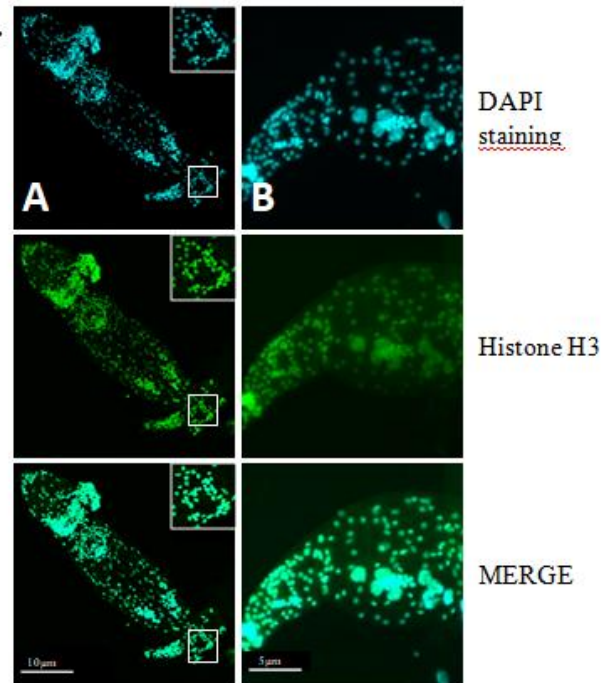
A.

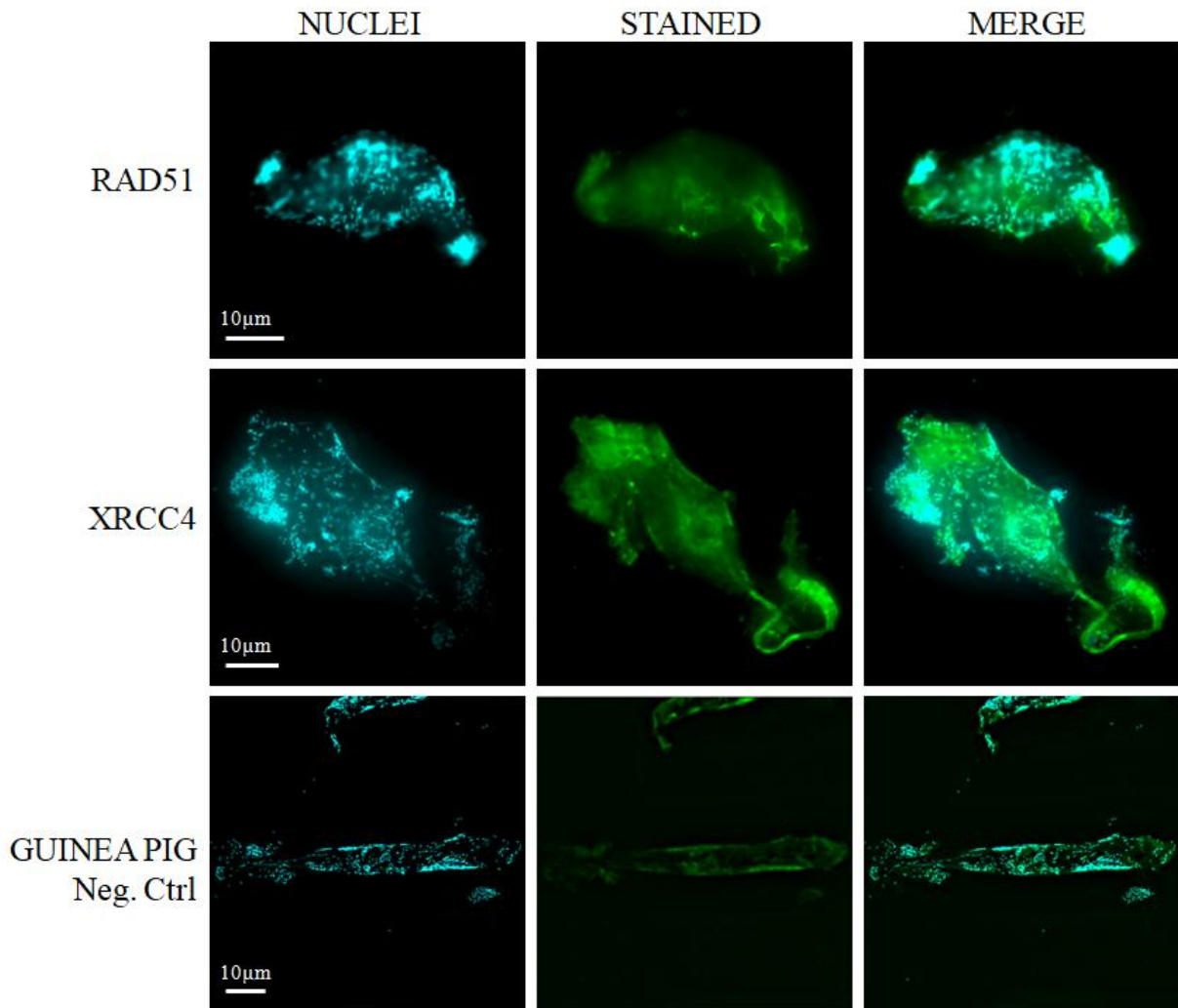|	Protocol A	Protocol B
Rotifers concentration	>10.000	500/5µl
Permeabilization	Freeze crack	Squash + Freeze Crack
Fixation	2% Formaldehyde	1% Formaldehyde
Blocking and permeabilization	3% BSA, 0,1% Triton X-100	3% BSA, 0,3% Triton X-100
Labelling	1:1000	1:150
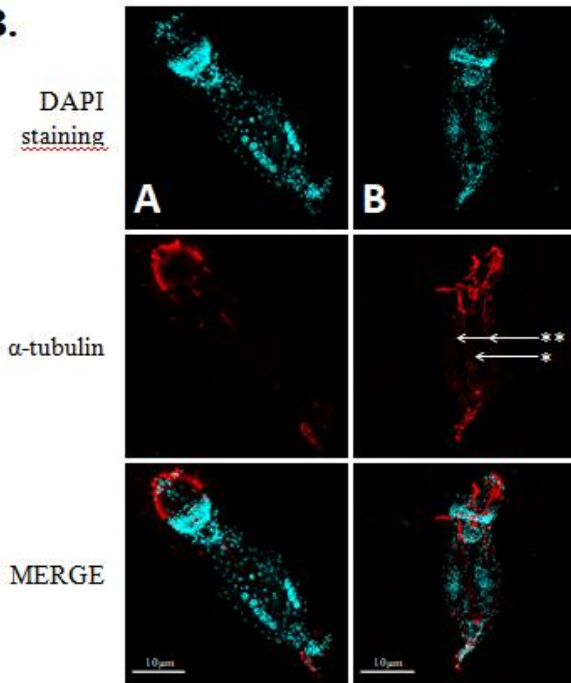
Figure 27 – Optimization of the staining protocol for the immunofluorescence protocol. *Adineta vaga* individuals are stained in order to test the different protocols and see if it can improve the staining of nuclear proteins. Per condition, individuals were permeabilized, fixed and blocked with 3% BSA and non-ionizing detergent. DNA was stained with DAPI and the proteins of interest were labelled using primary and fluorescent secondary antibodies. (A) Protocols tested. (B) The rotifer staining was done following protocol A for column A and following protocol B for column B. Here the α-tubuline antibody was used. (C) Staining of the *A. vaga* individuals following protocol A for column A and following protocol B for column B and using the histone H3 antibody. Slides were mounted with a slowfade mounting buffer for protocol A and with mowiol after DAPI staining for protocol B. The rotifers imaged in the columns B.-A. and C.-A. were made with the confocal microscope while the columns B.-B. and C.-B. were made with the Zeiss Axioimager Z.1 fluorescence microscope.

For the IF experiments on bdelloid rotifers, different methods of permeabilization and fixation were tested. *Adineta vaga* individuals were freeze cracked, fixated and permeabilized using two different protocols as outlined in figure 27. The antibodies were diluted in the same buffer as the blocking buffer. Antibodies against the α-tubulin serves as a permeabilization control for the staining of the cell cytoplasm. The antibody against histone H3 is our control for nuclei staining. The DNA was stained with DAPI. DAPI is a specific DNA label that binds to DNA regions rich in Adenine and Thymine. Therefore, if the green staining of the histone H3 overlaps with the blue staining of the DAPI, it shows that the antibodies reached the nuclei.

When looking at figure 27B and 27C (column A), rotifers were stained after freeze cracking and FA fixation with the α-tubulin and histone H3 antibodies. The α-tubulin signal is mainly observed in the head and the foot of the animal which is filled with tubulin filaments whereas the H3 signal is visible within all nuclei of the organism. However, using protocol A, the staining was not homogeneous throughout the slide or even throughout one rotifer. Furthermore, even when starting with more than >10.000 individuals, only a few were left on the slide due to the extensive washes of the IF protocol A. Therefore, to increase the rotifer quantity, individuals were concentrated in a small water volume and were squashed on the slide in order to improve their stickiness on the slide. To improve permeabilization, the percentage of FA was decreased in the fixation step of protocol B because the cuticle, being composed of proteins, might become fixed and interfere with the labelling. Secondly, the percentage of non-ionic detergent was increased in the blocking and antibody dilution buffers of protocol B to increase the permeabilization. Additionally, MeOH fixation by precipitation was also tested but gave bad results as the antibody could not pass the precipitated cuticle (Annexe D).

Performing IF using protocol B improved the staining: α-tubulin labelling was observed in the head, the toe but also the digestive system (asterisk, figure 27B-B) and muscles (double asterisks, figure 27B-B). Furthermore, the H3 signal is visible within all nuclei of the organism (Figure 27C-B). Negative controls were also performed by staining rotifers only with a secondary antibody in order to see if some non-specific staining would occur, they were all negative (Annexe E). Finally, the modifications made to protocol B also increased the adherence of rotifers to the slide allowing us to start with a lower number of individuals per slide.

After optimizing a labelling method for nuclear proteins in the bdelloid rotifer *A. vaga*, our purpose was to stain the nuclear proteins XRCC4 and RAD51 and see their localization upon ionizing radiation. However, we started by testing the IF experimental protocol on non-irradiated rotifers as our qPCR experiments showed that these two genes were already expressed in non-irradiated condition.

Figure 28 – XRCC4 and RAD51 staining using the IF protocol B. *Adineta vaga* individuals were stained with the antibodies RAD51 and XRCC4, per condition 500 individuals were used. After fixation they were blocked with 3% BSA and non-ionizing detergent. DNA was stained with DAPI 1:100 and the primary and secondary antibodies had concentrations of 1:150. Rotifers were imaged using the Olympus fluorescent microscope.
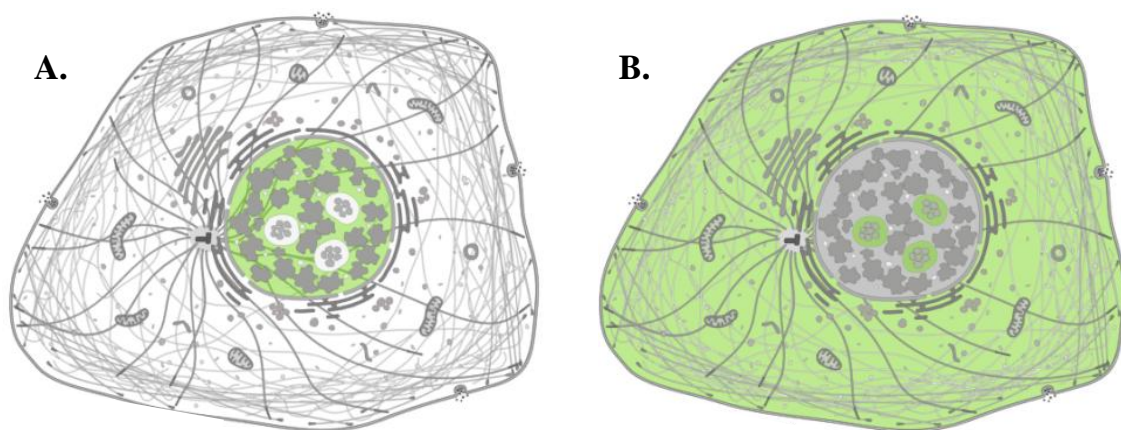
Figure 29 – Localization of XRCC4 and RAD51 in non-irradiated human cells. (A) In non-irradiated human cells XRCC4 localizes in the nucleoplasm (Green) while (B) Rad51 tends to be mainly localized in the nuclei but can also be found in the cytoplasm (The human atlas proteins, 2019a, 2019b).

3.2. Immunofluorescence staining trials using the antibodies against XRCC4 and RAD51

The polyclonal antibodies against XRCC4 and RAD51 were also tested for IF experiments using protocol B (Figure 27).

First, *Adineta vaga* individuals were concentrated in water, squashed and permeabilized by performing a FC. After FC, the rotifers were fixed using FA, blocked and permeabilized with BSA and Triton X-100. Finally, their XRCC4 and RAD51 were labelled using their primary antibody and a fluorescent secondary antibody.

When looking at the IF results, it seemed that the antibodies against RAD51 and XRCC4 mainly bind to the cuticle while we expected them to be located in the nucleus (Figure 28). In addition, the negative control containing only the fluorescent antibody showed a fluorescence pattern similar to the XRCC4 and RAD51 staining. In non-irradiated conditions, XRCC4 is expected to be localized in the nucleoplasm while Rad51 should be expected to localize in the nucleus and in the cytoplasm (Figure 29). In the case of *A. vaga*, maybe these proteins are located in the nuclei only after ionizing radiation creating many DNA DSBs. Therefore, XRCC4 and RAD51 labelling were also tested upon an 800Gy X-ray irradiation on hydrated *A. vaga* individuals. Furthermore, an increased permeabilization of the cuticle due to the irradiation might help the staining. The pattern of IF signals were similar to the NI state (Annex F) showing that the labelling observed with the antibodies RAD51 and XRCC4 seem mainly non-specific.

New optimizations are needed for the IF experiment with XRCC4 and RAD51. In this Master thesis we decided to focus on the "behaviour" of the histone H3 and the α-tubulin upon irradiation as the immunofluorescence seemed to be working with those antibodies.

3.3. Protein localization and behaviour upon irradiation using immunofluorescence

In order to see the impact of ionizing radiation on proteins, the histone H3 and α-tubulin localization and appearance was studied using immunofluorescence. Indeed, if ionizing radiation impacts the entire proteome in bdelloid rotifers, some modifications of the Histone H3 and α-tubulin labelling might be visible using IF.

In the case of the α-tubulin, ionizing radiation may have different impacts on the cytoskeleton such as an increase or decrease of signal intensity (due to degradation), uneven staining, disappearance of some structural staining or signal intensity increase (due to aggregation). These signal modifications could be due to distorted cytoskeleton structure possibly caused by ionizing radiation. It has been shown in cortical neurons that X-rays exposition could cause a sparse distribution of their β-tubulin resulting in the disappearance of some structures (Du *et al.*, 2014; Eriksson *et al.*, 2007).

Following irradiation event the histone H3 may experience different post-translational modifications such as phosphorylation, methtylation or acetylation. These different modifications may result in degradation of the modified histone (e.g. due to actelylation) (Friedl *et al.*, 2012) or in aggregation (e.g. methylation). Indeed, it has been shown that when undergoing ionizing irradiation chromatin remodelling impacts the radiosensitivity of the cells, this can result in the apparition of foci in the nuclei (Wang et al., 2017).
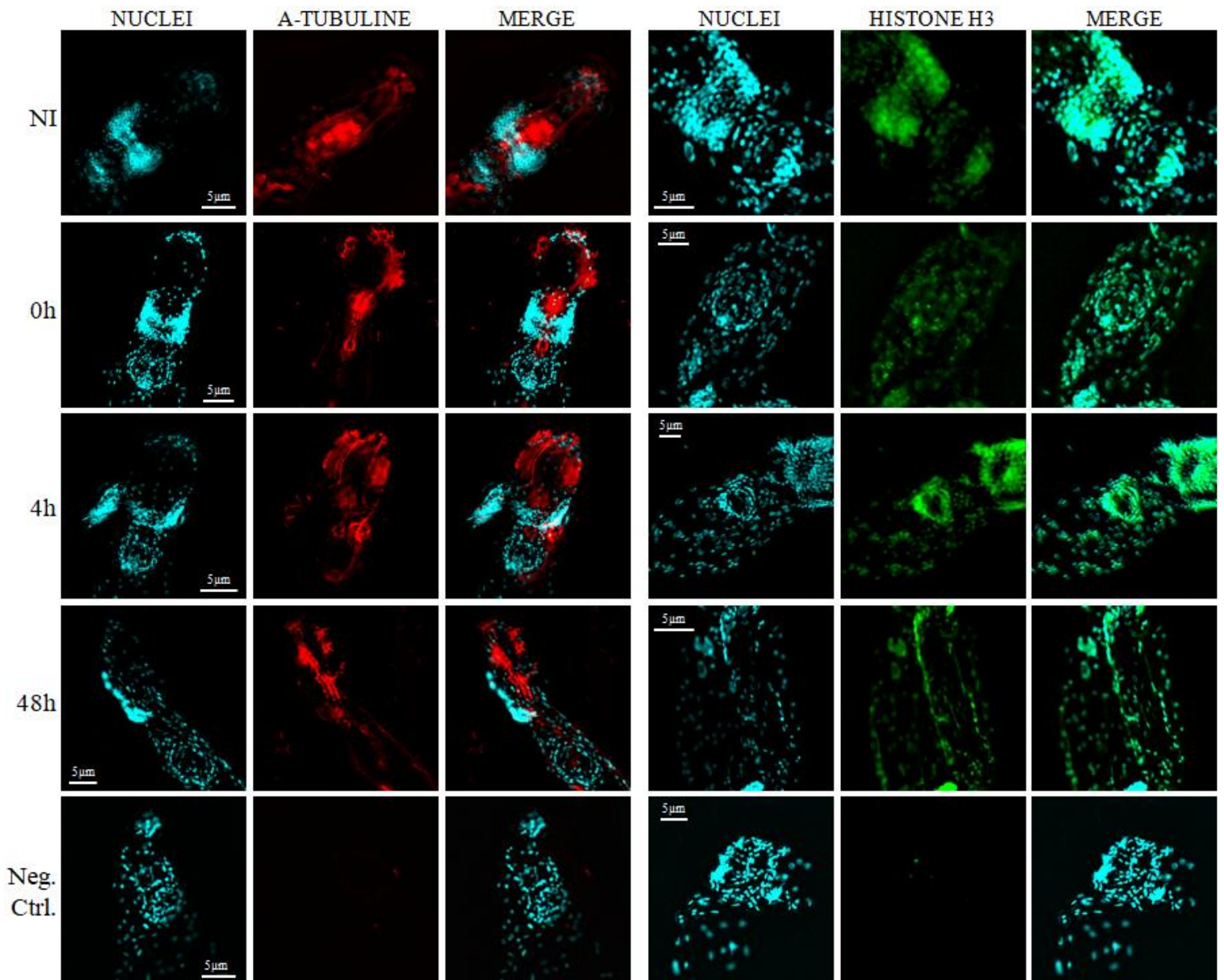
Figure 30 – Protein behaviour upon irradiation. *Adineta vaga* individuals were stained in order to see the integrity and localization of the α-tubulin and the Histone H3 upon 800Gy irradiation. Per condition, 500 individuals were fixed with formaldehyde after a freeze crack permeabilization. After fixation they were blocked with 3% BSA and non-ionizing detergent. DNA was stained with DAPI 1:100 and the primary and secondary antibodies were used at concentrations of 1:150. Rotifers were imaged using the Olympus fluorescent microscope.

Therefore, different behaviour could be expected. First a decrease of signal intensity or even a disappearance of some staining might be observed due to degradation. Second, an increase of signals or apparition of some foci could appear due to a potential aggregation.

In order to study the impact of radiation on bdelloid rotifers proteins, around 500 *A. vaga* individuals were squashed, freeze cracked and fixed with FA. The rotifers were then blocked and stained using antibodies against histone H3 and α-tubulin. This experiment was done on *A. vaga* individuals at different time-points post 800Gy of X-ray irradiation.

When checking the α-tubulin labelling post-irradiation, no differences can be observed between the different time-points and irradiation does not seem to have an impact on the tubulin profile (Figure 30). Indeed, the staining remained visible in the head, foot and digestive track. The same observations can be made for the histone H3 staining. While the staining is faint, the nuclei seem to be quite homogeneously stained throughout the different time-points post-irradiation and with comparable intensities between the different time-points.

4. Set up of neomycin lethal dose in *Adineta vaga* individuals in order to use it as a control for future microinjection and protein inactivation

One of the major objectives to study DNA repair in *A.vaga* is to knock out (KO) major genes and study the impact on bdelloid rotifer DNA repair kinetics. Indeed, ultimately, knowing the impact of complete inactivation or deletion of *Xrcc4* and/or *Rad51* genes within bdelloid rotifers would be a perfect tool to identify their function in DNA DSB repair upon irradiation. Indeed, if XRCC4 or RAD51 are inactivated and DNA repair kinetics are not visible anymore on PFGE profile, it would suggest that those proteins play a critical role in the DNA DSB. Moreover, it may also enable the identification of the NHEJ and/or HR repair pathway. Furthermore, making KO organisms is the one of the most efficient ways to see if antibodies can detect proteins of interest (Bordeaux *et al.,* 2010). Indeed KO organisms do not produce the protein anymore and therefore, it should not be detected during experiment such as WB.

Depletion/ inactivation of a gene can be done by multiple means such as RNA interference (RNAi) and CRISPR-Cas9 (Agrawal *et al.*, 2003). RNAi is a mechanism of post transcriptional gene expression regulation. It requires double stranded short interferent RNA (siRNA) causing specific depletion of an mRNA target containing their complementary sequence (Figure 31A). In the CRISPR-Cas9 system, the Cas9 enzyme causes a DSB at a specific DNA site guided by the gRNA, this break is repaired by NHEJ or HR if a homologous DNA template is provided together with the CRISPR-Cas9 system (Figure 31B) (Agrawal *et al.*, 2003; Bordeaux *et al.*, 2010). When the DSB is repaired by NHEJ, the DNA will suffer some modifications as some bases can be lost or added leading to mutagenesis of the targeted gene. The repair by HR will replace the targeted gene by the provided homologous template that may contain some mutations.

In order to study the *A. vaga* DNA repair mechanism using CRISPR-Cas9 or siRNA, microinjection is a crucial step that needs to be crossed. The aim is to microinject it inside their germovitellarium with a microinjector. *A. vaga* possesses two germovitellaria each made of a germarium (undifferentiated cells that form oocytes, nurse cells, and follicular cells (Hespeels, Flot, *et al*., 2014)) and a vitellarium (syncitial nurse gland) (Ricci & Fontaneto, 2009; Wigglesworth, 2017). Therefore, by microinjecting in their germovitellarium, a syncytial tissue, there is a chance that the oocytes can be reached through diffusion (Figure 31C).
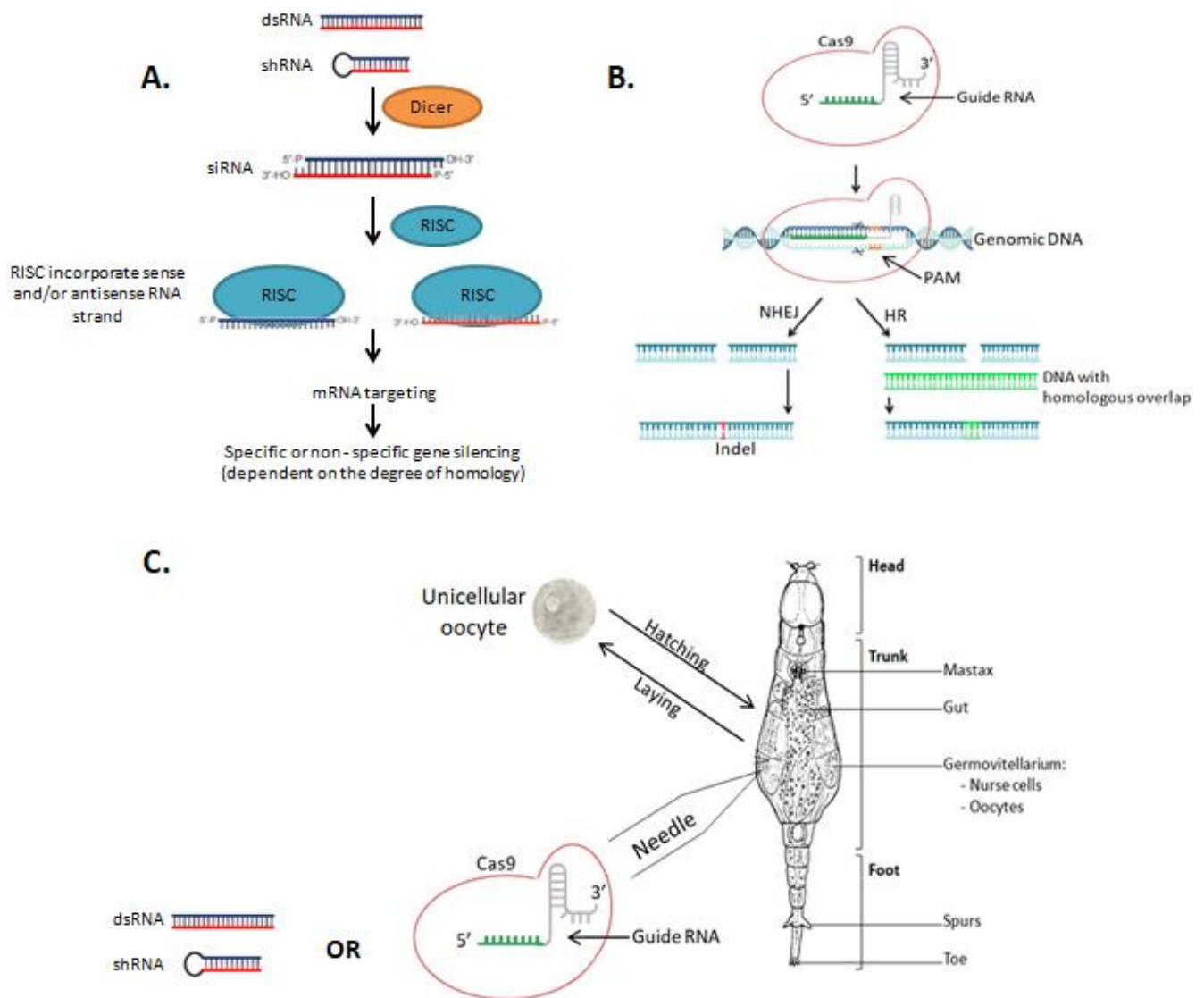
Figure 31 - Microinjection in an adult *A. vaga.* (A) RNAi is a two-step pathway involving ribonuclease enzymes Dicer and RISC. The RNAi starts by the processing of double stranded RNA (dsRNA) or short hairpin RNA (shRNA) into siRNA by the Dicer RNase. The siRNA is then incorporated into the dynamic multiproteic complex RISC (RNA-induced silencing complex). The ssRNA-RISC complex hybridizes with the mRNA target resulting in gene silencing by nucleolytic degradation. If the siRNA/mRNA duplex contains mismatches non-specific silencing can occurs (Agrawal *et al*., 2003). (B) CRISPR-Cas9 system is formed with two components: a Cas9 enzyme and a guide RNA that allows Cas9 to target a specific DNA region (with the guide sequence in green). The gRNA is composed of a Cas-binding scaffold sequence (grey) and a spacer sequence (green) that defines the genomic target. The target sequence is followed by a protospacer adjacent motif (PAM, orange) which differs depending on which Cas protein is used. Cas9 unzips the double helix, cleaves a given locus if sufficient homology is shared. The cleavage causes a DSB that can be repaired either with NHEJ or with HR if a homologous DNA template is provided together with the CRISPR-Cas9 system (Addgene, 2019). (C) Schematic representation of a bdelloid rotifer being microinjected with a CRISPR-Cas9 complex or dsRNA, implicated in RNA interference, inside its germovitellarium. Oocytes present are in a one-cell state, they will undergo mitosis with modification in every cell of the clone it will produce.

Oocytes are in a 1-cell state, therefore if they are modified with the CRISPR-cas9 system or by siRNA, the adult developing from this oocyte should have the modified gene in all its cells.

It has been shown in *C. elegans* that CRISPR-Cas9 or siRNA can enter nuclei through diffusion (Conte *et al*., 2015). *C. elegans* possesses a syncytium with stem cells that once microinjected can be modified with CRISPR-Cas9 (Amsellem & Ricci, 1982).

In order to confirm that the microinjection worked, protocols will be developed using a fluorescent dye. If after microinjection the individual can be seen through fluorescence, this confirms that the microinjection worked (figure 32). Common methods to detect specific gene knockdown by RNAi is to look at the target proteins behaviour through IF and WB using the specific antibodies (Agrawal *et al*., 2003). However, with bdelloid rotifers, WB and IF require either a large number of individuals or a long optimization. Therefore, the RNAi could be studied by performing RT-qPCR or by silencing genes that would result in obvious phenotypical modifications (e.g. inhibiting unc-22 in *C. elegans* gives twitching phenotypes). Finally, to observe if CRISPR-Cas9 has managed to reach the oocytes, different methods could be used. The first one is by PCR to identify the DNA damages at the CRISPR-Cas9 targeted loci.

However, another way to control if the CRISPR-Cas9 modification worked would be to incorporate an antibiotic resistance sequence by HR. Antibiotic resistance gene are commonly used for positive selection of cells that integrated the resistance cassette into their genome (Hall *et al*., 2009). Therefore, rotifers that resist the presence of the antibiotic would be the ones that have successfully been injected and modified with CRISPR. Furthermore, after the hatching of the oocyte coming from a microinjected mother, young individuals could be put in contact with spa water containing a lethal dose of this antibiotic. Therefore, using a resistance cassette gene could help, when growing populations of microinjected rotifers, to select organisms that indeed were modified.

In order to identify a lethal dose, a drug assay was performed on *A. vaga* with neomycin (G-418). The neomycin is the most common drug used for positive selection. Neomycin is an aminoglycoside interfering with protein synthesis in eukaryotic cells by inhibiting the elongation step of the polypeptide. The resistance cassette encodes for a phosphotransferase enabling resistance to neomycin (Hall *et al*., 2009).

We started by testing a large range of concentrations from 50 to 2500 µg/mL neomycin. Afterwards, concentrations between 50 to 500 µg/mL were used to determine more specifically the lethal dose for *A. vaga*.

When looking at the survival rate (Figure 33), we observed that after 2 days being in a medium containing neomycin at 300 µg/ml all *A. vaga* individuals died. We would therefore choose a concentration of 300 µg/mL for resistance selection. A higher concentration would not be chosen because it could lead to side-effects of the drug at high doses.

In addition to measuring the neomycin lethal dose, micro-injection protocols were started on 1-cell eggs and on adult individuals (Figure 32). In a petri dishe, an *A. vaga* individual was immobilized using a suction needle. The captured bdelloid rotifer was then microinjected with dextran-GFP around their germovitellarium. However, actually no micro-injection trials managed to introduce dextran-GFP within the organisms and keeping them alive.
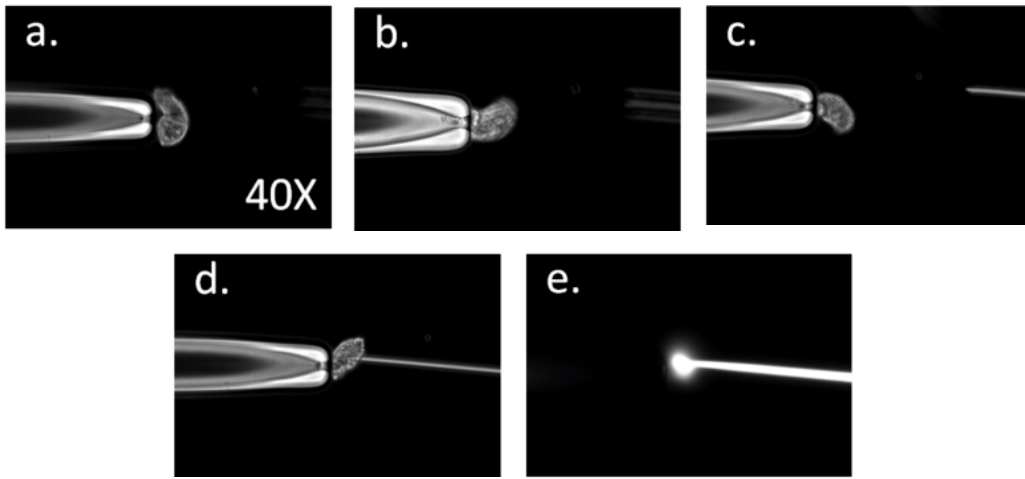
Figure 32 – Micro-injection in an *Adineta vaga* individual.

    a. An *A. vaga* is trapped at the "suction" position
    b. Capture of the individual
    c. Setting up the injection needle
    d. Micro-injection of the individual
    e. Visualisation of the Dextran-GFP injected

These micro-injection trials were made using an Olympus fluorescent microscope and a Narishige micro-manipulator andmicro-injector.
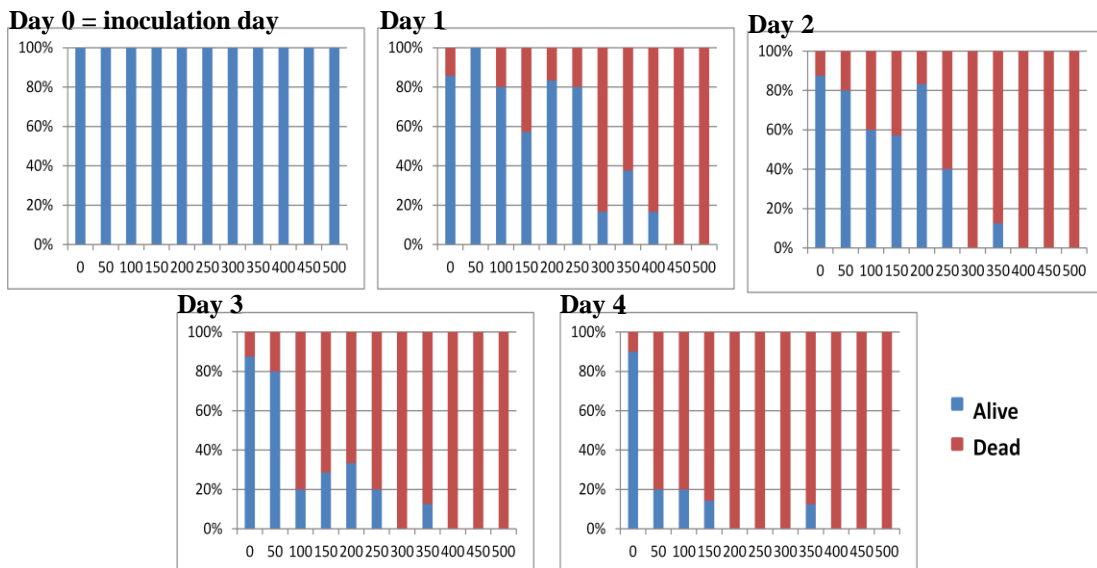
Figure 33 – Neomycin drug assay. To find the lethal dose of neomycin (G-418) needed to kill *Adineta vaga*, the survival of 8 individuals was measured during five days of exposure (Day 0 - 4). They were exposed to a concentration varying from 0 to 500 µg/mL. The blue bars represent the survival of the rotifers and the red bars represent their mortality.

5. Discussion

Adineta vaga is a bdelloid rotifer that has an extreme resistance to ionizing radiation causing DNA DSBs at a rate of ~0.004 DSB/Gy/Mbp (Daly, 2012). This resistance is associated with a capacity to prevent protein carbonylation (Krisko *et al*., 2012) and efficiently repair their DNA after high doses of radiation. However, the exact mechanism involved in DNA repair is not yet understood. Therefore, it would be interesting to discover the secret behind their DNA repair mechanisms and their extreme resistance.

In the present Master thesis, we managed to set up experimental conditions to perform RT-qPCR, WB with whole protein extracts of bdelloid rotifers and IF on fixed animals. At the exception of RT-qPCR, WB and IF procedures were never developed before for any bdelloid rotifer species. Optimising such methods will be of a great interest for the future experiments of the community working with similar organisms. In the host lab, these experimental pipelines will be used in future experiments to determine if either NHEJ or HR are active in the DNA repair of bdelloid rotifers upon irradiation.

When looking at PFGE results of irradiated rotifers, the DNA profile showed that repair does occur after creating DSBs in their DNA. In order to discover if HR or NHEJ is active inside irradiated bdelloid rotifers, we decided to look upon gene expression of genes responsible for the production of proteins implicated in these mechanisms by RT-qPCR. Therefore, with probes designed using the *Adineta vaga* assembled genome, the gene expression profile was analysed for Xrcc4 complete and partial genes (*Xrcc4_1* and *Xrcc4_2*) and for *Rad51* and *Rad51-Like* four different genes (*Rad51_1*, *Rad51_2*, *Rad51_L1* and *Rad51_L2*).

The first results from the RT-qPCR analyses was the constitutive expression of *Xrcc4* and *Rad51*. In non-irradiated conditions, *Rad51_L1* and *Rad51_L2* seem barely expressed in comparison to the other DNA DSB repair genes (***$P < 0.001$). On the other hand, even though all of the genes seem to show a constitutive expression, *Xrcc4_1* appears to be more expressed than any of the other genes (**$P < 0.01$ and ***$P < 0.001$). This is an interesting result as the somatic cells, which form the majority of the animal, are in G0/G1 phases and therefore their DNA are more likely to be repaired by NHEJ when encountering a DSB. Therefore, a constitutive expression of *Xrcc4* could help them repair quickly if the mRNA is ready to be translated at any time.

Upon encountering ionizing radiation, it can be seen that the gene expression of the genes of interest were changing. The significant higher expression of *Xrcc4_1* at early time-points (***$P < 0.001$) supports the hypothesis of NHEJ being involved but *Rad51_1*, although at a later time-point, also show a significant increase of gene expression after being exposed to ionizing radiation. Interestingly *Rad51_2* did not follow the same expression increase. This is not an unexpected pattern as it has been shown in plants, such as in the degenerate tetraploid *Coffea Arabica*, that homeolog gene silencing can be quite common (Vieira *et al*., 2019). Furthermore, the increase of expression is visible from time-point 2h for *Xrcc4,* and time-point 24h for *Rad51*, till time-point 48h when they seem to reach a peak of expression and then decrease. Interestingly, this correlates with the timing of the maximal DNA repair according to PFGE analysis. Indeed, at 48h the DNA repair profile is not evolving anymore on PFGE. These RT-qPCR profiles strongly suggest that XRCC4 and/or RAD51 are involved in DNA repair of *A. vaga*.

The variation of expression level of *Rad51_Like proteins* seems to illustrate another pattern of expression as unlike the other genes, its expression seems to be decreasing (*P< 0.05 and **P<0.01) until the time-point 24h. This could be explained by the fact that during extreme ionizing radiations, organisms would focus on expressing genes that are necessary for survival. Even though the increase of *Rad51_Like* has been shown to occur in other irradiated organisms, like human lymphocytes, they might not be crucial in bdelloid response to ionizing stresses (Fachin *et al*., 2007).

Bdelloid rotifers are multicellular eutelic organisms composed of 1,000 somatic cells in a G0/G1 state and oocytes in a G2 cell cycle state (Terwagne et al., in prep). Therefore, NHEJ would be more likely to occur in the somatic cells while the oocytes might be repaired by the HR mechanisms. However, this remains hypothetical at this stage.

Upon ionizing radiation, the general transcriptional apparatus can be impacted either by a decreased efficiency of the DNA-polymerase enzyme, or by a signalization cascade that favors pathways such as DNA DSB repair or DNA damage response (DDR). Indeed, it has been observed that upon IR cells undergo gene expression re-programming to strategically increase the expression of genes mandatory for the organism survival (or for apoptosis when the stress in too strong). Furthermore, it has been shown that ionizing radiations impact the post-transcriptional regulation of RNA, i.e. mRNA and Small noncoding RNAs (sRNAs). Indeed, the stability of expressed mRNA, therefore its post-transcriptional regulation, might play a role in DNA damage responses upon ionizing radiation (Venkata N. *et al*., 2017). Furthermore, sRNAs (<400 bp) are posttranscriptional regulators playing essential roles in response mechanisms to environmental stresses. When organisms suffer from environmental changes, these sRNAs possess the ability to simultaneously switch on and off a variety of metabolic pathways in response to environmental signals. In *D. radiodurans*, a radio-resistant species, it has been shown that sRNAs might play a role in their resistance to ionizing radiation by the regulation of pathways implicated in their survival (e.g. DNA DSB repair mechanisms) (Tsai *et al*., 2015).

Interestingly, at time-point 24h the genes that were not showing any increase in expression profile (*Xrcc4_2*, *Rad51_3*, *Rad51_L1* and *Rad51_L2*) suddenly increased their expression while the one that were highly expressed decreased (arrows Figure 17). This could be linked with the PFGE results. At time-point 24h, bigger fragments of DNA are again observed. Therefore, we might speculate that at time-point 24h the DNA fragments would be sufficiently repaired for the "general" transcription machinery to restart.

As RT-qPCR analyses showed the impact of ionizing radiation on the gene expression levels of specific DNA repair genes, we decided to also study the proteins of interest using western blotting (WB).

Using a WB approach, a reproducible protein extraction method was needed. Several buffers were tested and the one with a high salt buffer gave the best results for the nuclear fraction, allowing us to work on nuclear proteins. High salt concentration enhances nuclear membranes breakdown, solubilises chromatin-bound proteins, and thus increase their concentration in the final whole protein extract (Bass *et al*., 2017).

Therefore, the WB experiments were repeated using biological duplicates and we observed a lot of variability between replicates. This increasing variability, showing inconsistent results, was puzzling. Quantification measurements of the WB results only confirmed this observation. Therefore, the focus was made on the technical manipulations of rotifers during such experiments to standardize as much as possible. The question of rotifer cuticle weakening during ionizing radiation was assessed for protein extraction manipulation. Indeed, for protein extraction a mechanical lysis is performed using dounces and lysis is enhanced by using high salt buffer. Could this mechanical lysis impact ionized rotifers at a stronger level than non-ionized ones? Maybe the number of dounces were too high for irradiated rotifers than in addition to being permeabilized, ionized bdelloid rotifers proteins could be impacted. The experiment designed to answer this question showed that with few numbers of dounces (i.e. 100 dounces) the protein extraction was not optimal as the resulting concentration was too low. When undergoing 500 or 1000 mechanical dounces, the protein extraction concentration was higher and similar. However, the bands observed at 1000 dounces in irradiated and non-irradiated rotifers showed the same profile, no degradation profiles were seen in the irradiated condition.

Second, we tested whether high salt quantities in WB samples did impact the experiment and created the variability observed between replicates? After performing the WB experiment some differences could be seen between the 75k and the 150k rotifer samples in irradiated conditions. Indeed, it has been shown that high quantities of salt can cause migration problems due to the ions present in the sample or by osmoses resulting in large and "weird" shaped bands (BioRad, 2019; Uppsala, 2016). However, during our different WB analyses, such "strange" migration never occurred. Using the biological quadruplicates, the expression profile, the quantification and the quantity of protein extract in the samples were compared. This showed that the variability did not seem to originate from salt differences present in our samples as no clear correlation could be made between replicate variability and salt concentrations.

To conclude, WB results showed variability between samples, providing inconsistent results. However, in every WB experiment, a protein signal could be seen for XRCC4 and RAD51 at the expected molecular weight suggesting a constitutive production of the proteins. Constitutive production of the proteins, independently of the irradiation, correlates with the RT-qPCR results on non-irradiated rotifers that also showed constitutive gene expression.

Even though there is some variability, one main profile that could be observed is a decrease of signal at the 0h time-point in comparison to the non-irradiated state for both XRCC4 and RAD51. This is not observed in the qPCR analyses showing an increase of expression of *Xrcc4* and *Rad51* at early time-points while WB showed a tendency to decrease XRCC4 and RAD51 expressions at early time-points. However, this difference remains doubtful due to the technical issues of the WB experiment. Therefore, the focus should be on the RT-qPCR analyses as the results were consistent among replicates.

Finally, in order to see the impact of ionizing radiation on WB analyses, the variability in the results could be avoided for example dialyzing the samples, homogenizing the salt quantity in the samples, test the impact different mechanical lysis in order to have the same lysis between samples, etc.

Another experiment that was done to see if ionizing radiation could have an impact on proteins is immunofluorescence. Since RT-qPCR and WB analyses showed a constitutive production of the proteins XRCC4 and RAD51, studying their localization and "behaviour" upon irradiation using IF could be very informative.

However, like other experiments, IF required first some optimization steps on bdelloid rotifers. Therefore, different trials and errors were done. In the end we managed to reach an IF protocol that seemed to be working with the commercial antibodies directed against α-tubulin and histone H3 of *Adineta vaga*. However, after many attempts we did not manage to stain the rotifers using the polyclonal antibodies directed against XRCC4 and RAD51.

First and foremost, the negative control using only the secondary antibody showed some signals. This could suggest that the washing and the blocking (using BSA) need to be more stringent or maybe another blocking agent could be tried such as NFDM that in the WB experiment showed less non-specificity than BSA. The signals however observed in the labelled samples were more intense than the negative control showing some labelling. Many reasons could be at the origin of IF troubleshooting but labelling troubles mainly come from the ability of the antibody to bind to the antigen. Like for the WB experiment, the fact that the proteins were produced in guinea pig might impact the detection. While for the WB experiment, the proteins are partially denatured, which might help more antigen availability for the antibodies, the native conformation of the bdelloid rotifer proteins during in vitro experiments might impact the detection. However, it can also be seen during WB experiments that antibodies are non-specific especially when using BSA as blocking agents, this non-specificity could also be seen in the IF experiment. Therefore, this labelling trouble could be linked to the realization of the experiment itself. Finally, it has to be kept in mind that even though most of the commercial antibodies are designed for different experiments including WB, IF, ELISA, etc., it is not always the case. Therefore, our antibody against XRCC4 and RAD51 might be working for WB but not for IF.

Since the IF experiment did not worked with XRCC4 and RAD51, IF was performed with the Histone H3 and the α-tubulin antibodies following irradiation. The result did not show an impact of the irradiation on the protein fluorescence profile. This could be explained by a good protection of the proteome in bdelloid rotifers or by the fact that these proteins are present in sufficient quantity and subtle modifications cannot be seen. A protection of the proteome correlates with the Coomassie blue staining showing similar protein profiles in the batches of irradiated and non-irradiated rotifers. However, these analyses should be repeated in order to confirm these observations with other groups of irradiated rotifers. Furthermore, it would be interesting to observe the slides using a confocal microscope as it might show a more precise image and eventually subtle changes might be observed.

No matter how efficient the DNA repair mechanisms are in *Adineta vaga*, it is not the only mechanism behind rotifers' resistance. Since ionizing radiation stimulates the production of ROS, it causes oxidative damages to proteins impacting their functionality and efficiency (Daly, 2012; Krisko & Radman, 2010). In order to overcome this, resistant organisms developed effective antioxidant protections. *A. vaga* possesses enzymes (e.g. superoxyde dismutase), and non-enzymic free-radical scavengers (e.g. ROS-scavenging manganese complexes) that are upregulated upon undergoing stressful experiences (Berjak, 2006).

Therefore, their extreme resistance might not be due to an extremely efficient DNA repair mechanism but due to a better protection of the proteome, a protection that allows proteins, such as XRCC4 and RAD51, to work even under high doses of ionizing radiation. In addition to proteome protection, another factor impacting the effectiveness of the DNA repair could be gene redundancy. Indeed, the RAD51 protein can be expressed by two different genes (Hecox-Lea & Mark Welch, 2018). Even though, in the case of RAD51, it would seem that those genes might be silenced in bdelloid rotifers (e.g. *Rad51_2* barely expressed upon irradiation), it has been seen in polyploid organisms that when genes become unable to perform, usually silenced redundant genes can take their place (Vieira, 2019). That redundancy could be another survival resistance mechanism of *A. vaga*. If the protein is suppressed or lose its activity, another non-affected copy of the protein could take its place in the DNA repair mechanism.

In the environment, organisms are never exposed to thousands gray of ionizing radiation, why would rotifer be able to resist to such high doses? Two still ongoing hypotheses could explain why bdelloid rotifers exhibit incredible resistances to stresses leading to DNA damages. They are often called the "desiccation-adaptation hypothesis" and "radiation-adaptation hypothesis" (Berjak, 2006). The "desiccation-adaptation hypothesis" is based on the type of habitats of bdelloid rotifers. *A. vaga*, can be found in semi-terrestrial environments that undergo frequent drought episodes. Therefore, these bdelloid rotifers are able to survive desiccation and enter a stage of life suspension, anhydrobiosis (Crowe *et al*., 1992; Ricci & Fontaneto, 2009). It has been shown that desiccation is associated with many damages including DNA DSB (Hespeels, Knapen, *et al*., 2014). Therefore, surviving desiccation requires the ability to maintain functional macromolecules, i.e. DNA and proteins, and membranes (Hespeels, Knapen, *et al*., 2014; Tunnacliffe *et al*., 2005). This maintenance can be achieved either by preserving the integrity of these molecules using antioxidants and LEA proteins or by repairing damages that occurred, such as efficient DNA repair mechanisms (Gladyshev & Meselson, 2008; Tunnacliffe *et al*., 2005). All these adaptations to resist desiccation could have had an impact on *A. vaga's* ability to resist irradiation since the damages it causes (DNA DSBs and oxidative stress) are similar to the desiccation damages (Azzam *et al*., 2012). Thus, the resistance mechanisms that bdelloid rotifers developed could be due to an evolutionary adaptation to a desiccation-prone environment.

The "radiation-adaptation hypothesis" is also based on an extreme environment resistance that bdelloid rotifers managed to "conquer", i.e. permafrosts and thaw lakes (Bégin & Vincent, 2017). In such environments, ionizing radiation of relatively low intensity can accumulate creating damages that piles up in cryopreserved organisms (Cheptsov *et al.*, 2018). These damages caused by accumulated irradiation are DSBs, lipid peroxidation and protein oxidation, similar to desiccation damages (Cheptsov *et al.*, 2018; Hecox-Lea & Mark Welch, 2018). When the permafrost is thawing, organisms that accumulated damages need to be able to repair them in order to survive and reproduce. Therefore, the defence mechanisms that bdelloid rotifers developed against these accumulations of irradiation damage could also be at the origin of their ability to survive in ephemeral water environments.

In addition to desiccation and radiation, bdelloid rotifers efficient DNA repair and high resistance to stresses might come from their mode of reproduction. *Adineta vaga* reproduce through an apparent obligate parthenogenesis, a monoparental mode of reproduction based on mitotic divisions of oocytes or a modified meiosis (Krisko, Leroy, Radman, & Meselson, 2012).

The individual produced is therefore a clone of its mother (Krisko *et al.*, 2012; Mirzaghaderi & Hörandl, 2016). As an asexual, following the Muller's ratchet principle, rotifers would accumulate deleterious mutations that would lead to the extinction of the species (Maciver, 2016) unless they have a mechanism preventing mutation accumulation. Repairing frequently DNA DSBs through homologous recombination in its germline following cycles of desiccation could be a putative mechanism preventing this increase of deleterious mutations in their genome, leaving signatures of gene conversion.

On the other, it hand has been shown that asexual organisms posses a larger geographical distribution area than their sexual relatives. This phenomenon, called geographical parthenogenesis, is therefore an exception in the predominance of sex in nature. Furthermore, according to Baker's law, since there is no need of a mating partner for founding a new population, uniparental reproduction is advantageous for colonization (Baker 1965, 1967; Cosendai *et al.*, 2013). Additionnaly, the Baas-Becking's hypothesis (aka the 'everything is everywhere' hypothesis) state that microscopic organisms are globally distributed due to high dispersal resulting of small size and an ability to enter dormancy (Baas_Becking, 1934; Fontaneto *et al.*, 2008).

Finally, bdelloid rotifers are asexual micro-organisms, however their reproductive rate is quite low in comparison to other organisms therefore the ability to resist many stresses and colonize new environment through a single asexual female might be another key player explaining their evolutionary success large broad-scale distributions. Bacteria, such as *E. coli*, presenting moderate stress tolerances were also able to conquer many ecological niches based on other strategies, fast multiplication and genetic shuffling. However, this strategy leads to many deaths in the bacterial population when there is a sudden environmental modification but the species is maintained because population are large and because there are always a few individuals that are genetically different that will start a new population (Jayaraman, 2011).

CONCLUSIONS AND PERSPECTIVES

Adineta vaga, microscopic metazoan, is an organism that has shown numerous times an ability to survive extreme conditions. This can be directly observed through their survival rate after undergoing ionizing radiation (up to 2,000Gy). In many organisms, it has been shown that the mortality of ionizing radiation is linked to an accumulation of DNA DSBs and enhanced oxidative stress following radiation. However, even though A. vaga also suffers from those DNA DSB accumulations, they manage to repair them. Therefore, different questions can be asked such as: is their survival linked to their DNA DSB repair mechanisms? Which DNA DSB repair mechanisms does A. vaga use? How does it protect his DNA repair proteins?

The objective of this master thesis was to participate in the discovery of their DNA DSB repair mechanisms. Looking at the literature and previous results, we decided to focus our research on the two main DNA DSB repair mechanisms present throughout the tree of life: NHEJ and HR, with a specific focus on the proteins XRCC4 and RAD51.

Upon working on this subject, using transcriptomic analyses, A. vaga showed a constitutive expression of the genes XRCC4 and RAD51. The constitutive expression of DNA DSB proteins can be observed in many organisms, this could be a way for them to be ready whenever a DSB occurs. However, in the case of A. vaga, it seemed that Xrcc4 might be more expressed. Furthermore, ionizing radiation seemed to have an impact on XRCC4 and RAD51 expression as their gene expression seemed to vary depending on the time post-irradiation.

Furthermore, during the start of my master thesis we have made an extraction buffer that allowed us to reach the nuclear proteins. Analysis of irradiated rotifer protein profiles seemed to indicate an impact of ionizing radiation on DNA DSB repair mechanism. However, upon performing biological replicates, a high level of variability in the results was observed which might be due to the manipulation of the rotifers. Therefore, apart for a constitutive expression of our proteins in the non-irradiated state, no conclusion can be drawn for the impact of ionizing radiation on protein expression using the Western blot experiment.

Finally, an IF protocol was developed using antibodies against the α-tubulin and the Histone H3. Furthermore, optimizations are still needed in order to use IF experiments with the antibody against XRCC4 and RAD51. However, the study of the impact of ionizing radiation on the labelling profile of α-tubulin and the Histone H3 was performed. At different time-points upon ionizing radiation, the α-tubulin and the histone H3 staining did not seem to vary. It could be speculated that in addition to an efficient DNA DSB repair mechanism, the extreme resistance of bdelloid rotifers to ionizing radiation comes from their proteome protection, through an efficient antioxidant mechanism.

Scientists are still uncertain about the origins of their resistance. Hypotheses are still being debated and it could come from their adaptation to desiccation, to radiation accumulation in extreme environments or even to a combination of these factors. Finally, asexuality associated with effective DNA repair mechanisms might have helped bdelloid rotifers to survive for millions of years without sex without accumulating deleterious mutations as expected for most asexual lineages.

In order to progress on the deciphering of DNA DSB repair mechanisms in the bdelloid rotifer *Adineta vaga* different aspects of this phenomenon could be studied. A few examples can be found below:

a. **Confirmation of the RT-qPCR results.** This should be done by realising a biological triplicate**.** Furthermore, to complete the study of the RNA, mRNA FISH could be used to localize the subcellular expression of the different RNAs.

b. **Getting rid of the WB variability**. The WB showed lots of variability. This can be due to a accumulation of factors such as the impact of salt and the mechanical lysis. It might also be the consequence of other aspects of our analysis we have yet assessed or even due to biological reasons. However, it would be informative to be able to see the impact of ionizing radiation for XRCC4 and RAD51 protein profile expression. Therefore, the lysing method could be improved by testing other mechanical lysis such as beads. Using monoclonal antibodies instead of polyclonal could reduce the non-specificity. By precaution, the quantity of salt should be harmonized between samples even though no direct effect seems to be observed.

c. **Optimization of the IF approach.** Optimization of the IF experiment using XRCC4 and RAD51 by trying different blocking agents or incubation periods. Furthermore, it would be interesting to compare staining of the general histone H3 with specifically modified histone H3 like the H3K9m3, implicated in chromatin remodeling (Wang *et al.*, 2017). In human cells, it has been evocated that histone methylation could be implicated in the DNA repair pathway choice, e.g. H3K36me3-enriched loci might prefer HR while H4K20me2 can recruit 53BP1 for NHEJ repair (Wei *et al.*, 2018).

d. **Inactivating genes**. The micro-injection protocol will be further developed and will be used for the CRISPR-Cas9 or siRNA experimental set up. This could allow us to see the behaviour of KO bdelloid rotifers for DNA DSB repair proteins. Even though siRNA is an experiment that might be easier to set up than CRISPR-cas9, it causes mainly gene knock down with an average efficiency of 70% (i.e. 30% of mRNA is not impacted) and off target effects can be high. Furthermore, the dsRNA would have to be stabilised in a complete population and over a long period of time. Therefore, if micro-injection succeeds, it might be interesting to focus on CRISPR-cas9 first.

c. **Analysing desiccated rotifers**. During this Master thesis, during the ionizing radiation bdelloid rotifers were in a hydrated condition. This means that *Adineta vaga* individuals could start repairing during exposure to ionizing radiation while breaks accumulate. Therefore, it would be interesting to desiccate bdelloid rotifers prior to irradiating them. Indeed, in anhydrobiosys, the bdelloid rotifers have a metabolism slowed down and do not repair DNA DSB. By performing ionizing radiation on desiccated individuals, DSB would accumulate and the individuals would repair them only after re-hydration. This might show us a « real » 0h time-point post-ionizing radiation

d. **Uncovering potential impacts of ROS**. Indeed, ROS causes irreversible negative modifications to proteins by carbonylation, it could be interesting to evaluate the carbonylated states of the proteins (Daly, 2012). Furthermore, in addition to the protein stability, ROS might impact RNA stability, therefore it would be interesting in our RT-qPCR to quantify the quantity of stabilized and newly transcribed RNA (Ventaka *et al*., 2017). Furthermore, sRNAs might have an impact on transcription regulation in D. radiodurans upon encountering ionizing radiation. It could be interesting, like in *D. radiodurans*, to identify such sRNA using whole-transcriptome deep sequencing by performing Small RNA Illumina, sequencing the result and analyze them and their potential activity in radiation-resistance (Tsai et al., 2015). *A. vaga*, also radio-resistant, might possess the same kind of transcription regulation upon ionizing radiation.

f. **Localizing DSBs.** A way to observe and localize DNA DSBs would be very informative since bdelloid rotifers do not possess H2AX, an important DNA DSB sensor (Van Doninck *et al*., 2009). Therefore, it could be interesting to study other potential sensors such as the SIRT6 (Lior *et al*., unpublished – 2019) and the protein ATM at the origin of the activation of DDR and DNA DSB repair pathways (Ventaka *et al*., 2017). A SIRT6 homolog present in *A. vaga* genome would be verified by blasting the gene sequence on the chromosome-scale haploid genome assembly of *A. vaga* (Narayan *et al*., in prep.).

g. **Discovering potential new DNA DSB repair mechanism**. During this master thesis, even though based on previous analyses, we assumed that *Adineta vaga* might possess NHEJ or HR. However, bdelloid rotifers might also have developed another efficient mechanism, different from NHEJ or HR. With this idea in mind, a comparative proteomic analysis is realised without a priori in order to discover potential other proteins implacated in DSB repair.

Annex A - qPCR complementary informations

A. RT-qPCR primers specificity and efficiency

Gene	Efficiency (% - log)			Slope	R²
HSP70	97,57	-	1,99	-3,37	0.995
GAPDH	88,58	-	1,95	-3,63	0.991
Xrcc4_1	84,24	-	1,93	-3,77	0.997
Xrcc4_2	104,27	-	2,02	-3,22	1.000
Rad51_1	93,23	-	1,97	-3,50	0.992
Rad51_2	94,8	-	1,98	-3,45	0.998
Rad51_L1	110,38	-	2,04	-3,10	1.000
Rad51_L2	135,04	-	2,13	-2,67	0.967

Performance of the RT-qPCR assay and primers efficiency verified by performing calibration curves using tenfold serial dilutions and assessing the PCR efficiency. The standard curves showed an R^2 of 0.967 or more with an efficiency varying between 84 and 135%. Seeing the efficiency and slope of *Rad51_2* every analysis performed on this gene were made with caution.

B. PFGE analysis of the effect of 800Gy ionizing irradiation on *Adineta vaga* genome using bdelloid rotifers used for the RT-qPCR experiment
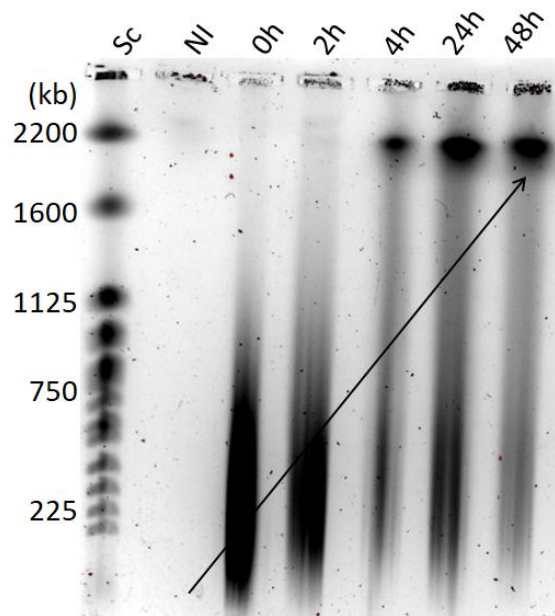
The different lanes of the gel contain the DNA profile of 1,000 individuals showing that with time bigger DNA fragment are formed. This could be due to DNA repair mechanisms such as NHEJ or HR.
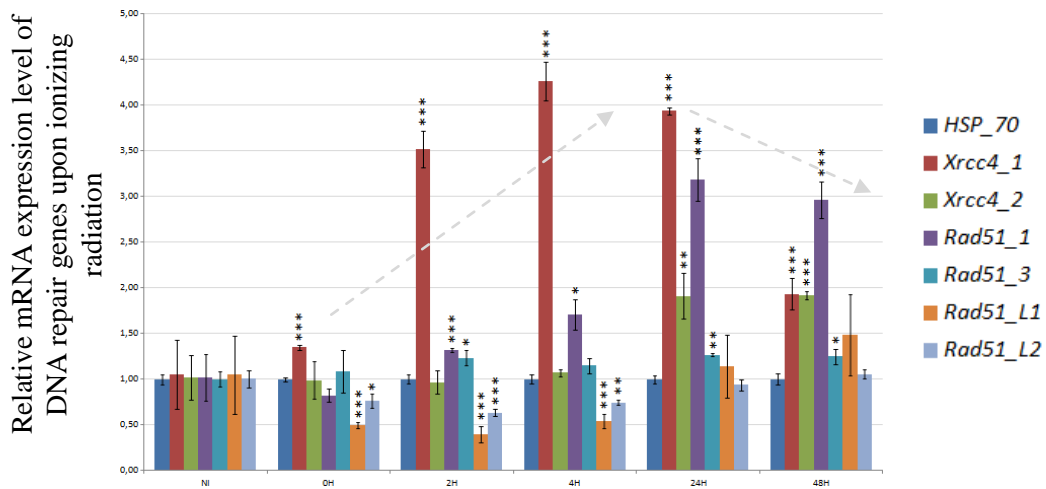
C. Amplicon verification by cloning & sequencing

| Query	Subject	% similarity	Alignment length	Nb mismatch	Nb indels	Start Query	End Query	Start on subject	End on subject	E-value	Bit score
*GAPDH*_Cloning	Chrom_2	93.617	47	2	1	1	46	1651669	1651623	2.67e-11	69.4
		99.405	168	0	1	33	199	1651580	1651413	6.71e-82	303
*HSP70*_Cloning	Chrom_4	98.964	193	2	0	1	193	13618919	13618727	1.06e-94	346
*XRCC4_1*_Cloning	Chrom_5	98.947	95	1	0	1	95	12157090	12157184	7.87e-42	171
		100.000	57	0	0	94	150	12158826	12158882	2.25e-22	106
		100.000	69	0	0	151	219	12158949	12159017	4.81e-29	128
*XRCC4_2*_Cloning	Chrom_2	97.500	120	2	1	76	195	1761702	1761584	6.84e-52	204
		97.333	75	2	0	1	75	1761827	1761753	4.24e-29	128
*RAD51_3*_Cloning	Chrom_5	100.000	148	0	0	1	148	10243206	10243353	5.35e-73	274
		96.552	58	2	0	145	202	10243400	10243457	1.24e-19	97.1
*RAD51_L1*_Cloning	Chrom_2	99.010	202	2	0	1	202	6529054	6528853	1.11e-99	363
*RAD51_L2*_Cloning	Chrom_6	98.561	139	1	1	1	139	10601300	10601163	4.20e-64	244
		100.000	68	0	0	135	202	10601111	10601044	1.59e-28	126

C. *Adineta vaga* mRNA kinetics after 800Gy irradiation using *HSP70* as housekeeping gene

Gene expression of DNA repair mechanism proteins upon 800Gy ionizing radiation realised in technical triplicates. The expression was measured using RT-qPCR analyses on RNA from *A. vaga* individuals exposed to X-ray IR. The analyses were performed on 8 different targets: *Xrcc4_1*, *Xrcc4_2*, *Rad51_1*, *Rad51_2*, *Rad51_L1* and *Rad51_L2*. The relative expression levels were referred to the expression of *HSP70*. The Data represent the mean ± standard deviation. Two-tailed P values were calculated between indicated column and its left adjacent column using Student's t-test (*, P<0.05; **, P<0.01; ***, P<0.001). This statistical analysis allows us to see the variation of gene expression at different time-points post irradiation in comparison to the non-irradiated (NI) gene expression level.

## D. *Adineta vaga* DNA repair mechanisms genes expression
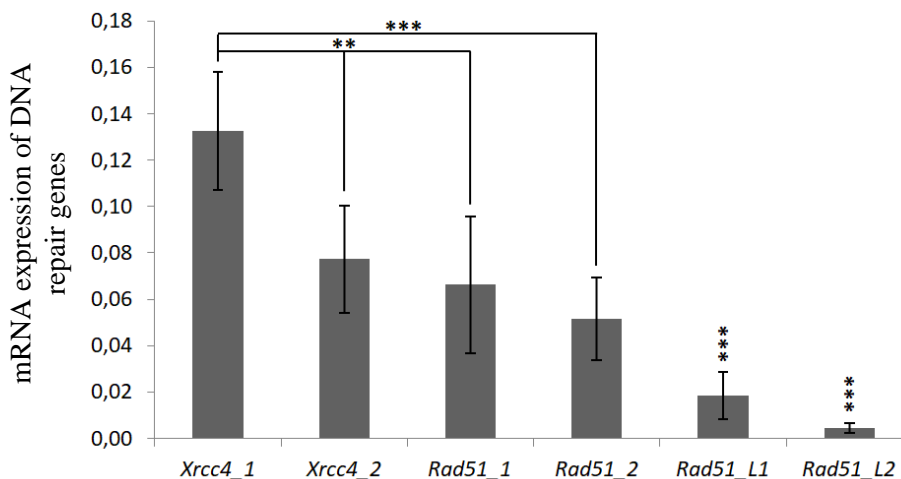
Gene expressions of specific proteins in non-irradiated biological duplicates (technical triplicates). The expression was measured using RT-qPCR analyses of RNA extracts coming from non-irradiated *A. vaga*. The analyses were performed on 8 different targets: *Xrcc4_1*, *Xrcc4_2*, *Rad51_1*, *Rad51_2*, *Rad51_L1* and *Rad51_L2*. The relative expression levels were referred to the expression of *HSP70*. The data represent the mean of Delta Ct measures ± standard deviations. Two-tailed P values were calculated using a two tailed Student's t-test (*, P<0.05; **, P<0.01; ***, P<0.001). The gene expression for *Xrcc4_2*, *Rad51_1* and *Rad51_2* were analysed regarding the *Xrcc4_1* gene expression. Furthermore, the expression of *Rad51_L1* and *Rad51_L2* were statistically analysed in comparison to every other gene expression showing a statistically less important expression than the other DNA repair genes.

Annex B – *Rad51* genes sequences alignment
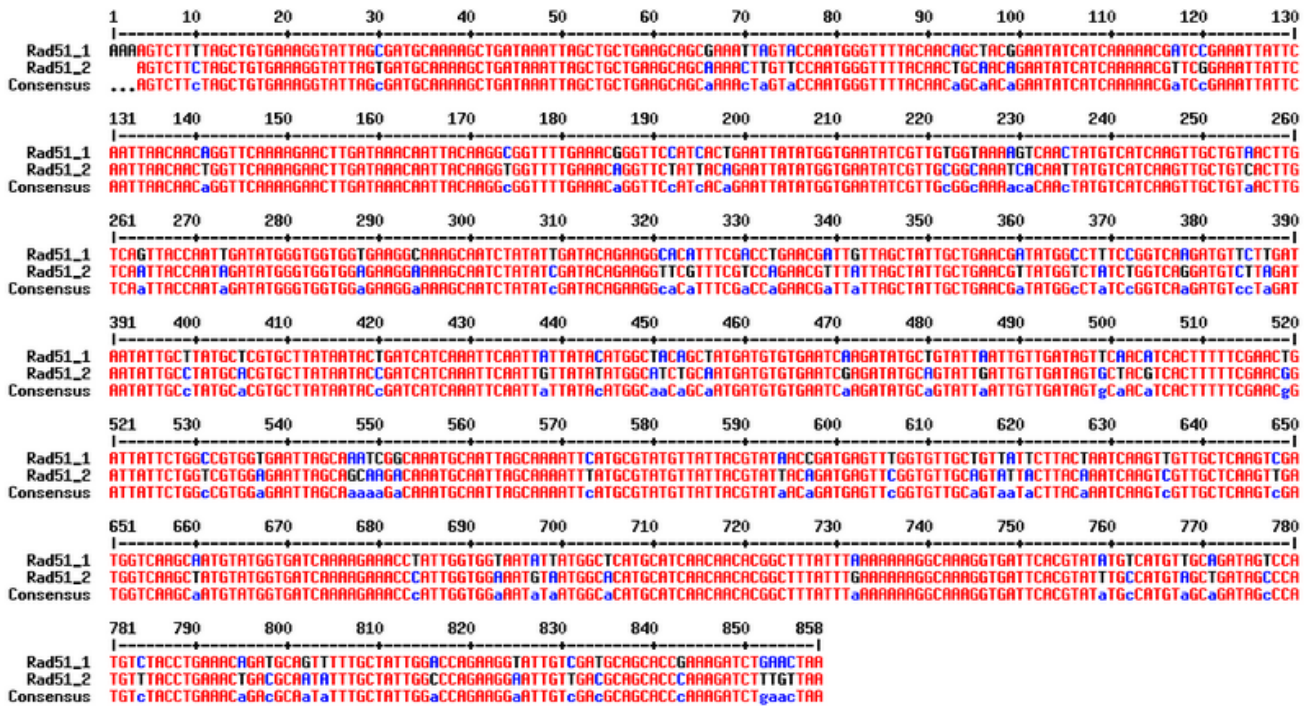
Alignment of *Rad51_1* and *Rad51_2* sequences. The high consensus values (in red) possess 86% of similarity while the low consensus values (in blue) possess ≤50% of sequences similarity. The sequences alignment was realised using the MultAlin website (Corpet, 1988) and the similarity measurement was realised using NCBI BLAST global alignment.

Annex C - 800Gy irradiation impact on whole protein extract at different time-points
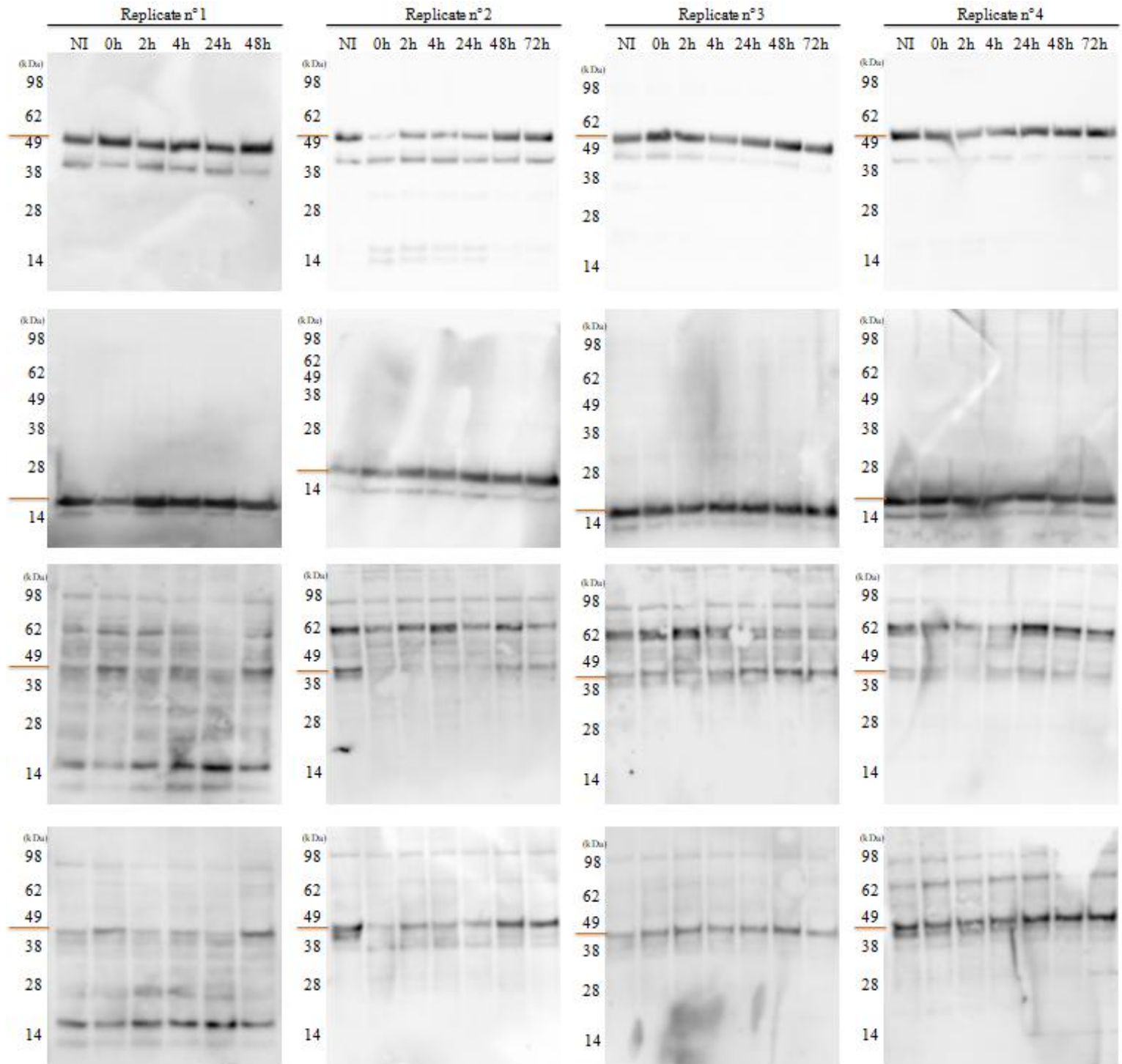
Western blotting detected with antibodies against α-tubulin, Histone H3, RAD51 & XRCC4 made with the same sample as the Coomassie blue staining. The replicate n°1 was loaded with 5µg of proteins and blocked with BSA while the other replicates were realised according to the Materials &Methods.

Annex D – Impact of MeOH fixation on IF experiments
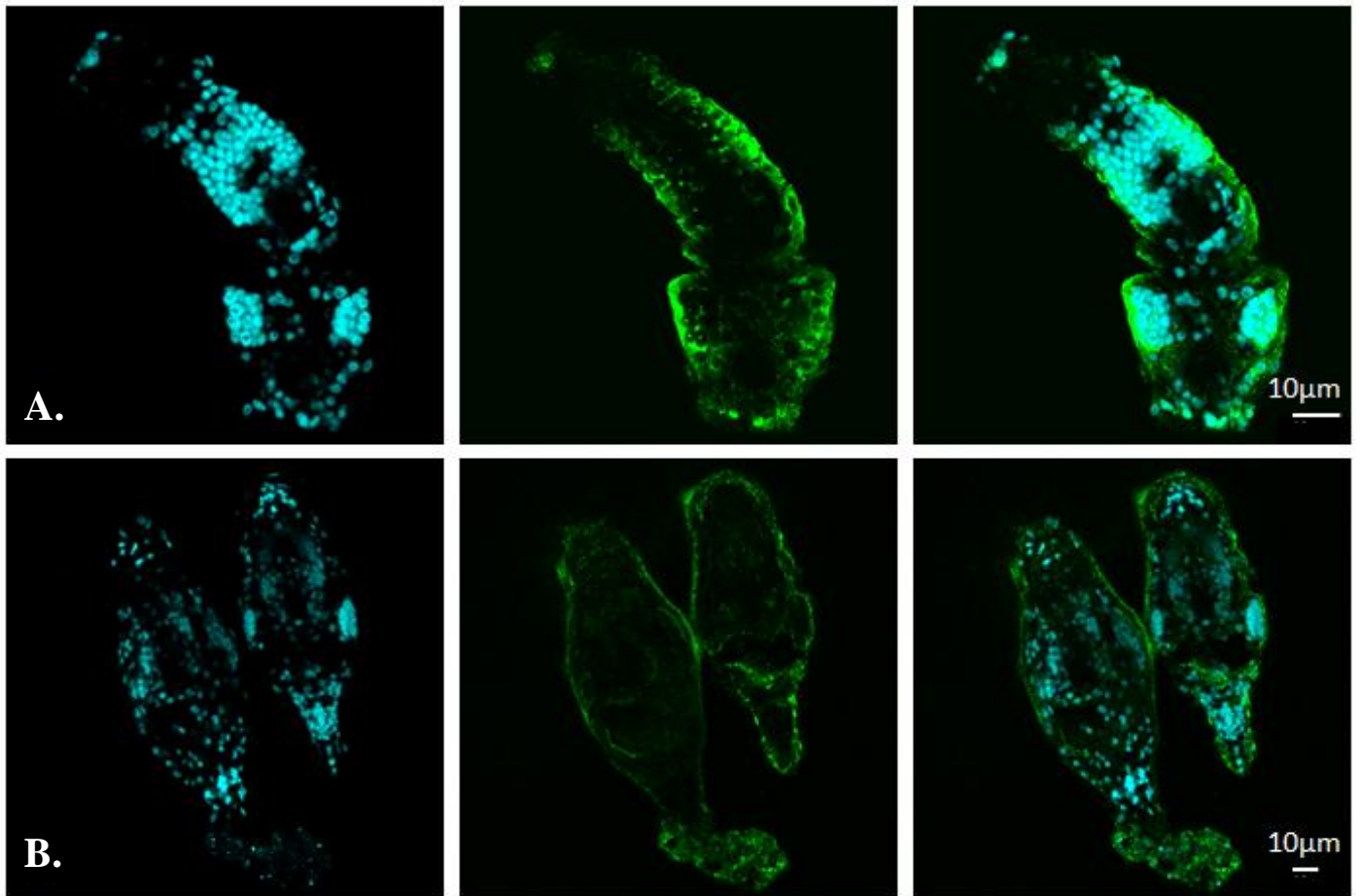
Adineta vaga individuals rotifers were stained in order to test different fixation methods and the impact it has on nuclear protein staining. Per condition, 20,000 individuals were fixed, blocked with 3% BSA and non-ionizing detergent. DNA was stained with DAPI and the primary and secondary antibodies had concentrations of 1:150. (A) After being freeze cracked bdelloid rotifers were fixed with MeOH followed by acetone. (B) The individuals were fixed in a solution of MeOH: acetone (1:1) before being disposed on a slide, undergoing freeze crack and being blocked and stained. Rotifers were imaged using the confocal microscope.

# Annex E - Optimization of staining protocol negatives controls
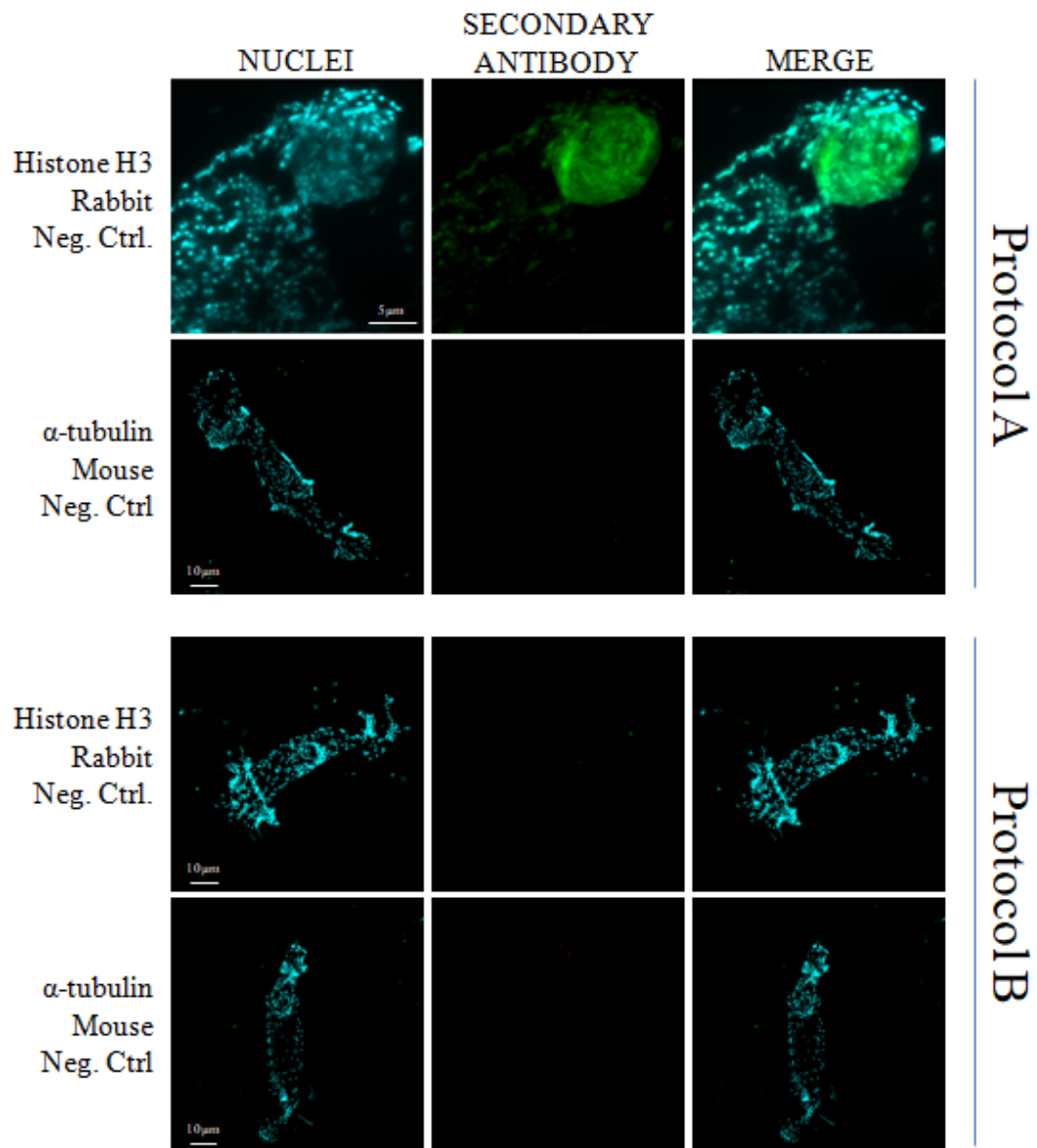
Adineta vaga individuals rotifers were only stained with fluorescent secondary antibody to confirm that signals are due to labelling and not to non-specificity. This figure shows the negative controls of the protocols presented in the figure 27.

Per condition, 500 individuals were fixed with formaldehyde after a freeze crack permeabilization. After fixation they were blocked with 3% BSA and non-ionizing detergent. DNA was stained with DAPI 1:100 and secondary antibody at a concentrations of 1:150. Rotifers were imaged using the Olympus fluorescent microscope.

Annex F – XRCC4 and RAD51 labelling upon 800Gy ionizing radiation
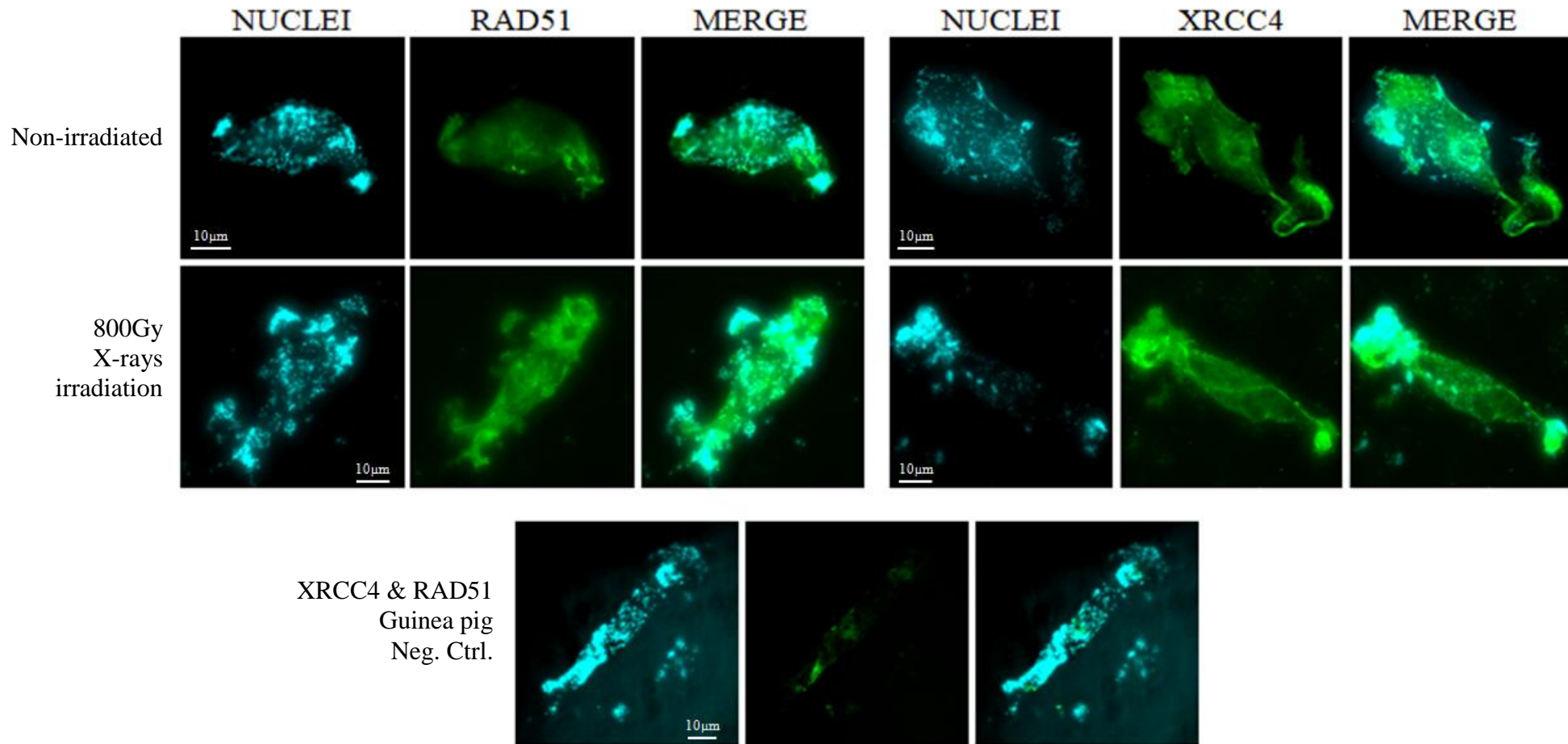
Adineta vaga individuals were stained in order to see if RAD51 and XRCC4 stainings would occur upon 800Gy irradiation. Per condition, 500 individuals were fixed with formaldehyde after a freeze crack permeabilization. After fixation they were blocked with 3% BSA and non-ionizing detergent. DNA was stained with DAPI 1:100 and the primary and secondary antibodies were used at concentrations of 1:150. Rotifers were imaged using the Olympus fluorescent microscope.

BIBLIOGRAPHY

Addgene. (2019). CRISPR Guide. Retrieved from https://www.addgene.org/crispr/guide/

Agrawal, N., Dasaradhi, P. V. N., Mohmmed, A., Malhotra, P., Bhatnagar, R. K., & Mukherjee, S. K. (2003). RNA Interference: Biology, Mechanism, and Applications. *Microbiology and Molecular Biology Reviews, 67*(4), 657-685.

Amsellem, J., & Ricci, C. (1982). Fine structure of the female genital apparatus of Philodina (Rotifera, Bdelloidea). *Zoomorphology, 100*(2), 89–105.

Attwood, D. (Ed.) (2007). *Soft X-rays and extreme ultraviolet radiation: Principles and Applications* (1 ed.). University of Cliorni, Berkeley.

Azzam, E. I., Jay-Gerin, J.-P., & Pain, D. (2012). Ionizing radiation-induced metabolic oxidative stress and prolonged cell injury. *Cancer letters, 327*(0), 48-60.

Bártová, E., Krejčí, J., Harničarová, A., Galiová, G., & Kozubek, S. (2008). Histone Modifications and Nuclear Architecture: A Review. *Journal of Histochemistry & Cytochemistry, 56*(8), 711-721.

Bass, J. J., Wilkinson, D. J., Rankin, D., Phillips, B. E., Szewczyk, N. J., Smith, K., & Atherton, P. J. (2017). An overview of technical considerations for Western blotting applications to physiological research. *Scandinavian Journal of Medicine & Science in Sports, 27*(1), 4-25.

Bégin, P. N., & Vincent, W. F. (2017). Permafrost thaw lakes and ponds as habitats for abundant rotifer populations. *Arctic Science, 3*(2), 354-377.

Beltrán-Pardo, E., Jönsson, K. I., Wojcik, A., Haghdoost, S., Bermudez-Cruz, R. M., & Bernal, J. (2013). Sequence analysis of the DNA-repair gene rad51 in the tardigrades Milnesium cf. tardigradum, Hypsibius dujardini and Macrobiotus cf. harmsworthi. *Journal of limnology, 72*, 80-91.

Berjak, P. (2006). Unifying perspectives of some mechanisms basic to desiccation tolerance across life forms. *Seed Science Research, 16*(1), 1-15.

BioRad. (2019). Western Blot Doctor™ — Protein Band Appearance Problems.

Bordeaux, J., Welsh, A., Agarwal, S., Killiam, E., Baquero, M., Hanna, J., Anagnostou, V., & Rimm, D. (2010). Antibody validation. *BioTechniques, 48*(3), 197-209.

Bradbury, A., & Plückthun, A. (2015). Reproducibility: Standardize antibodies used in research. *Nature, 518*(7537), 27–29.

Burma, S., Chen, B. P. C., & Chen, D. J. (2006). Role of non-homologous end joining (NHEJ) in maintaining genomic integrity. *DNA Repair, 5*(9), 1042-1048.

Butlin, R. (2002). The costs and benefits of sex: new insights from old asexual lineages. *Nature Reviews Genetics, 3*(4), 311-317.

Cheptsov, V., Vorobyova, E., Belov, A., Pavlov, A., Tsurkov, D., Lomasov, V., & Bulat, S. (2018). Survivability of Soil and Permafrost Microbial Communities after Irradiation with Accelerated Electrons under Simulated Martian and Open Space Conditions. *Geosciences, 8*(8), 298 (291-224).

Choi, E.-H., Yoon, S., Hahn, Y., & Kim, K. P. (2017). Cellular Dynamics of Rad51 and Rad54 in Response to Postreplicative Stress and DNA Damage in HeLa Cells. *Molecules and cells, 40*(2), 143-150.

Comeron, J., Williford, A. & Kliman, R. (2018). The Hill–Robertson effect: evolutionary consequences of weak selection and linkage in finite populations. *Heredity 100*, 19–31.

Conte, D., Jr., MacNeil, L. T., Walhout, A. J. M., & Mello, C. C. (2015). RNA Interference in Caenorhabditis elegans. *Current protocols in molecular biology, 109*, 26.23.21-26.23.30.

Corpet, F. (1988). Multiple sequence alignment with hierarchical clustering. *Nucleic Acids Research, 16*(22), 108881-110890.

Crowe, J. H., Hoekstra, F. A., & Crowe, L. M. (1992). Anhydrobiosis. *Annual Review of Physiology, 54*(1), 579-599.

Daly, M. J. (2012). Death by protein damage in irradiated cells. *DNA Repair, 11*(1), 12-21.

Danchin, E. G. J., Flot, J.-F., Perfus-Barbeoch, L., & Van Doninck, K. (2011). *Genomic Perspectives on the Long-Term Absence of Sexual Reproduction in Animals*: Springer.

Deepti, J., & Dinakar, S. M. (2019). Antibody specificity and promiscuity. *Biochemical Journal, 476*(3), 433-447.

Derveaux, S., Vandesompele, J., & Hellemans, J. (2010). How to do successful gene expression analysis using real-time PCR. *Methods, 50*(4), 227-230.

Desai, M. M. & Fisher, D. D. (2007). Beneficial Mutation–Selection Balance and the Effect of Linkage on Positive Selection. *Genetics, 176*(3), 1759-1798.

Dong, W.-H., Wang, T.-Y., Wang, F., & Zhang, J.-H. (2011). Simple, time-saving dye staining of proteins for sodium dodecyl sulfate-polyacrylamide gel electrophoresis using Coomassie blue. *PLoS One, 6*(8), e22394-e22394.

Du, Y., Zhang, J., Zheng, Q., Li, M., Liu, Y., Zhang, B., Liu, B., Zhang, H., & Miao, G. (2014). Heavy ion and X-ray irradiation alter the cytoskeleton and cytomechanics of cortical neurons. *Neural regeneration research, 9*(11), 1129-1137.

Duerr, J. S. (2013). Antibody Staining in C. Elegans Using "Freeze-Cracking". *Journal of Visualized Experiments*(80), e50664.

Dueva, R., & Iliakis, G. (2013). Alternative pathways of non-homologous end joining (NHEJ) in genomic instability and cancer. *Translational Cancer Research, 2*(3), 163-177.

Eriksson, D., Löfroth, P.-O., Johansson, L., Riklund, K. Å., & Stigbrand, T. (2007). Cell Cycle Disturbances and Mitotic Catastrophes in HeLa Hep2 Cells following 2.5 to 10 Gy of Ionizing Radiation. *Clinical Cancer Research, 13*(18), 5501s-5508s.

Fachin, A. L., Mello, S. S., Sandrin-Garcia, P., Junta, C. M., Donadi, E. A., Passos, G. A. S., & Sakamoto-Hojo, E. T. (2007). Gene Expression Profiles in Human Lymphocytes Irradiated In Vitro with Low Doses of Gamma Rays. *Radiation Research, 168*(6), 650-665.

Friedl, A., Mazurek, B., & Seiler, D.(2012). Radiation-induced alterations in histone modification patterns and their potential impact on short-term radiation effects. Frontiers in Oncology, 2(117): 1-10

Flot, J.-F., Hespeels, B., Li, X., Noel, B., Arkhipova, I., Danchin, E. G. J., Hejnol, A., Henrissat, B., Koszul, R., Aury, J.-M., Barbe, V., Barthélémy, R.-M., Bast, J., Bazykin, G. A., Chabrol, O., Couloux, A., Da Rocha, M., Da Silva, C., Gladyshev, E., Gouret, P., Hallatschek, O., Hecox-Lea, B., Labadie, K., Lejeune, B., Piskurek, O., Poulain, J., Rodriguez, F., Ryan, J. F., Vakhrusheva, O. A., Wajnberg, E., Wirth, B., Yushenova, I., Kellis, M., Kondrashov, A. S., Mark Welch, D. B., Pontarotti, P., Weissenbach, J., Wincker, P., Jaillon, O., & Van Doninck, K. (2013). Genomic evidence for ameiotic evolution in the bdelloid rotifer Adineta vaga. *Nature, 500*, 453.

Fontaneto, D., Barraclough, T. G., Chen, K., Ricci, C., & Herniou, E. A. (2008). Molecular evidence for broad-scale distributions in bdelloid rotifers: everything is not everywhere but most things are very widespread. *Molecular Ecology, 17*(13), 3136-3146.

Galis, F., & van Alphen, J. J. M. (2019). Parthenogenesis and developmental constraints. *Evolution & Development, e12324*(0), 1-13.

GeneCards. (2016). RAD51B Gene. Retrieved from https://www.genecards.org/cgi-bin/carddisp.pl?gene=RAD51B

Gladyshev, E. A., & Arkhipova, I. R. (2010). Genome Structure of Bdelloid Rotifers: Shaped by Asexuality or Desiccation? *Journal of Heredity, 101*(1), 85-93.

Gladyshev, E. A., & Meselson, M. (2008). Extreme resistance of bdelloid rotifers to ionizing radiation. *Proceedings of the National Academy of Sciences, 105*(13), 5139-5144.

Gladyshev, E. A., Meselson, M., & Arkhipova, I. R. (2008). Massive Horizontal Gene Transfer in Bdelloid Rotifers. *Science, 320*(5880), 1210-1213.

Hall, B., Limaye, A., & Kulkarni, A. B. (2009). Overview: generation of gene knockout mice. *Current protocols in cell biology, Chapter 19*, Unit-19.12.17.

Hecox-Lea, B. J., & Mark Welch, D. B. (2018). Evolutionary diversity and novelty of DNA repair genes in asexual Bdelloid rotifers. *BMC Evolutionary Biology, 18*(1), 177.

Hespeels, B., Flot, J.-F., Derzelle, A., & Van Doninck, K. (2014). Evidence for Ancient Horizontal Gene Acquisitions in Bdelloid Rotifers of the Genus Adineta. In P. Pontarotti (Ed.), *Evolutionary Biology: Genome Evolution, Speciation, Coevolution and Origin of Life* (pp. 207-225). Cham: Springer International Publishing.

Hespeels, B., Knapen, M., Hanot-Mambres, D., Heuskin, A.-C., Pineux, F., Lucas, S., Koszul, R., & Van Doninck, K. (2014). Gateway to genetic exchange? DNA double-strand breaks in the bdelloid rotifer Adineta vaga submitted to desiccation. *Journal of Evolutionary Biology, 27*(7), 1334-1345.

Hur, J. H., Van Doninck, K., Mandigo, M. L., & Meselson, M. (2008). Degenerate Tetraploidy Was Established Before Bdelloid Rotifer Families Diverged. *Molecular Biology and Evolution, 26*(2), 375-383.

Jackson, S. P. (2002). Sensing and repairing DNA double-strand breaks. *Carcinogenesis, 23*(5), 687-696.

Jayaraman, R. (2011). Hypermutation and stress adaptaion in bacteria. *Journal of Genetics, 90*(2), 383 - 391.

Khanna, K. K., & Jackson, S. P. (2001). DNA double-strand breaks: signaling, repair and the cancer connection. *Nature Genetics, 27*(3), 247-254.

Kong, Q., & Lin, C.-L. G. (2010). Oxidative damage to RNA: mechanisms, consequences, and diseases. *Cellular and molecular life sciences : CMLS, 67*(11), 1817-1829.

Kozera, B., & Rapacz, M. (2013). Reference genes in real-time PCR. *Journal of applied genetics, 54*(4), 391-406.

Krisko, A., Leroy, M., Radman, M., & Meselson, M. (2012). Extreme anti-oxidant protection against ionizing radiation in bdelloid rotifers. *Proceedings of the National Academy of Sciences, 109*(7), 2354-2357.

Krisko, A., & Radman, M. (2010). Protein damage and death by radiation in *Escherichia coli* and *Deinococcus radiodurans. Proceedings of the National Academy of Sciences, 107*(32), 14373-14377.

Latta, L. C., Tucker, N. K., & Haney, R. A. (2019). The relationship between oxidative stress, reproduction, and survival in a bdelloid rotifer. *BMC Ecology, 19*(7), 1-10.

Lee, H. O., Davidson, J. M., & Duronio, R. J. (2009). Endoreplication: polyploidy with purpose. *Genes & development, 23*(21), 2461-2477.

Lieber, M. R. (2010). The Mechanism of Double-Strand DNA Break Repair by the Nonhomologous DNA End-Joining Pathway. *Annual Review of Biochemistry, 79*(1), 181-211.

Lillehoj, E. P. (1994). Protein immunoblotting. In V. S. Malik & E. P. Lillehoj (Eds.), *Antibody Techniques* (pp. 273-289). San Diego: Academic Press.

Maciver, S. K. (2016). Asexual Amoebae Escape Muller's Ratchet through Polyploidy. *Trends in Parasitology, 32*(11), 855-862.

Malu, S., Malshetty, V., Francis, D., & Cortes, P. (2012). Role of non-homologous end joining in V(D)J recombination. *Immunologic Research, 54*(1), 233-246.

Mark Welch, D. B., Mark Welch, J. L., & Meselson, M. (2008). Evidence for degenerate tetraploidy in bdelloid rotifers. *Proceedings of the National Academy of Sciences of the United States of America, 105*(13), 5145-5149.

Mirzaghaderi, G., & Hörandl, E. (2016). The evolution of meiotic sex and its alternatives. *Proceedings. Biological sciences, 283*(1838), 1-10.

Nowell, R., Wilson, C., Smith, T., Fontaneto, D., Crisp, A., Micklem, G., Tunnacliffe, A., Boschetti, C., & Barraclough, T. (2018). Comparative genomics of bdelloid rotifers: Insights from desiccating and nondesiccating species. *PLoS Biology, 16*, e2004830.

Rao, X., Huang, X., Zhou, Z., & Lin, X. (2013). An improvement of the 2ˆ(-delta delta CT) method for quantitative real-time polymerase chain reaction data analysis. *Biostatistics, bioinformatics and biomathematics, 3*(3), 71-85.

Renglin Lindh, A., Schultz, N., Saleh-Gohari, N., & Helleday, T. (2007). RAD51C (RAD51L2) is involved in maintaining centrosome number in mitosis. *Cytogenetic and Genome Research, 116*(1-2), 38-45.

Ricci, C., & Caprioli, M. (2005). Anhydrobiosis in Bdelloid Species, Populations and Individuals1. *Integrative and Comparative Biology, 45*(5), 759-763.

Ricci, C., & Fontaneto, D. (2009). The importance of being a bdelloid: Ecological and evolutionary consequences of dormancy. *Italian Journal of Zoology, 76*(3), 240-249.

Sebesta, M., & Krejci, L. (2016). Mechanism of Homologous Recombination. In F. Hanaoka & K. Sugasawa (Eds.), *DNA Replication, Recombination, and Repair: Molecular Mechanisms and Pathology* (pp. 73-109). Tokyo: Springer Japan.

Shrivastav, M., De Haro, L. P., & Nickoloff, J. A. (2007). Regulation of DNA double-strand break repair pathway choice. *Cell Research, 18*, 134.

Snyder, A. R., & Morgan, W. F. (2004). Gene expression profiling after irradiation: Clues to understanding acute and persistent responses? *Cancer and Metastasis Reviews, 23*(3), 259-268.

Space. (2017). Western Blot – Cell Lysate Protocol. Retrieved from http://www.spacesrl.com/risorse-tecniche/recommended-protocols/western-blot-cell-lysate-protocol/

The protein human atlas (2019a). RAD51. Retrieved from https://www.proteinatlas.org/ ENSG00000051180-RAD51/cell

The protein human atlas (2019b). XRCC4. Retrieved from https://www.proteinatlas.org/ ENSG00000152422-XRCC4/cell

Tripathi, R., Boschetti, C., McGee, B., & Tunnacliffe, A. (2012). Trafficking of bdelloid rotifer late embryogenesis abundant proteins. *The Journal of Experimental Biology, 215*(16), 2786-2794.

Tsai, C.-H., Liao, R., Chou, B., & Contreras, L. M. (2015). Transcriptional analysis of Deinococcus radiodurans reveals novel small RNAs that are differentially expressed under ionizing radiation. *Applied and environmental microbiology, 81*(5), 1754-1764.

Tunnacliffe, A., Lapinski, J., & McGee, B. (2005). A Putative LEA Protein, but no Trehalose, is Present in Anhydrobiotic Bdelloid Rotifers. *Hydrobiologia, 546*(1), 315-321.

Uppsala. (2016). Western Blotting: Principles and Methods. 176p.

Van Doninck, K., Mandigo, M. L., Hur, J. H., Wang, P., Guglielmini, J., Milinkovitch, M. C., Lane, W.S.? & Meselson, M. (2009). Phylogenomics of Unusual Histone H2A Variants in Bdelloid Rotifers. *PLOS Genetics, 5*(3), e1000401.

Vagenende, V., Yap, M., & Trout, B. (2009). Mechanisms of Protein Stabilization and Prevention of Protein Aggregation by Glycerol. *Biochemistry, 48*, 11084-11096.

Venkata Narayanan, I., Paulsen, M. T., Bedi, K., Berg, N., Ljungman, E. A., Francia, S., Veloso, A., Magnuson, B., di Fagagna, F d'A., Wilson, T. E., & Ljungman, M. (2017). Transcriptional and post-transcriptional regulation of the ionizing radiation response by ATM and p53. *Scientific Reports, 7*, 43598-43598.

Vieira, N. G., Ferrari, I. F., Rezende, J. C. d., Mayer, J. L. S., & Mondego, J. M. C. (2019). Homeologous regulation of Frigida-like genes provides insights on reproductive development and somatic embryogenesis in the allotetraploid Coffea arabica. *Scientific Reports, 9*(1), 1-15.

Wang, P., Yuan, D., Guo, F., Chen, X., Zhu, L., Zhang, H., & Shao, C. (2017). Chromatin remodeling modulates radiosensitivity of the daughter cells derived from cell population exposed to low- and high-LET irradiation. *Oncotarget*, *8*(32), 52823–52836.

Wei, S., Li, C., Yin, Z., Wen, J., Meng, H., Xue, L., & Wang, J. (2018). Histone methylation in DNA repair and clinical practice: new findings during the past 5-years. *Journal of Cancer*, *9*(12), 2072-2081.

Wharton, D. A. (2015). Anhydrobiosis. *Current Biology, 25*(23), 1114-1117.

Wigglesworth, V. B. (2017). Insect: Arthropod class: Forms & function: Reproductive system. Retrieved from https://www.britannica.com/animal/insect/Circulatory-system#ref250919

Wilson, C. G. (2011). Desiccation-tolerance in bdelloid rotifers facilitates spatiotemporal escape from multiple species of parasitic fungi. *Biological Journal of the Linnean Society, 104*(3), 564-574.

Wilson, T. E. (2008). Non-Homologous Recombination. In Begley (Ed.), *Wiley Encyclopedia of Chemical Biology* (pp. 1 - 9): John Wiley & Sons.